THESIS

DEVELOPMENT OF THE PIEZOVANE FOR ESTIMATING LIQUEFACTION POTENTIAL OF SATURATED SANDS

Submitted by

Leo Wm. Butler

Department of Civil Engineering

In partial fulfillment of the requirements

for the Degree of Master of Science

Colorado State University

Fort Collins, Colorado

Fall 1994

COLORADO STATE UNIVERSITY

FEBRUARY 21, 1992

WE HEREBY RECOMMEND THAT THE THESIS PREPARED UNDER OUR SUPERVISION BY LEO WM. BUTLER ENTITLED DEVELOPMENT OF THE PIEZOVANE FOR ESTIMATING LIQUEFACTION POTENTIAL OF SATURATED SANDS BE ACCEPTED AS FULFILLING IN PART REQUIREMENTS FOR THE DEGREE OF MASTER OF SCIENCE.

COMMITTEE ON GRADUATE WORK

Thomas J. Siller

Donald ...

Wayne A. Charlie

Advisor

...

Department Head

ABSTRACT OF THESIS

DEVELOPMENT OF THE PIEZOVANE FOR THE ESTIMATING LIQUEFACTION POTENTIAL OF SATURATED SANDS

The Piezovane was developed for determining in situ liquefaction potential of saturated sands by measuring the porewater pressure response of saturated sand during and after shearing of the soil. A negative porewater pressure response is an indication that the material is in a dense (dilative) state; therefore is not susceptible to liquefaction failure. Positive porewater pressure response is an indication that the sand is in a loose (contractive) state and is susceptible to liquefaction-type failure. This project included design, fabrication of the Piezovane apparatus and the calibration chamber for the initial laboratory testing. Sands were placed within the calibration chamber at densities greater than or less than densities at the steady state which had been developed by using CU triaxial and CD direct shear tests. Trends indicate that the Piezovane testing can predict contractive or dilative behavior of soils. Additional testing both in the laboratory and in the field is required to determine whether these measured porewater pressure responses and measured shear resistances provide parameters needed for evaluating liquefaction potential and their possible use for design. A patent for the Piezovane has been awarded.

Leo Wm. Butler
Civil Engineering Department
Colorado State University
Fort Collins, Colorado 80523
Fall 1994

ACKNOWLEDGMENTS

I take this opportunity to express my appreciation and gratitude to Mr. Walt Patzer, Mr. Bob Brennan, Mr. Bob Kiesel and Ms. Marilee Schenkel with the College of Engineering for their time and technical expertise; my friends and colleagues at STS Consultants, Ltd., for their patience and prodding when necessary; and to Ms. Lisa Duff and Ms. Carol Douglas for typing this manuscript.

I am deeply indebted to my fellow researchers in the Blast Induced Liquefaction Research Program at Colorado State University (without their help, advice and encouragement, this project would not have been possible): Mr. Dave Allard, Mr. Wayne Lewis, Mr. Paul Jacobs, Mr. Clint Scott, Mr. Chris Hatton, Ms. Lynne Schure, Dr. Tom Bretz, and Dr. Hassen Hassen. I give special thanks to my advisor, Dr. Wayne Charlie, who initially came up with the theory behind the Piezovane, for his time patience and understanding. I am grateful to the Air Force Office of Research for its funding and continuing efforts to patent the Piezovane. I thank Mr. John W. France of GEI Consultants, Inc. of Englewood, Colorado, for his technical guidance. Thanks are extended to Dr. Donald Doehring and Dr. Thomas Siller for serving on my graduate committee. I would like to thank Dr. JWN Fead for his time and advice during my undergraduate and graduate studies at Colorado State University.

I thank my parents, Mr. L. William Butler and Mrs. Nancy J. Brady and my mother-in-law and father-in-law, Dr. and Mrs. Vincent Bavisotto, for their support and encouragement. I thank my children, Michael and Maria, for their patience throughout my graduate studies. Above all, I thank my wife, Nancy, for her time, patience, loving support and sacrifices throughout my research efforts.

DEDICATION

This manuscript is dedicated to Ken Malone, a good friend and fellow student, who was taken from us before he had the opportunity to make his contribution to the engineering community.

TABLE OF CONTENTS

LIST OF TABLES

LIST OF FIGURES

LIST OF SYMBOLS

Symbol	
a	spherical radius of influence, cm
C	pore pressure parameter
cc	cubic centimeter
cm	centimeter
CD	consolidated, drained
CU	consolidated, undrained
C_u	coefficient of uniformity
CPT	Cone Penetration Test
C_v	coefficient of consolidation, m^2/s
CSU	Colorado State University
D	vane diameter, cm
D_r	relative density, %
D_{50}	diameter of 50% passing, mm
e	void ratio
e_c	void ratio at end of consolidation
e_i	initial void ratio
f_v	poison factor
fΔ	expansion factor
g	gravitational constant, 9.81 m/s^2
H	vane height, cm
K	coefficient of lateral stress
K_o	coefficient of lateral stress at rest
k	coefficient of permeability, cm/s
kPa	kilopascal
M	torque, N-m
m	meter
m_v	coefficient of compressibility, 1/kPa
ms	millisecond
mv	millivolt
N	newton
p'	$(\sigma'_1 + \sigma'_2)/2$, kPa
p'_s	$(\sigma'_1 + \sigma'_2)/2$, at steady state, kPa
pwp	porewater pressure, kPa
PVS	Poudre Valley Sand
q	$(\sigma_1 - \sigma_2)/2$, kPa
q_s	$(\sigma_1 - \sigma_2)/2$, at steady state, kPa
r	vane radius, cm
R	correlation coefficient

R^2	coefficient of determination
S	shear strength, kPa
S_p	peak shear strength, kPa
S_{ref}	reference shear strength, kPa
S_s	steady state shear strength, kPa
S_{su}	undrained steady state shear strength, kPa
S_{uv}	undrained vane shear strength, kPa
S_{vs}	vane shear strength at steady state, kPa
S_{vp}	peak vane shear strength, kPa
SPT	Standard Penetration Tests
s	standard deviation
S	second
T	dimensionless time factor
t_f	time to failure from start of shear, s
U	pore pressure dissipation, (%)
u	pore pressure, kPa
v	angular shear velocity, cm/sec
ξ_s	strain at steady state, %
γ_d	dry unit weight, kN/m^3
γ	unit weight, kN/m^3
γ_w	unit weight of water, kN/m^3 (9.81 kN/m^3)
ϕ'	effective angle of internal friction, degrees
ϕ'_s	effective angle of internal friction at steady state, degrees
σ	stress, kPa
σ'	effective stress, kPa
σ'_f	effective stress normal to failure plane, kPa
σ_{fs}	effective stress normal to failure plane, at steady state, kPa
σ_1'	effective major principal stress, kPa
σ_3'	effective minor principal stress, kPa
$\sigma_3'_c$	effective isotropic consolidation stress, kPa
$\sigma_3'_s$	effective minor principal stress at steady state, kPa
σ_v'	effective vertical stress, kPa
σ_{vc}'	effective vertical consolidation stress, kPa
σ_h'	effective horizontal stress, kPa
τ_f	shear strength, kPa
τ_d	driving shear stress, kPa
w	rotation rate, rad/sec

CHAPTER I

INTRODUCTION

A. Statement of Problem

On October 17, 1989, the Loma Prieta earthquake, having a magnitude of 7.1, occurred 70 km south of San Francisco, California. The effects of liquefaction were observed over a radius of 70 km from the epicenter. Damage in the San Francisco Bay Area was in excess of $10 billion, some of which can be associated to liquefaction. This damage included sand boils, lateral spreading, soil bearing failures of foundations, pavement distress, and damage to underground utilities. The fracturing of water mains led to loss of fire protection and the fracturing of gas lines caused numerous fires (Seed et al., 1990).

Present methods for evaluating the in situ liquefaction potential are empirical and need to be improved (Peck, 1979; Poulos, 1988). Current in situ techniques are restricted to correlations with the Standard Penetration Test (SPT), Cone Penetration Test (CPT), or shear wave test results. Soil parameters associated with laboratory liquefaction evaluation (dilative/contractive states and/or cyclic shear strength) cannot be directly associated with the in situ properties (Castro, 1982b). There are three common methods for evaluation of liquefaction potential: the steady state method by Poulos and Castro of Geotechnical Engineering, Inc.; the SPT (or CPT) and cyclic analysis by Seed of the University of California at Berkeley; and the threshold strain approach by Dobry at Rensselaer Polytech. Inst. (Hausner, 1985).

The Piezovane was developed to measure the soil state and residual steady state strength in situ. The device was designed to be adapted to current subsurface exploration methods. The Piezovane consists of a modified vane shear apparatus which has been equipped with a porewater pressure transducer, rotation potentiometer and torque transducer. A patent application was granted by the U.S. Patent and Trademark Office (Charlie and Butler, 1990) in 1992. The Piezovane and CSU Piezovane are trademarks of Colorado State University.

B. Objective of Study

The goals of this research are to develop and evaluate the Piezovane, a new in situ device for determining liquefaction potential. The objectives of the research are to determine if the Piezovane can:

- Determine contractive or dilative soil states,
- Determine shear strength at large deformation (steady state shear strength).

The scope of this thesis is limited to design, construction and preliminary testing of this device. This will include the design and construction of laboratory equipment for testing feasibility of the device. In addition, laboratory equipment and procedures were developed to evaluate the steady state behavior of soil used in this study.

CHAPTER II

LITERATURE REVIEW

A. Liquefaction

1. Introduction

Liquefaction, the act or process of transforming any substance into a liquid, was first applied to a soil failure by Hazen (1920) in describing the failure of Calaveras Dam in California, and by Casagrande (1940) in describing the failure of Fort Peck Dam in Montana. It was not until the Niigata, Japan and Alaskan earthquakes of 1964 that liquefaction was identified as a Geotechnical failure. The Alaskan earthquake induced liquefaction which destroyed harbor facilities, runways, roads, railroads, buildings and homes. In Niigata, several apartment buildings tilted or fell over due to liquefaction of the underlying soil. Empty underground tanks also surfaced after the earthquake. In the United States there have been several dam failures due to liquefaction including: Fort Peck Dam, Sheffield Dam, and Lower San Fernado Dam (Seed, 1987).

Liquefaction may cause damage due to several phenomena, including flow failures, lateral spreads, increased ground oscillation, loss of bearing capacity, ground settlements, and sand boils (Housner, 1985). When a saturated cohesionless soil is subject to a trigging event, (i.e. earthquake, blasting, construction vibration or additional static loadings) particle rearrangement occurs. If the particle rearrangement causes a net decrease in void ratio and if the decrease

occurs under undrained conditions, it will result in excess porewater pressure. Increase in porewater pressure (u) decreases the effective stress, σ' defined as:

$$\sigma' = \sigma - u \qquad \text{Eq. 2.1}$$

where σ is the total stress. This concept was first introduced by Terzaghi (1943). Liquefaction transpires when the magnitude of the effective stress decreases to near zero.

2. Definition of Liquefaction

There have been several variations in the definition of liquefaction. Casagrande (1975) suggested the use of the following definitions.

> Actual Liquefaction - "It is the response of loose, saturated sand when subjected to strains or shocks that result in substantial loss of strength and in extreme cases leads to flow slides."
>
> Cyclic Mobility - "The response of a test specimen of dilative sand to cyclic loading in a triaxial test when the peak porewater pressure rises momentarily in each cycle to the confining pressure."

The Committee on Soil Dynamics of the Geotechnical Engineering Division (Marcuson, 1978) recommended the following definition:

> Liquefaction: "The act or process of transforming any substance into a liquid. In cohesionless soil, the transformation is from a solid state to a liquefied state as a consequence of increased pore pressure and reduced effective stress... Liquefaction is thus defined as a changing of state which is independent of initial disturbance that could be static, vibratory, sea wave, shock loading or a change in groundwater pressure. The definition also is independent of deformation or ground failure movements that might follow the transformation. Liquefaction always produces a transient loss of shear resistance but does not always produce a longer-term reduction of shear strength".

Castro and Poulos (1977) and Castro et al., (1982a) proposed the following definition which will be used in this report.

> Liquefaction - "Is a phenomenon wherein a mass of soil loses a large percentage of its shear resistance, when subjected to undrained monotonic, cyclic or shock loading, and flows in a manner resembling a liquid until the shear stresses acting on the mass are as low as the reduced shear resistance."

The shear strength referred to in this definition is the strength at large strains. (Poulos, 1988).

B. Critical Void Ratio

1. Development of Critical Void Ratio

It was first noticed in 1885 by O. Reynolds, that a dense granular material would dilate when deformed. He demonstrated this property on lead shot and sand, and termed it "dilatancy." He used a closed rubber bag filled with dense, saturated material. The bag was connected to an open graduated vessel containing water. As the bag was deformed the material dilated, the void volume increased, which caused it to fill with water from the graduated vessel (Castro, 1969).

Casagrande (1940) observed during direct shear tests, that a loose sand when sheared, decreases in volume ("contracts") and eventually approaches a "steady state volume". He also noted that a dense sand when sheared increases in volume, ("dilates"), until it also reaches the same steady state volume, which he termed the "critical void ratio". When he first lectured on this subject before the Boston Society of Civil Engineers (Casagrande, 1940), he was under the impression that the critical void ratio was independent of the normal stress.

In 1936, while investigating methods of determining the critical void ratio for the design of the Franklin Falls dam for the U.S. Army Corps of Engineers, a great number of direct shear tests were performed on a wide range of normal stresses on sands obtained from the dam. Casagrande concluded from these laboratory tests that:

- The direct shear test is not suitable for the determination of the critical void ratio, because of the limited deformation possible and because of the lack of accuracy in the determination of the initial void ratio and of its subsequent changes during the tests.
- In spite of the limitations of the direct shear tests, it is possible to conclude from such tests that the critical void ratio is not a constant for a given sand, but that it decreases with increasing normal stress. (Casagrande, 1975).

Casagrande and Watson (1938) then designed a triaxial apparatus and a technique for consolidated drained (CD) tests on soil samples. From these tests it was concluded that:

- Sand with void ratios greater than the critical void ratio (a loose state), will decrease in volume throughout the test, with a small increase in volume at a large strain near the end of the test.
- Sand with a void ratio lower than the critical void ratio (dense initial state) would have an initial decrease in volume at the start of the test. As the peak compressive stress is approached, the sand dilates and the volume increase continues to the end of the test.
- The critical void ratio was found to decrease with increased confining pressure.

Casagrande and Watson (1938) reported two limitations of using the triaxial apparatus to determine the actual critical void ratio.

- In tests with a dense initial state, one or more failure planes would develop shortly after the peak deviator stress. Further deformation occurs along the narrow failure zone, which cannot be correlated with the volume change of the entire specimen.
- In tests with a loose initial state, no failure planes develop, but the specimen fails gradually by bulging. Large strains are needed to reach the critical void ratio. Constant shear stress and constant volume are only approximately reached with large vertical strains.

Even with these limitations, the triaxial tests on loose specimens permit a conservative estimate of the critical void ratio, which were based on the volume changes at the peak compressive stresses. Casagrande introduced the term "lower critical void ratio" in the same paper. He defined it as that void ratio for which the volume change at the peak compressive stress is passing through zero, and for some strain after the peak the specimen continues to dilate (Casagrande and Watson, 1938).

By the time Casagrande presented his second lecture on liquefaction in 1938, the early test results led him to the following conclusions.

- All combinations of void ratios and effective normal stresses which would put the initial state below or to the left of the critical void ratio line would develop a dilative behavior (point B on Figure 2.1) which is safe against liquefaction failure.
- Any combination of void ratios and/or effective normal stresses which would put the initial state to the right or above the critical void ratio line (point A on Figure 2.1) would result in contractive behavior. For liquefaction to occur, the initial state must be substantially to the right of the critical void ratio line so that in the liquefied state the effective stresses would decrease to below the existing shear stresses in the soil mass.
- The greater the effective normal stress, the lower the critical void ratio, so a heavily loaded, medium dense sand may be susceptible to liquefaction.

After the second lecture, a major liquefaction failure occurred at Fort Peck Dam in Montana. The upstream toe liquefied with about eight million cubic meters of sand moving 400 meters. The U.S. Army Corps of Engineers carried out a major investigation which included obtaining large diameter undisturbed samples of the sands which had failed. The undisturbed samples were obtained by coring columns of sand which had been frozen in situ. Casagrande and Watson (1938) determined the critical void ratio on the hydraulically filled sand used in the dam. These tests concluded that the sand was at a void ratio smaller (below) than its critical void ratio, so liquefaction could not have occurred. This was a major factor in influencing the investigating

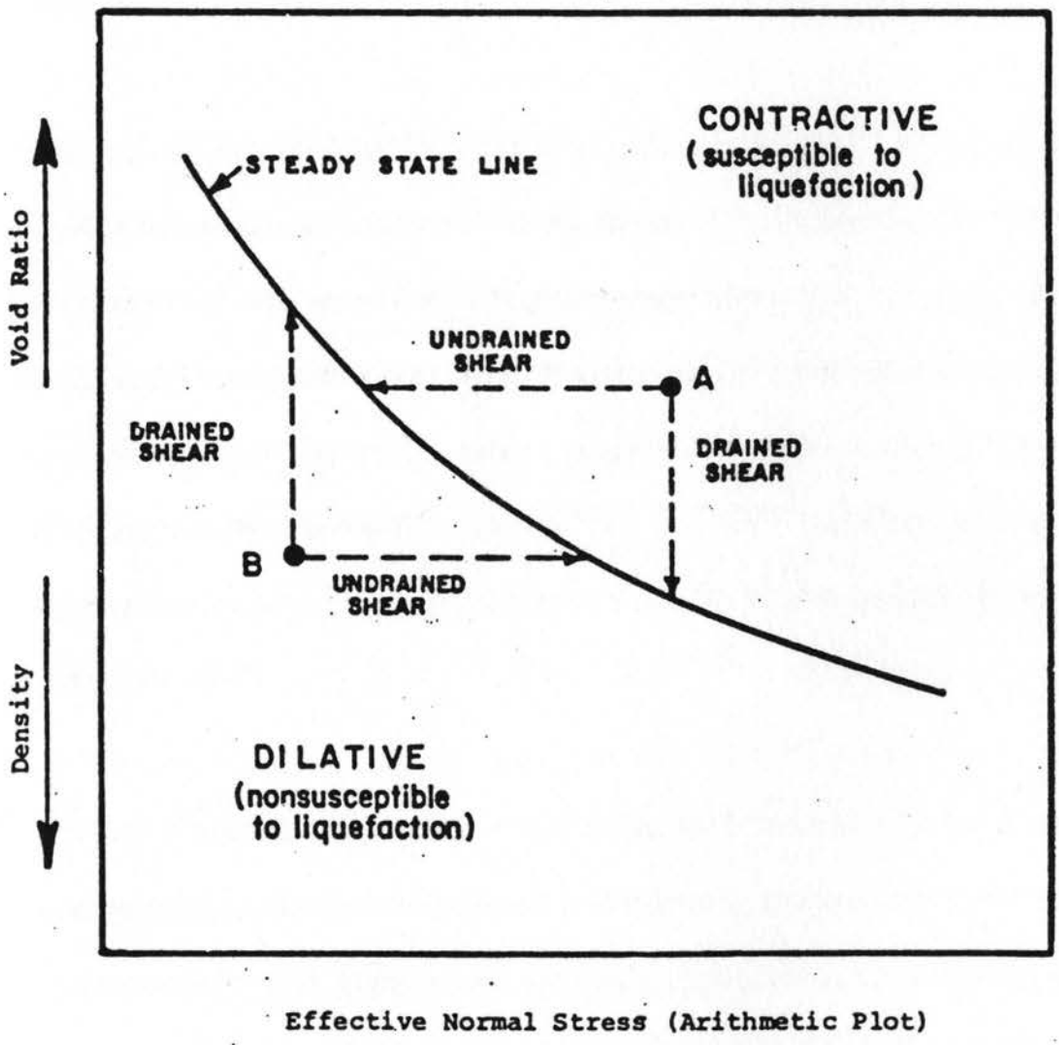

Figure 2.1 Steady State / Critical Void Ratio Diagram (Castro et al., 1982b).

board that the failure was not due to liquefaction. Casagrande disagreed with the majority of the board, pointing out that the speed of movement and topography of the slide afterward could only have resulted from a liquefaction failure. However, the data indicated that the sand void ratio was located below the critical void ratio line. This, he assumed, was due to the type of laboratory test that did not define correctly the critical void ratio and led to dangerous design errors. He then warned against the use of this method in design (Casagrande, 1975).

In the years that followed Fort Peck dam failure, Casagrande developed the hypothesis that when a sand liquefies into a flow failure, there is a change in state from a granular structure to a liquid with a minimum shear resistance. The grains would start to flow in a chain reaction and would remain in this liquid state during flow. When the flow stops, the grains would rearrange as the excess pore pressure dissipates to a more compacted state than pre-flow condition. The term he used to describe this intermediate state was "flow structure". As in the Fort Peck dam failure the sand's state went from a loose initial state to a state which was no longer prone to liquefaction (Casagrande, 1975).

After several unsuccessful attempts at simulating the flow structure in the laboratory, he asked Castro to design a triaxial test that would maintain a constant load while the sample deformed. Previous attempts with strain control tests were unsuccessful, due to the fact that the driving force could not be maintained, so the sand would "relax". With a constant load, the driving force would be constant as the flow structure is being developed and as the mass accelerates, which starts the chain reaction for the flow structure.

Castro (1969) developed a stress control test which allowed constant load to be applied to the sample during failure. After consolidating a specimen in a triaxial cell, increments of stress were applied to the specimen by adding weights to a hanging bracket attached to the specimen. The specimen's strain induced by the stress increment was measured.

In Test "a" (Figure 2.2) of Castro (1969), the relative density (D_{rc}) of the specimen after consolidation was 27%. At 1% strain, the peak deviator stress [$(\sigma_1-\sigma_3)/2$] was reached, when the next increment of stress was applied, the specimen liquefied and strained to about 25% in a fraction of a second. During the flow failure the deviator stress had decreased to 15% of the peak deviator stress and remained constant. The induced porewater pressure increased to 377.5 kPa and remained constant during the flow failure. This resulted in a decrease in effective minor principal stress from σ_{3f} = 400.0 kPa to σ_{3f} = 24.5 kPa.

The after consolidation relative density was D_{rc} = 44% in Test "b". This specimen achieved greater peak deviator stress before liquefaction occurred, and strained to approximately 18% in 0.4 seconds. During the flow failure the deviator stress decreased slightly compared to the peak deviator stress before the flow failure. After the flow failure it was necessary to increase the deviator stress for additional strain to occur.

In Test "c" the D_{rc} = 47%, the specimen started to develop a peak deviator stress slightly higher than "b", but then rapidly increased strength as the specimen began to dilate. This is also indicated by the porewater pressure response. The porewater pressure decreased to zero at 14% strain.

In Figure 2.2 the deviator stress and porewater pressure response of the three tests are shown. Castro classified a type "a" failure as a liquefaction failure, a type "b" as a limited liquefaction failure, and a type "c" as a dilative response. By plotting the void ratio after consolidation against the logarithm of the effective minor principal stress (σ'_3), the critical void ratio can be determined as shown in Figure 2.1.

Poulos (1971) introduced the term "Steady State Void Ratio" to be synonymous with Casagrande's (1940) critical void ratio. The term critical state had been applied by other authors to describe different soil states other than what Casagrande had intended. It also conveys the steady state flow of liquids used in fluid mechanics theory (Castro et al., 1982a).

2. Steady State Lines

Steady state concepts can be best explained through the use of graphical representation of the effective stress (σ'_3), shear stress (τ) and void ratio (e). This three-dimensional representation can be conveniently represented by any two dimensions with a common axis. The most common representation is by plotting void ratio versus logarithm of either minor effective stress or shear stress as indicated on Figure 2.3.

Castro and Poulos (1977) reported that the steady state line is not unique but is a function of soil type. Therefore, relative density alone is not a variable for susceptibility for liquefaction. Poulos et al., (1985) concluded the following:

- The slope of the steady state line on a semi-log scale is effected by grain shape, with subrounded grains having less of a slope than angular grains (Figure 2.4).
- The vertical position of the steady state line can be contributed to the grain size distribution.

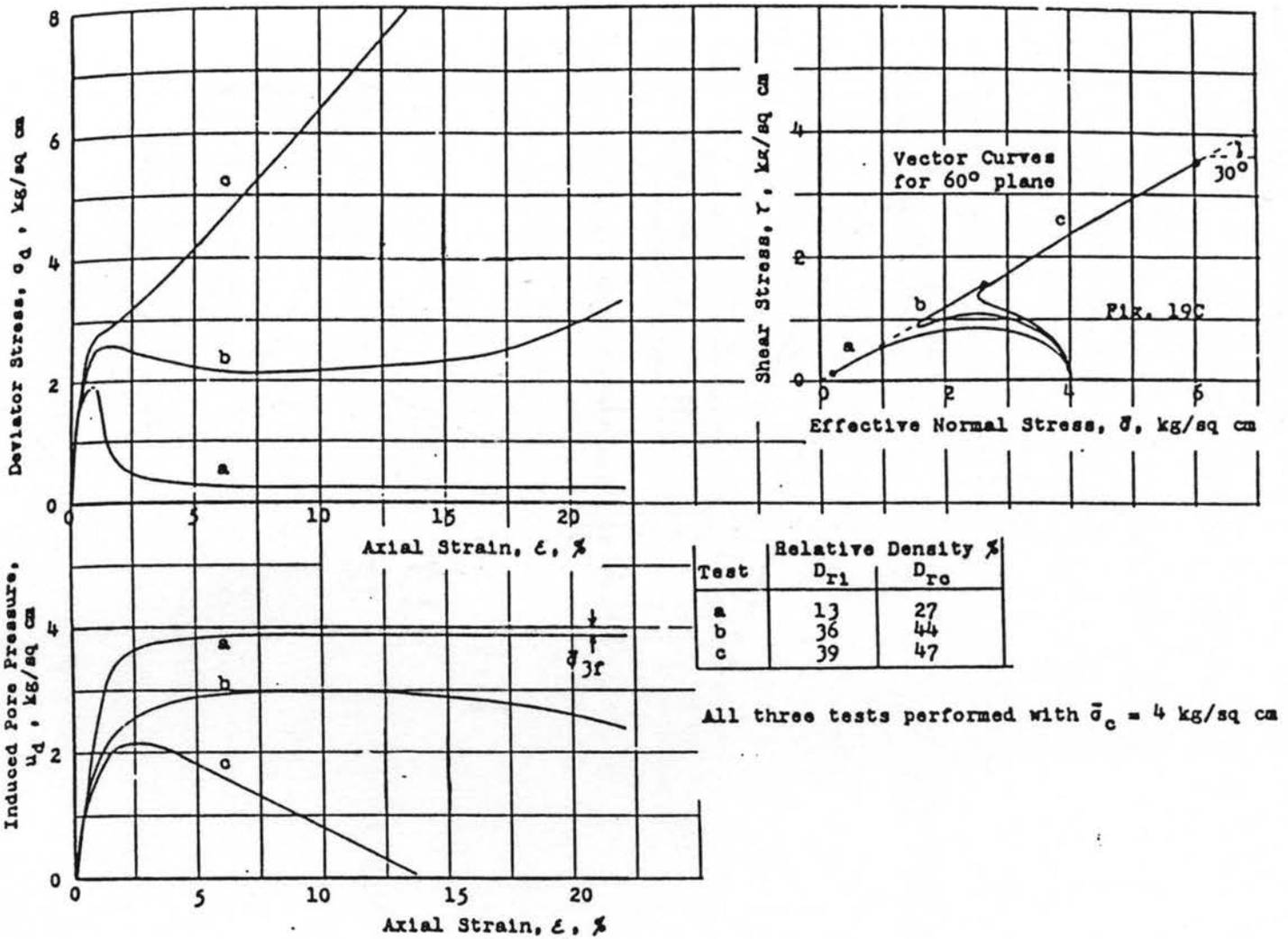

Figure 2.2 Example of Triaxial Test Results (Castro, 1969).

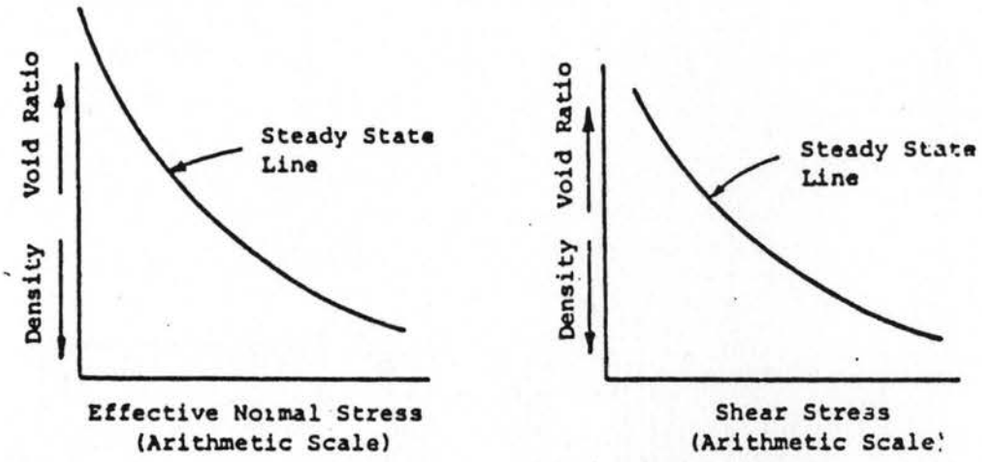

a) Steady State Lines in Arithmetic Plots

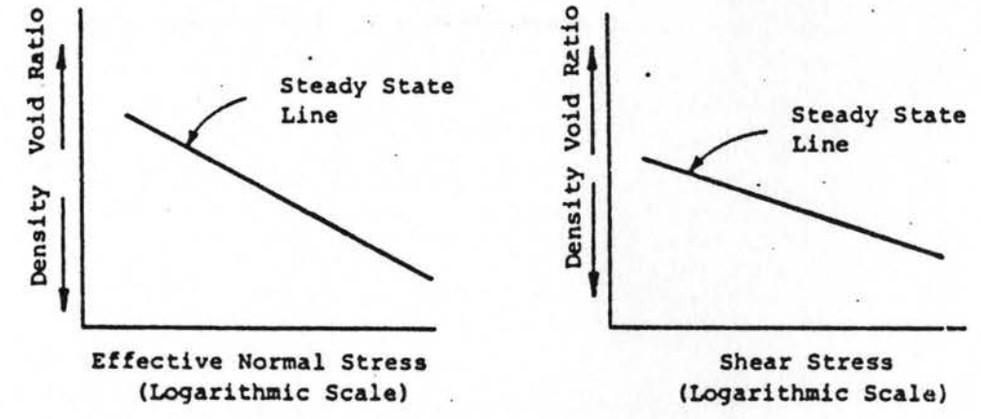

b) Steady State Lines in Semi-Logarithmic Plots

Figure 2.3 Examples of Steady State Line Plots (Scott, 1984).

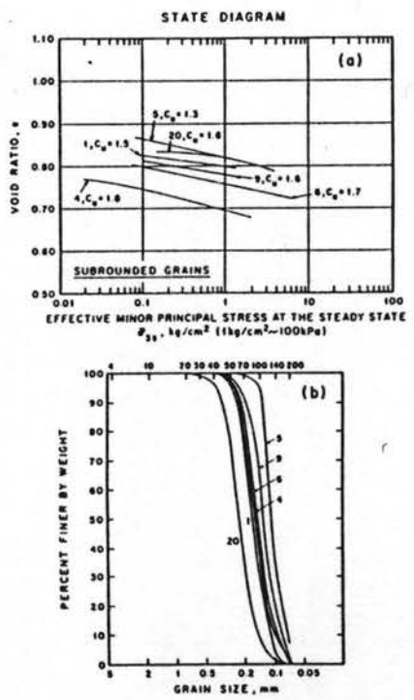

Steady-State Lines for Sands—Subrounded Grains (Castro, et al., 1982)

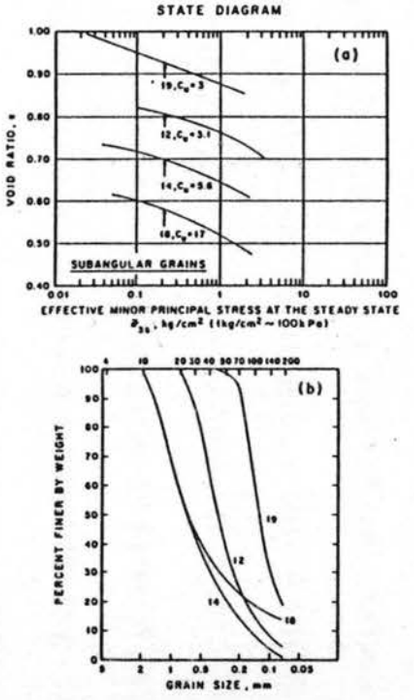

-Steady-State Lines for Sands—Subangular Grains (Castro, et al., 1982)

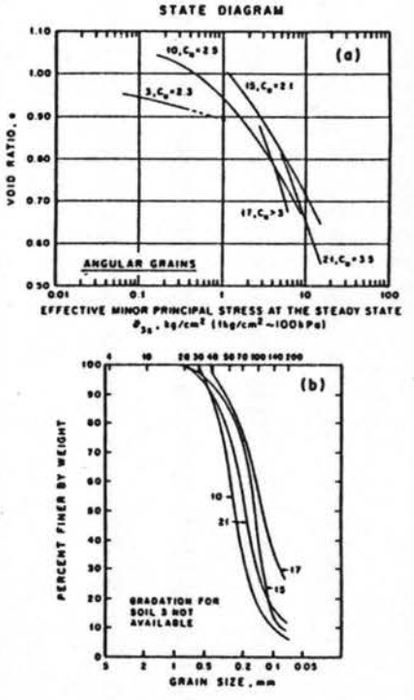

.—Steady-State Lines for Sands—Angular Grains (Castro, et al., 1982)

Figure 2.4 Steady State Lines For Subrounded, Subangular and Angular Sands

(Poulos et al., 1985)

3. Steady State Deformation

Poulos (1971, 1981, 1988) noted that there is a special structure of soil that is achieved after all of the grains have reached an orientation termed "steady state condition." When a sand is strained at the "steady state condition", there is no change in shear stress and/or volume. Poulos termed this "Steady State of Deformation", which he defined as:

> "The steady state deformation for any mass of particles is that state in which the mass is continuously deforming at a constant volume, constant normal effective stress, constant shear stress, and constant velocity. The steady state of deformation is achieved only after all orientation has reached a statistically steady state condition and after all particle breakage, if any is completed, so that the shear stress needed to continue deformation and velocity of deformation remain constant" (Poulos, 1981).

During liquefaction of a flow type failure of a saturated sand, the original soil particle structure is completely destroyed and rearranged into what Casagrande (1975) termed "flow structure". He had observed this during undrained triaxial tests where the grains oriented such that the shear stress for continued deformation reaches a constant value. Steady state deformation occurs in clays during drained shear tests and is commonly called the "residual" shear strength which is reached at large strains. There are three important points to steady state of deformation which relate to the understanding of liquefaction:

- The steady state of deformation is not a static state of a soil, but rather occurs only during continuous deformation at constant velocity (Poulos, 1971).
- Steady state deformation is a special soil structure which allows continuous straining of the soil with minimum shearing resistance and no tendency for loss of shear stress or volume changes (Castro, 1969; Casagrande, 1975; Poulos, 1981).
- The steady state deformation can only be achieved after all grain reorientation and particle breakage, if any, is completed. Large strains are normally required to achieve this condition. (Poulos, 1971, 1981).

From laboratory triaxial tests it can be concluded that: (1) The stresses during steady state deformation are dependent only on the void ratio and are independent of stress history. (2) During steady state condition the mobilized friction angle is equal to the friction angle determined in drained tests at large strains on samples having contractive initial state (Castro et al., 1982a).

For steady state of deformation to occur the soil must have the following conditions:

- The soil's void ratio (e) and effective confining stress (σ'_3) point must be situated on the steady state line.
- The soil's void ratio (e) and shear stress (τ) point must also be situated on the steady state line.
- There must be sufficient strain so that the soil continues to strain without changes in stress, volume, or velocity (Castro et al., 1982).

4. Steady State Strength

The stress response of a loose saturated cohesionless soil undergoing undrained shearing indicates there are unique soil strengths. The peak shear strength occurs during the initial shear strains and the steady state shear strength transpires at large shear strains (i.e. during the steady state deformation). The steady state strength controls the ultimate stability of a permanent structure. The peak shear strength is a temporary condition. If the initial stresses produced by the triggering mechanism are greater than the steady state shear strength there is a potential for liquefaction to occur. However, if the steady state shear strength is less than the initial stresses then liquefaction will not occur. When static loadings are the triggering mechanism, the initial (driving) stresses need to be near or at the peak shear strength for liquefaction to occur. When dynamic loadings are the triggering mechanism, large strains are required for liquefaction to occur. Liquefaction due to different types of loading is illustrated on Figure 2.5.

The steady state strength is unique for a given soil. It can be measured by tests which can shear a specimen at very large strains, i.e. clean sands - triaxial tests; and finer grained soils - shear vane test or rotation shear test. The steady state strength is independent of structure, initial void ratio, effective stress, or method of loading (Poulos, 1988).

5. Steady State and Liquefaction

Liquefaction occurs when the shear resistance of a mass of a loose saturated sand decreases when subjected to undrained monotonic, cyclic, or shock loading. The loss in shear resistance during loading is due to the conversion in the structure from a drained state to an essentially undrained state. At this point, the shear resistance of the soil mass is less than the induced driving shear stresses, commencing in liquefaction. The soil mass undergoes very large unidirectional shear strains (flows) until the shear stresses acting on the soil mass decrease to the steady state strength. The following sequence of events must occur to liquefy a sand deposit:

- The sand state is situated above the steady state line and is fully a saturated.
- Driving shear stresses develop under drained conditions, until they are greater than the undrained steady state shear strength, but are still lower than the drained shear strength.
- A trigger mechanism (e.g. an earthquake, an increase in dead load, a change in seepage pressure, or blasting) must occur so that the sand deposit is converted from a drained state to a practically undrained state.
- As the sand deposit undergoes deformation, the shear resistance is reduced from the drained shear strength to the significantly lower undrained shear strength.
- Consequently, large strains occur (flow), which continues until the driving shear stresses are reduced to the undrained steady state strength (S_{us}). (Castro et al., 1982a)

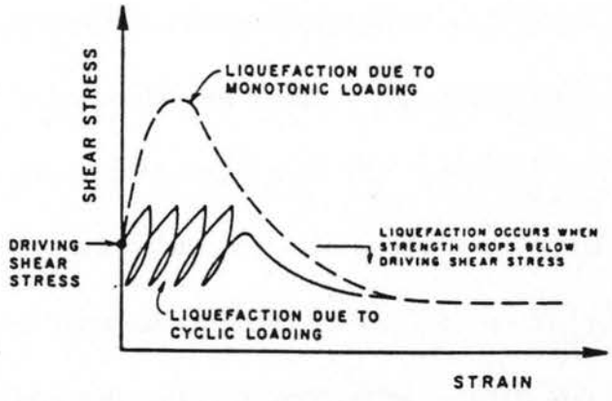

-Liquefaction Due to Monotonic or Cyclic Loading (Schematic)

Figure 2.5 Liquefaction Due To Different Types of Loadings (Poulus et al., 1985).

C. Methods of Determining the Steady State Line

1. Direct Shear Tests

Taylor (1939) suggested that several consolidated drained (CD) direct shear tests be performed to determine the steady state line. Since the normal stress does not change during the test, dense and loose sand's void ratios would shift to the steady state void ratio during shearing of the sample. To determine one point on the steady state line, several tests were conducted at the same initial void ratio with various normal stresses. The changes in void ratio at the peak shear stress during the CD direct shear tests were plotted versus the confining stress. The point of the linear regression of the change in void ratio versus normal stress plot at which no change in void ratio occurred was determined to be the steady state point. An example is shown in Figure 2.6. This procedure was repeated for several initial void ratios to develop the steady state line.

Taylor (1939) also conducted a series of CD triaxial tests to determine the steady state line. Several tests were performed at the same initial void ratio, with the confining stress varying. The change in void ratio at the peak deviator stress was plotted versus the confining stress. Using the same procedure as used with the direct shear tests, the steady state line was developed. Taylor found relatively small differences between CD direct shear tests and CD triaxial tests. However, he reasoned that since liquefaction is associated with shearing at constant volume, CD triaxial tests would be a more rational procedure.

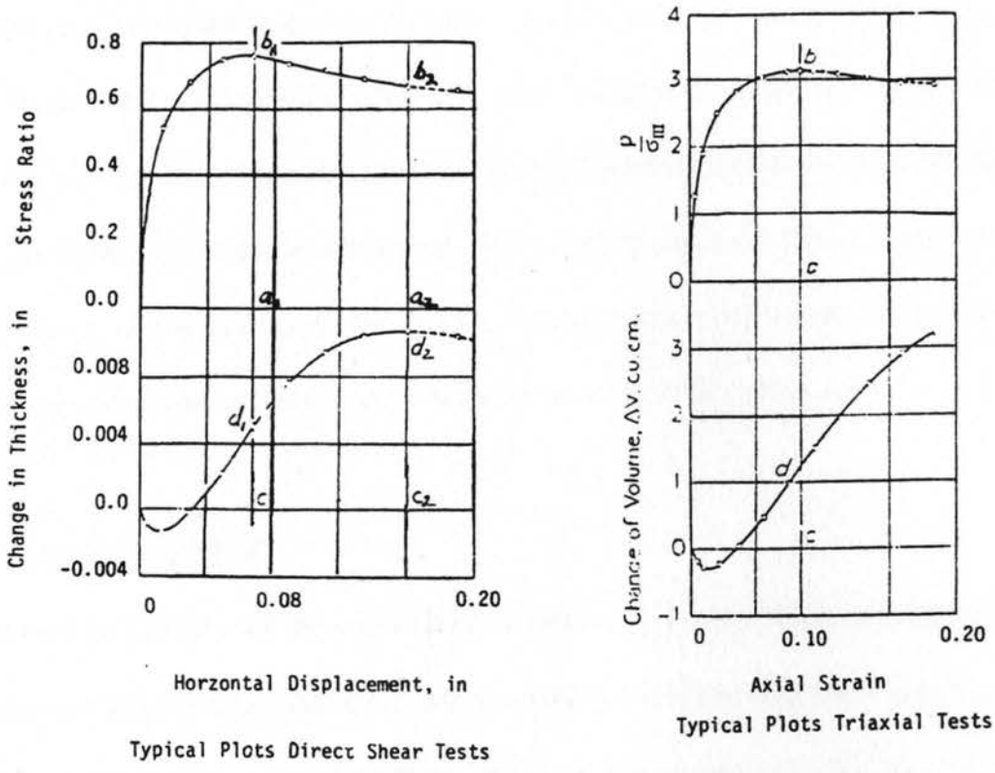

Figure 2.6 Typical Plots For Direct Shear and Triaxial Tests (Taylor, 1939).

Void ratio and displacement for a direct shear test are shown in Figure 2.7. Curve L depicts a loose sand, Curve D depicts a dense sand and Curve M depicts a sand at the steady state condition. As the specimens were sheared, the loose sand contracted to the same void ratio as sand M, while the dense sand to dilated the same void ratio as sand M. Sand M does not change its volume during the test. Samples were tested at a constant void ratio with varying normal stresses until the steady state condition was reached. By varying the void ratios the steady state line was developed. Scott (1989) stated that the redistribution of the void ratios is significant during shearing and stresses imposed at the boundaries are not fully understood.

2. Simple Shear Test

Roscoe (1953) designed the simple shear apparatus to apply uniform two dimensional shear strain while permitting measurement of volume change during shear on a rectangular sample. The simple shear apparatus is similar to a direct shear box, except that one pair of platens is allowed to rotate so that the sample deforms uniformly. Roscoe (1958) compared drained and undrained triaxial tests to the simple shear apparatus using steel balls, glass beads, and sand. Tests were conducted with initial void ratio either above or below the steady state line. The sample was sheared until a constant state was reached. Steel balls reached a critical void ratio with insufficient scattering of the data. Glass bead results were similar to the steel balls but with some scattering in the data. The sand results had a higher scattering of the data than did the glass beads or steel balls. The scatter was particularly higher at greater normal stresses. This was attributed to the breaking of the particles during shearing.

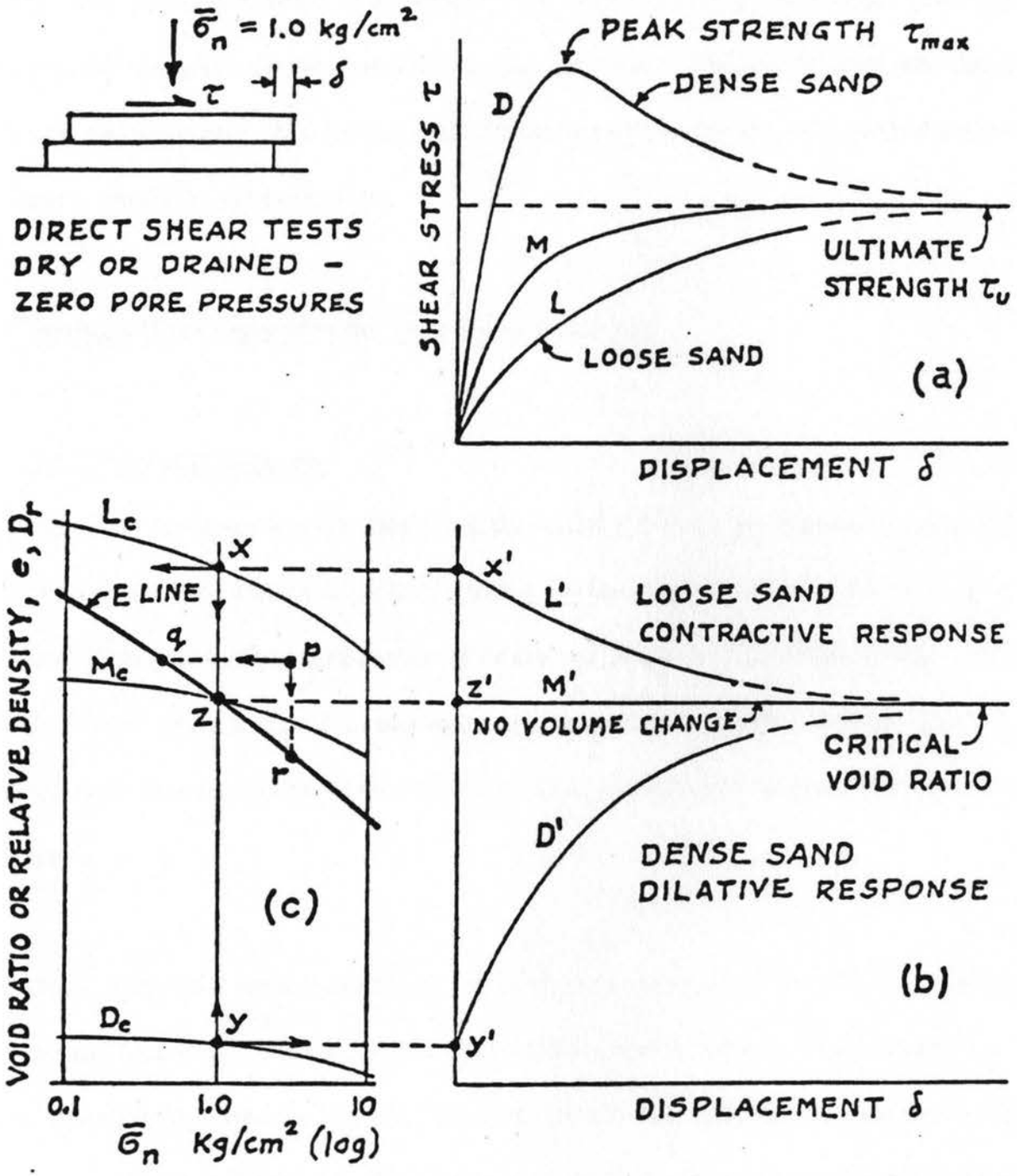

Figure 2.7 Result of Direct Shear Test and Steady State Line (Casagrande,1975).

3. Triaxial Tests

There have been several methods of triaxial testing suggested for evaluating the steady state condition of a soil (Casagrande and Watson, 1938; Taylor, 1939; Castro, 1969; and Castro et al., 1982). The procedure which is accepted today is outlined in Poulos et al., (1985) using isotropically consolidated, monotonically loaded, undrained (CU) triaxial tests with porewater pressure measurements. The triaxial tests are performed on several recompacted contractive samples to obtain the steady state line.

D. Previous Work Done with the Vane Shear Apparatus

1. The Vane Shear Apparatus

The vane shear apparatus was simultaneously developed in Sweden and Germany around 1928. It was not documented until the Swedish Geotechnical Institute in 1947 used the vane on several projects. This data was consolidated into a report by Cadling and Odenstad (1950). Skempton (1948) independently designed a vane borer and also used it for shallow testing. The vane test permits rapid determinations of the undrained shear strength of fine grain soils under in situ conditions.

The shape of the vane shear is cruciform and there are a variety of sizes. American Society for Testing and Materials Standard Specification ASTM D-2573 Standard Test Methods for Field Vane Shear Testing Cohesive Soil (ASTM, 1989) specifies the height of the vane to be twice the diameter as shown in Figure 2.8. To minimize disturbance effects during insertion, the blades should be beveled on the bottom and/or have a point at the bottom. The most common dimensions are summarized by Arman et al., (1975) in Table 2.1.

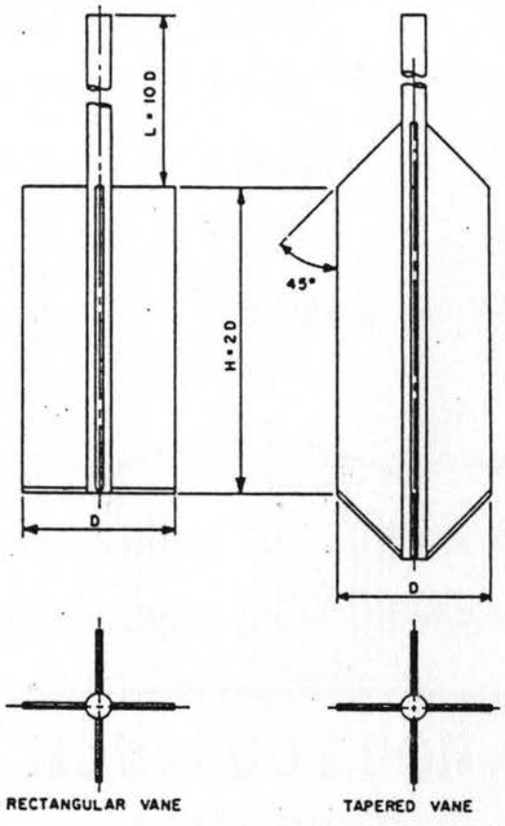

FIG. 1 Geometry of Field Vane

Figure 2.8 Vane Shear Apparatus From ASTM D 2573 (ASTM, 1989)

Table 2.1: Recommended Dimensions of Vane Shear Apparatus (ASTM D-2573)

Casing Size	Diameter in. (mm)	Height in. (mm)	Thickness of Blade in. (mm)	Diameter of Vane Rod in. (mm)
AX	1 1/2 (38.1)	3 (76.2)	1/16 (1.6)	1/2 (12.7)
BX	2 (50.8)	4 (101.6)	1/16 (1.6)	1/2 (12.7)
NX	2 1/2 (63.5)	5 (127.0)	1/8 (3.2)	1/2 (12.7)
4 in. (101.6 mm)	3 5/8 (92.1)	7 1/4 (184.1)	1/8 (3.2)	1/2(12.7)

The selection of a vane size is directly related to the consistency of the soil being tested (i.e. softer soils require a larger vane diameter). There have been investigations into the effects of the shear vane shape (Osterberg, 1956; Vickers, 1983; and Arman et al., 1975). The investigators agreed that the size of the vane is directly proportional to the amount of disturbance to the shearing zone. The ratio of the cross-sectional area of the vane to cross-sectional area of the shearing zone defines the Area Ratio. The Area Ratio is defined as:

$$\text{Area Ratio (\%)} = \frac{8t\,(D - d) + \pi d^2}{\pi D^2} \times 100 \qquad \text{Eq. 2.2}$$

where t is the thickness of the blade, d is the diameter of the vane rod, and D is the overall diameter of blades when rotated (Vickers, 1983). An area ratio ranging between 10% to 25% for vanes is recommended by Arman et al. (1975), and Vickers (1983) recommends an Area Ratio less than 12%.

The following assumptions are often used to calculate the undrained shear strength (S_{uv}).

- The soil is completely undrained.
- There is no disturbance of the soil during boring or installation of the vane.
- The remolded zone around the vane is very small.
- There is no progressive failure. The maximum applied torque overcomes the fully mobilized shear strength along failure surface.
- The soil mass has isotropic strength conditions.
- The distribution of shear strength around the cylindrical surface area and circular ends is uniform.

With the above assumptions, the torque (M) at failure can be expressed as a function of the undrained shear strength (S_{uv}) using Cadling's equation:

$$S_{uv} = \frac{M}{\pi D^2 \left(\frac{H}{2} + \frac{D}{6} \right)} \qquad \text{Eq. 2.3}$$

where H is the vane's height and D is the vane diameter.

When the diameter of the vane is equal to twice the vane's height, the strength can be determined by the following equation:

$$S_{uv} = \frac{6M}{7\pi D^3} \qquad \text{Eq. 2.4}$$

The torque, M, in Equation 2.3 and 2.4 is the torque applied to the vane. If shaft or bushing friction is present, then the applied torque must be corrected for torque induced by shaft and bushing friction (Cadling and Odenstad, 1950). The angular shear velocity (v) at the outside edge of the vane determines the angular shear rate. The angular shear rate has a significant influence on the measured shear strength of fine grained soils. Angular shear velocity (v) can be calculated by:

$$v = r\,\omega \qquad \text{Eq. 2.5}$$

where r is the blade radius and ω is the vane rotation rate in radians per time. Several studies have shown the undrained shear strength increased with angular shear velocity (Cadling and Odenstad, 1950; Perlow and Richards, 1977).

Blight (1968) proposed a method of testing which enables the vane shear to measure shear strength under fully drained conditions. When the vane shear performs a completely undrained test, the porewater pressure is effected by (1) the insertion of the vane shear to the depth of measurement, and (2) the rotation rate of the vane shear. In a drained test, full drainage must occur for both insertion and during rotation.

By using the following assumptions, a theoretical approach was derived.

- All induced porewater pressure is dissipated from the insertion of the vane before starting to shear the sample.
- During shearing, a sphere of influence is formed with a radius of "a" (Figure 2.9a). The excess porewater pressure is uniform within this sphere. The excess porewater pressure is proportional to the resistance of the vane blades, therefore also proportional to shear stress on the surface of the potential failure (Figure 2.9b).
- The torque increases uniformly with time until failure is reached as shown in Figure 2.9b. If completely undrained conditions could be maintained within the sphere of influence, the excess porewater pressure would rise uniformly to u_0 at failure (time t_f). When drainage is possible, the pressure rises to a value u_f ($<u_0$) at failure and thereafter declines as further drainage occurs.
- The porewater pressure on the surface of the sphere of influence remains equal to the hydrostatic porewater pressure at all times. This surface is thus assumed to represent a drainage surface.

Using the above stated assumptions, Blight (1968) developed the following analytical model

where U is the excess porewater dissipation.

$$U = 1 - \frac{1}{T}\left\{\frac{1}{8} + \frac{4}{\pi^3}\sum_{n=1}^{\infty}\frac{(-1)^n}{n^3}\sin\frac{n\pi}{2}\exp(-\pi^2 n^2 T)\right\} \qquad \text{Eq. 2.6}$$

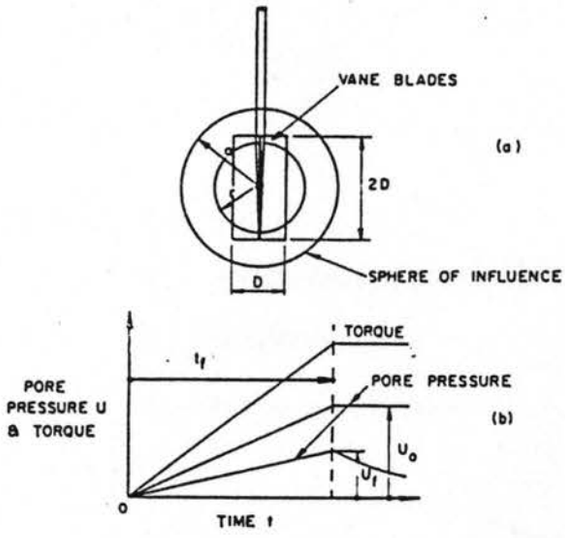

(a) Proportions of vane and sphere of influence. (b) Idealized pore pressure changes in vane test

Figure 2.9 The Vane's Sphere of Influence (Blight, 1968)

U will vary from 0% on a rapid vane test in which no drainage occurs (drained test), to 100% during a slow test which is fully drained (undrained test); T is a dimensionless time factor defined as:

$$T = \frac{C_v t_f}{a^2} \qquad \text{Eq. 2.7}$$

C_v - coefficient of consolidation

t_f - the test duration

a - sphere of influence

Blight (1968) assumed that the sphere of influence (a) was between one diameter (D) and 3/2 D. This model was developed for silt size particles but could be useful in determining strain rates for drained and undrained tests in coarse grain materials also.

The vane shear test has been limited to determining the undrained shear strength of fine grain soils due to the dilatant characteristics of coarse grain soils. Wilson's (1963) hypothesis was that negative porewater pressure would occur during shearing, which would result in higher than actual shear strength. Barros and Barros (1989) presented an analytical approach based on the solution for a thick-wall cylinder in a 3 dimensional stress field to evaluate the internal friction angle (ϕ). The internal friction can be expressed as:

$$\frac{M}{D^3 \sigma_v'} = \frac{\pi}{6} \left[\frac{3H}{D} \left[((f_\Delta f_V + 1) - \sin \phi') 1 \right] \text{TAN} \phi' \right] \qquad \text{Eq. 2.8}$$

where f_v is "poison factor" defined as:

$$f_v = \frac{1}{1+v} \qquad \text{Eq. 2.9}$$

v = Poison ratio

$f\Delta$ is the "expansion factor" defined as:

$$f\Delta = \frac{\Delta d\, E}{d\, \sigma'_v} \qquad \text{Eq.2.10}$$

σ'_v - Normal vertical effective stress
E - Young's modulus
Δd - Diameter of expansion
M - Torque
D - Vane diameter

The value of the internal friction angle can only be determined if Young's Modulus E, Poison's Ratio (v) and the diameter expansion of the failure surface are known.

2. Wilson's Vane

Wilson (1963) conducted an investigation into erroneous results using the shear vane in coarse-grained soils. The hypothesis for this study stated that vane tests in dilatant soils give erroneous values for the shear strength. This was based on the fact that negative porewater stresses induced during shear deformation would increase the effective stresses, resulting in apparently high values for the shear strength. His study included tests on clay, silt and sand. The shear strength was measured using Cadling's equation.

A Wykeham-Farrance laboratory vane tester with modifications made to a 19.0 mm (3/4 inch) diameter and 25.3 mm (1 inch) high laboratory vane was used in the investigation. The modifications to the vane involved, cutting a 19.0 mm (3/4 inch) slot in one of the 0.8 mm (1/32 inch) thick blades. The slot was attached to a 3.2 mm (0.0614 inch) O.D. hypodermic needle. To prevent the slot from being obstructed with soil particles, a No. 200 stainless steel mesh covered the opening. Pressure was measured with a Norwegian porewater pressure device (a type of null indicator). Some alterations were made so that rotation of the vane would not interfere with the measurement of shear strength and porewater pressure. Wilson's Vane is shown in Figure 2.10.

The Wykeham-Farrance laboratory vane apparatus was considered to be a stress-controlled machine with torque applied using torsion springs. The stress could not be applied at a predetermined rate as the angular strains of the vane blades in the soil affects the applied stress. After testing it was established that the tests were neither rigorously stress-controlled nor strain-controlled.

The sand tested was Zircon sand (Cu = 1.4, D_{10}= 0.06 mm, e = 0.595) which was described as a medium-fine sand with well rounded grains and "characteristics of a dilatant soil". Zircon sand was used by foundries and test specimens could be built having constant void ratios. There was no mention of how specimens were prepared or saturated.

Tests were conducted with various speeds, sizes of container, and rigid or non-rigid boundaries. The diameter ratio (the ratio of diameter of the container to the diameter of the vane) ranged from 5.3 to 13.3, which may explain the side boundary effects observed. Another variable in the tests was the depth of insertion of the vane. As would be expected with an increase of depth, shear strength also increased.

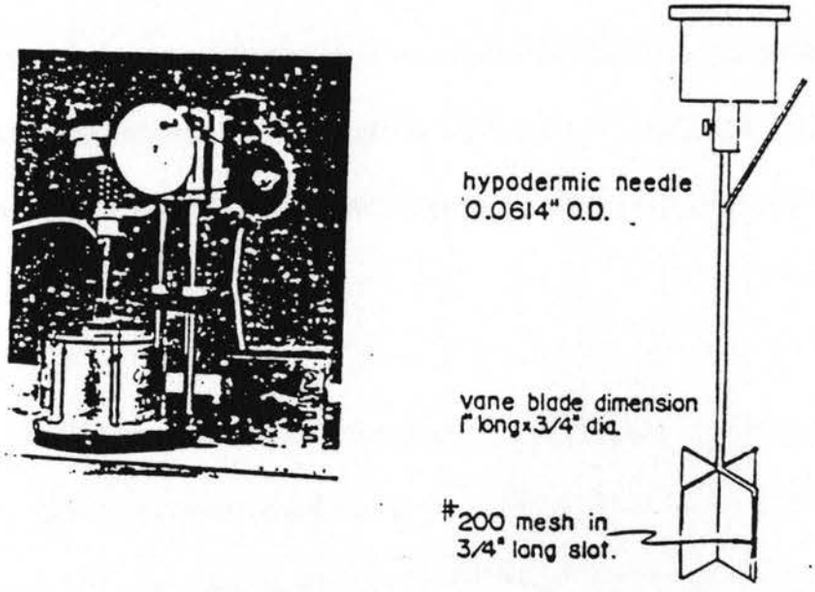

Variable speed type.
Laboratory Vane Apparatus.

Figure 2.10 Laboratory Vane Apparatus (Wilson, 1963).

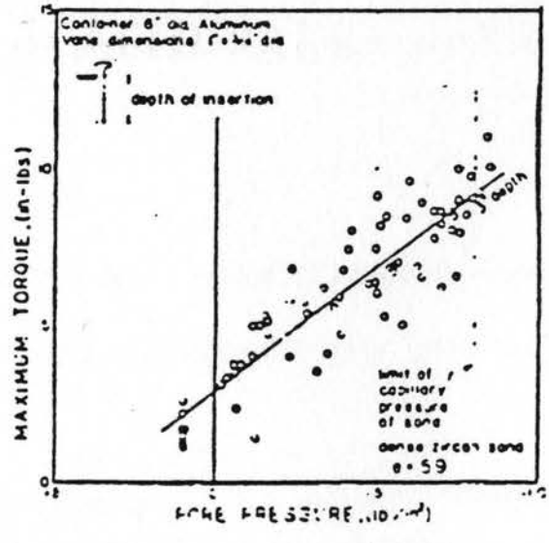

(b) MAXIMUM TORQUE vs PORE PRESSURE. AT CONSTANT DEPTH

-Vane Tests in Sand.

Figure 2.11 Vane Tests in Sand (Wilson, 1963).

The vane speeds were varied, and found to be independent of the measured value of torque. It was observed that a straight line relationship exists through both the negative and positive porewater pressure response when plotted versus maximum torque as shown in Figure 2.11. It was noted that the calculated shear strength using Cadling's equation was greater than the shear strength measured in triaxial tests, therefore supporting Wilson's hypothesis. (Wilson, 1963).

3. GEI VANE

Castro et al., (1982b) was the first to attempt using a vane shear device to evaluate liquefaction potential. The vane shear device results would be interpreted in terms of the steady state concept of liquefaction. The vane design was modeled after a self-boring shear vane, developed in France. The main consideration in using this type of vane was minimum disturbance during insertion and rotation. The vane design had eight (8) short fins mounted on a cylindrical shaft. The diameter of the vane was 3.81 cm and the height was 6.5 cm with a diameter ratio of 7.2. At the center of the vane was a shaft with two pressure ports. The pressure ports connected to a duct at the center of the shaft which led to the outside of the cell, where a porewater pressure transducer was mounted.

Besides measuring the porewater pressure, torque and angular displacements were measured. Torque, displacement, and porewater pressure were recorded using a strip chart recorder.

The vane shear device was tested using a 27.3 cm diameter aluminum K_oConsolidation cell. Vertical consolidation pressure was applied by fluid pressure on a rubber membrane at the bottom of the cell. The cell's rigid sides prevented lateral deformation which maintained a K_o condition. The shear vane was fixed into a set position at the center of the cell and the sample was built around it, at constant density. The vane and K_o Consolidation cell are shown on Figure 2.12.

The two sands used in the study were Banding sand No. 6 and mine tailing sand for which the steady state lines and physical properties were determined in previous research (Castro et al., 1982b). Samples for tests were compacted in layers using a spring-loaded static tamper. The number of layers varied with the target density for that test. The samples were saturated using a backpressure technique, and the Skempton "B" parameter was used to determine the degree of saturation. A sample was assumed to be saturated when the B-parameter was greater than 0.9. The samples were consolidated to an effective vertical stress (σ'_v) of 98.1 kPa. Volume changes were measured during consolidation by monitoring both the volume changes of water entering the bottom of the membrane to supply pressure to the sample and water exiting the sample due to the decrease in pore volume. Both methods were in general agreement with each other.

The vane was rotated by hand at approximate constant velocity. Rotation was continued until the torque reached a constant value (steady state of deformation). The tests were performed under undrained and drained conditions. Additional tests were conducted after the initial test on each sample. The results of these tests varied from the initial test.

The results of the drained tests are plotted in Figure 2.13 and both measured peak and steady state shear stresses for the initial tests are recorded. Also shown are two reference lines: (1) the steady state void ratio, e_{ss}, at the initial effective normal stress on the failure surface (σ'_f), and (2) the drained steady state shear strength (τ_{ss}). It was assumed that $K_o = 0.5$, therefore since all of the tests were conducted with the same vertical consolidation (98.1 kPa), the horizontal effective normal stress after consolidation was 49.0 kPa. The value of the reference drained steady state shear strength at the initial effective normal stress was estimated from the effective stress friction angle obtained from CU triaxial tests. Figures 2.15 and 2.16 show typical shear strength on the failure surface for a dilative and contractive sample, respectively.

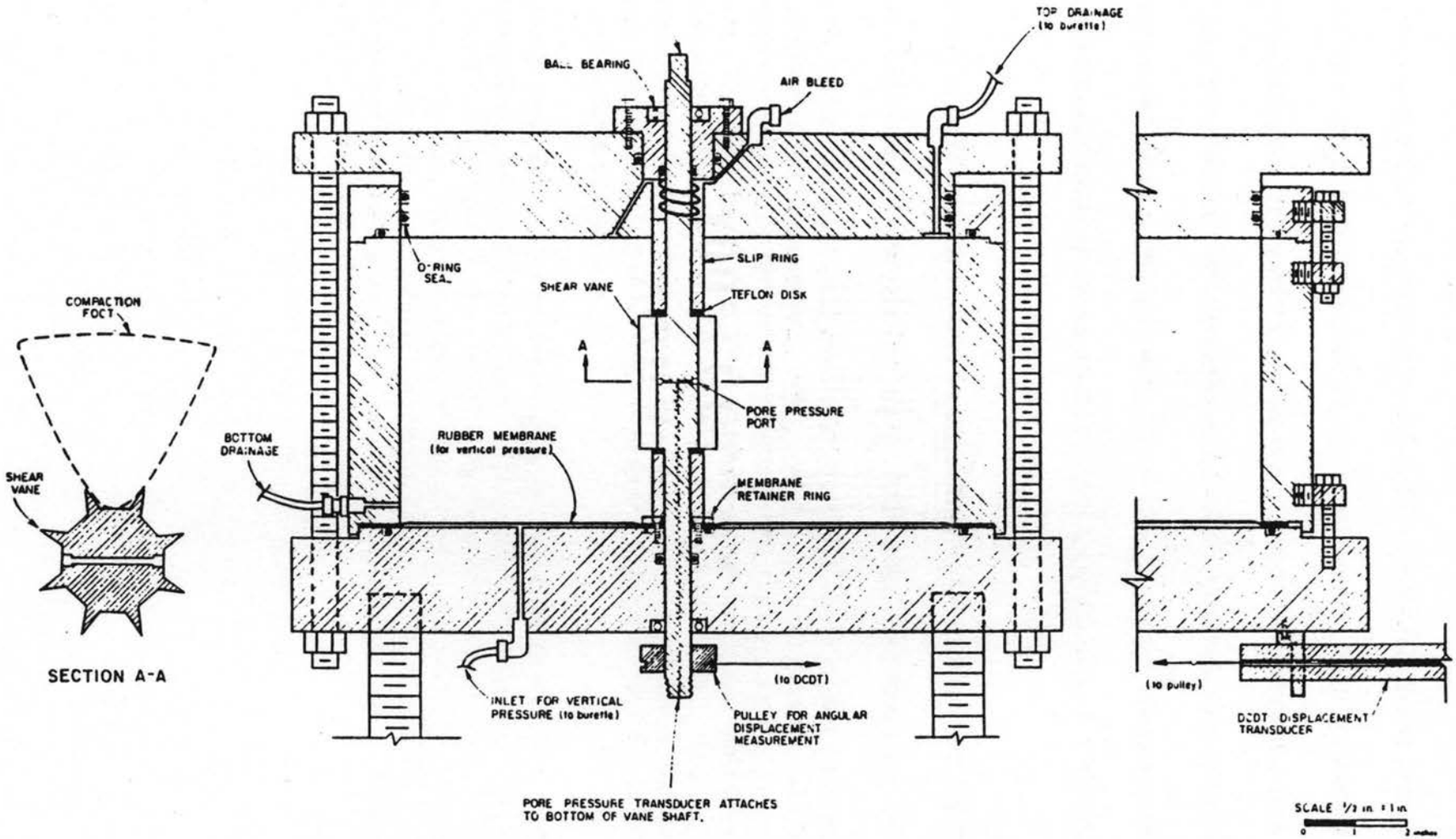

Figure 2.12 G.E.I.'s Vane and K_o Consolidation Cell (Castro et al., 1982b).

A general trend was observed. At high void ratios the measured shear stresses were less than the reference steady state shear stresses. The measured shear stresses would abruptly increase at void ratios lower than the reference void ratio. To explain this, the test results were presented in terms of the state diagram. The results from the vane tests converted to steady state points by (1) the effective normal stress on the failure surface at steady state was determined from using the CU triaxial tests, effective stress friction angle along with the measured steady state shear stress, and (2) it was assumed that the void ratio along the failure zone, while continuously shearing the vane (at steady state deformation) was the same void ratio determined from CU triaxial tests.

The steady state plots illustrated the complex interaction which occurred with effective stress changes in the failure zone. The results were interpreted in steady state philosophy as:

- "When the initial state of the soil is above the steady state line (i.e. loose), the soil in a thin shear zone around the vane contracts. As the soil in the shear zone contracts, a reduction in the horizontal effective stress in the shear zone occurs due to arching in the surrounding soil. (i.e., Test No. 5 in Figure 2.13). As a result of this effective stress reduction, the drained steady state shear strength (measured in the vane shear test) is less than the reference steady state shear strength (i.e. as measured in a drained direct shear test without arching). Thus, the steady state shear stress measured in the vane shear test plots below the τ_{ss} reference in Figure 2.14.

- Conversely, when the initial state of the soil is below the steady state line, the soil in the shear zone dilates, resulting in an increase in the effective normal stress in the shear zone (i.e., Test No. 4 in Figure 2.13). In this case, the drained steady state shear strength measured in the vane shear test is greater than the reference drained steady state shear strength (i.e., as measured in a direct shear test without this "reverse" arching). Thus, the steady state shear stress measured in the vane shear test plots above the τ_{ss} reference line in Figure 2.14." (Castro et al., 1982b).

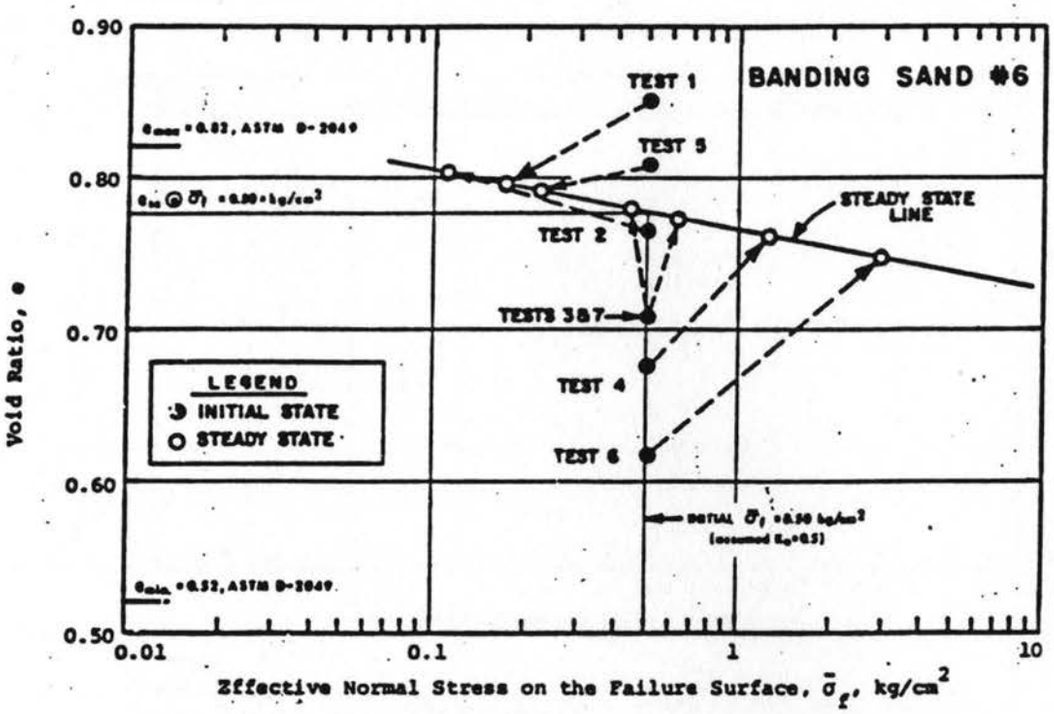

Figure 2.13 Steady State Plot For Drained Vane Tests (Castro et al., 1982b).

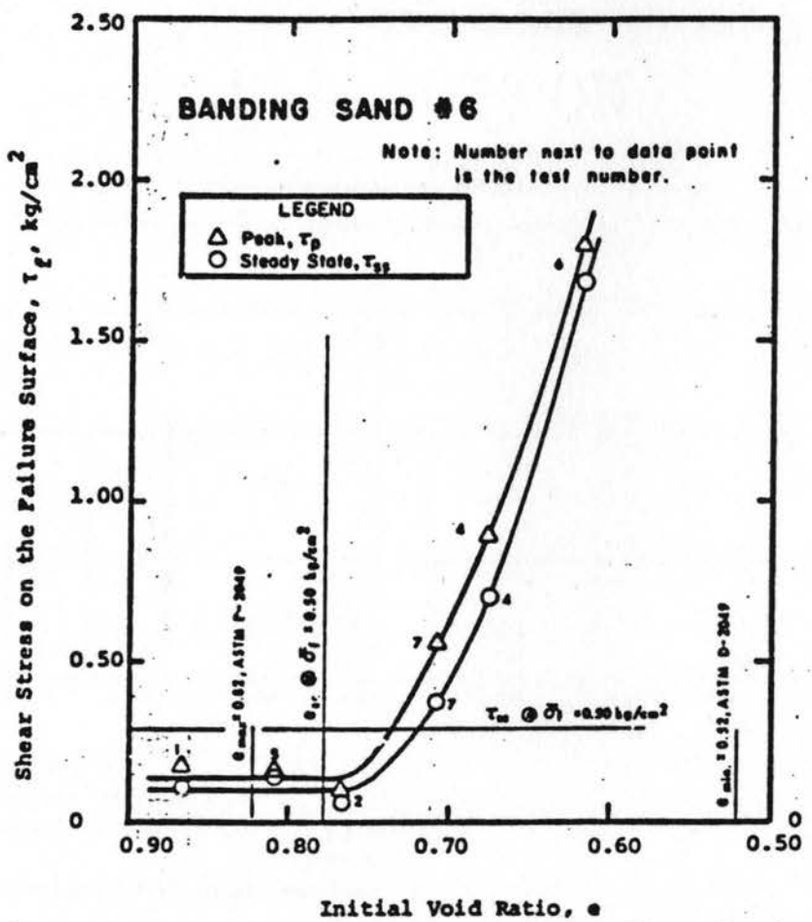

Figure 2.14 Summary of Shear Stress Results From Drained Vane Tests (Castro et al., 1982b).

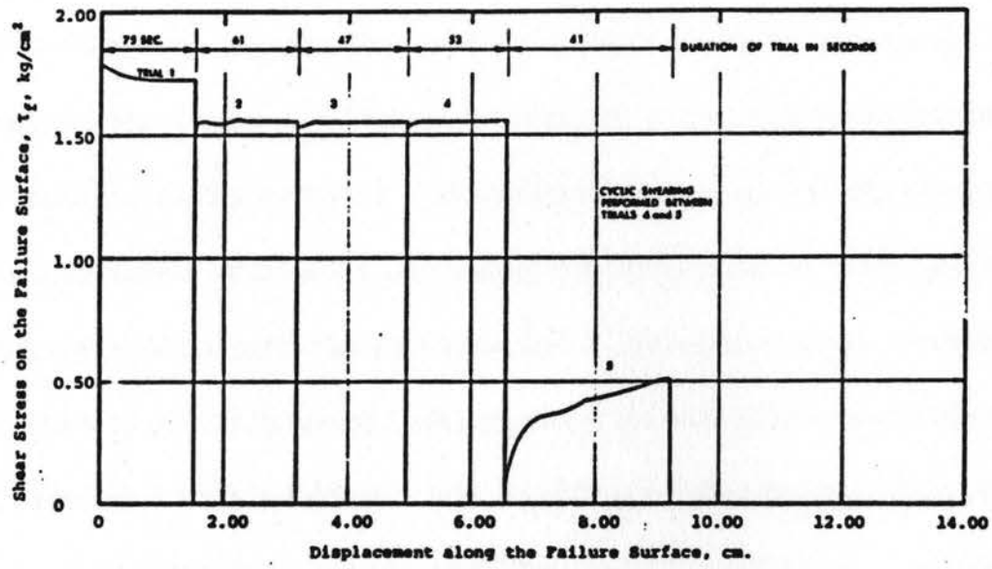

Test No. 6

Material: Banding Sand #6

State after Consolidation: $\bar{\sigma}_v$ = 1.00 kg/cm^2

e_c = 0.618

Method of Loading: Drained Vane Shear

Figure 2.15 Typical Dilative Test From Castro et al., (1982b).

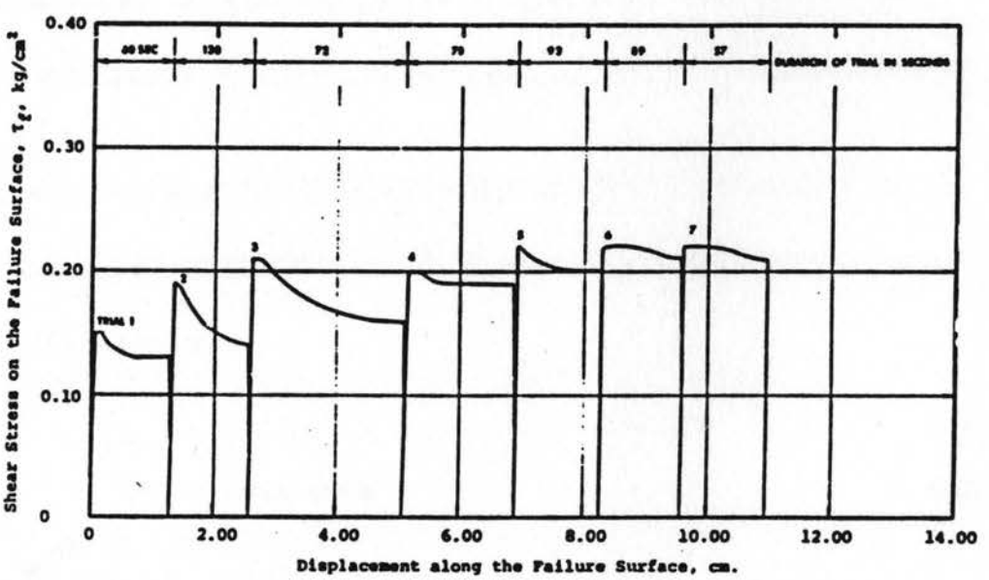

Test No. 5

Material: Banding Sand #6

State after Consolidation: $\bar{\sigma}_v$ = 1.00 kg/cm^2

e_c = 0.808

Method of Loading: Drained Vane Shear

Figure 2.16 Typical Contractive Test From Castro et al., (1982b).

It was also observed that samples with an initial state slightly below the steady state underwent a decrease in effective normal stress at the start of the shearing. With continued strain the soil then dilated and there was an unloading and loading cycle within the shear zone. Two possible explanations were offered: (1) Dilative soils generally undergo a slight initial contraction at the start of shear deformation which would result in this initial decrease in effective normal stress. If inelastic deformation occurs in the surrounding soil during shearing, there must be dilation past the initial void ratio for there to be a net increase in effective normal stress. A weakly dilative soil (initial state very close to the steady state line) would not recover from the initial contraction, and would experience a net reduction in effective normal stress due to arching effect. (2) The reference steady state determined by triaxial tests could be positioned too high due to strain limitation of the triaxial test. This is discussed in more detail in Castro et al., (1982b).

Castro et al., (1982b) concluded:

- That undrained vane shear tests were not practical due to rapid dissipation of the shear-induced porewater pressure.
- However, it might be possible to measure porewater pressure changes if the transducer was located closer to the shear zone.
- The device could be used in evaluating the susceptibility to liquefaction using drained tests.

The liquefaction potential could be determined by comparing the peak shear stress (τ_p) measured by the vane to a reference drained steady state shear stress τ_{ss} at corresponding to zero change in effective normal stress.

$$\tau_{ss} = \sigma_f' \tan \phi' \qquad \text{Eq. 2.11}$$

Effective normal stress on the failure surface (σ_f') is an estimate from analysis of the in situ stresses. Using $K_o = 1$ for a normally consolidated deposit on level ground is reasonable. The friction angle must be estimated or determined by other tests (e.g. $\phi' = 30°$ to $35°$). If the

measured steady state shear stress (τ_p) by the vane is lower than the reference shear stress τ_{ss}, the initial state lies above the steady state line, then material is susceptible to liquefaction. If the measured steady state shear stress is greater than the reference shear stress τ_{ss}, the initial state lies below the steady state line, then liquefaction is not a problem. There is some indication that this method is conservative. (Castro et al. 1982b).

E. Laboratory Evaluation of In Situ Testing Methods

To better understand the effects of soil type, normal and vertical stress on in situ equipment (i.e. piezocones, pressuremeters, vanes, etc.) under controlled conditions are required to use laboratory test calibration chambers. These chambers usually consist of steel cylindrical cells where porewater, and confining stresses can be controlled. Such calibration chambers have been developed by Bunnell (1978); Woods and Henke (1981); Bellotti et al., (1982), A1-Mukhtar et al., (1988).

Samples prepared within calibration chambers are usually placed at a predetermined density by either an undercompaction methods or freefalling a constant distance through defusers. Samples are saturated using a combination of vacuum, carbon dioxide (CO_2), and back pressure. (Bellotti et al., 1982 and 1988; and Bunnell 1978). An evaluation of calibration chambers and possible sources of error include density determination, the non-uniformity of stresses due to arching, chamber size and boundary effects was described by Been et al. (1988).

F. In Situ Tests for Determining Liquefaction Potential

Several methods have been used to determine liquefaction potential in place. These methods include Standard Penetration Test (SPT), and Cone Penetration Tests (CPT), and are discussed in more detail below. There is a need to develop in situ evaluation of liquefaction potential to avoid the affects of sample disturbance and cost.

1. Standard Penetration Test (SPT)

The most common in situ test used in evaluating soils for liquefaction is the SPT test. Various studies have shown large variability in results from this standardized test. The test measures the number of blows required to drive a standard split-spoon sampler O.D. = 5.08 cm (2.00 inches) and I.D. = 3.45 cm (1.375 inches) using a 63kg (140 pound) hammer freefalling a distance of 76.2 cm (30 inches). Actual energy delivered to the drill rods may vary between 40% to 90% of the theoretical energy of 158 N-m (4200 in-lbs) for this system. This variation is caused by a combination (Seed 1985, 1987) of several factors including:

1) Type of hammer
2) The number of turns of the rope around the cathead
3) Length and type of drill rods
4) The use of drilling mud versus hollow stem augers
5) Use of non-standard sampling tubes or inserts
6) Depth of measurement (effective stress)
7) The depth range over which the penetration resistance is measured (0.0m to 0.3m or 0.15m to 0.45m) Robertson et al., (1982).

Therefore, SPT test results must be "corrected" or standardized with other investigations. Seed (1985) proposed a new standard based on standardized equipment and procedures indicated in Table 2.2.

Table 2.2: Recommended Standardized SPT Procedures (Seed, 1985)

Sampler:	Std. sampler with: (a) O.D. 5.08 cm (2.00 inches) and (b) I.D. = 3.492 cm (1.375 inches) (constant - i.e. no room for liners in barrel).
Drill Rods:	A or AW for depths less than 15.2 meters (50 feet) N or NW for depths 15.2 meters (50 feet) or greater
Energy Delivered to Sampler:	284.7 N-m (2520 in-lbs.) (60% of theoretical freefall maximum)
Blowcount Rate:	30 to 40 blows per minute
Penetration Resistance:	The number of blows (N) to advance the sampler from 15.2 to 45.72 cm (6 to 18 inches).

The standardized penetration resistance N_{60} is defined as the number of blows to drive the standard sampler using 60% of the theoretical "freefall" energy (284.7 N-m) for recommended standardized SPT procedures. For other procedures the following correction to the data is required to obtain the standardized N_{60} value.

$$N_{60} = N \times \frac{(ER)}{60\%} \qquad \text{Eq. 2.12}$$

The energy ratio (ER) is the efficiency or theoretical freefall energy delivered by the hammer system. This can be measured using a pile analyzer or estimated using Table 2.3.

Table 2.3 - Summary of Energy Ratios for SPT Procedures (Seed, 1985)

Country	Hammer Type	Hammer Release	Estimated Rod Energy (%)	Correction Factor for 60% Rod Energy
Japan[a]	Donut	Freefall	78	78/60 = 1.30
	Donut[b]	Rope and pulley with special throw release	67	67/60 = 1.12
United States	Safety[b]	Rope and pulley	60	60/60 = 1.00
	Donut	Rope and pulley	45	45/60 = 0.75
Argentina	Donut[b]	Rope and pulley	45	45/60 = 0.75
China	Donut[b]	Freefall[c]	60	60/60 = 1.00
	Donut	Rope and pulley	50	50/60 = 0.83

[a]Japanese SPT results have additional corrections for borehole diameter and frequency effects.

[b]Prevalent method in this country today

[c]Pilcon type hammers develop an energy ratio of about 60%.

In addition to standardized N_{60} values from equipment and procedures a correction must be made to account for effective overburden stress. To standardize for effective overburden stress, N_{60} values are referenced to a equivalent penetration resistance having a hypothetical overburden stress of 98.1 kPa (1 ton/sq ft). The corrected penetration resistance $(N_1)_{60}$ can be computed using:

$$(N_1)_{60} = N_{60} \times C_N \qquad \text{Eq. 2.13}$$

C_N is a correction coefficient for effective overburden pressure. $(N_1)_{60}$ is then compared to the cyclic stress ratio (τ_{av}) which is the ratio of average horizontal shear stress to effective overburden stress which is developed using cyclic triaxial tests. Based on field performance Seed (1985) suggests three ranges of $(N_1)_{60}$ Potential Damage from liquefaction (Seed, 1990 and Seed et al., 1985).

Table 2.4: SPT and Potential Liquefaction Damage (Seed, 1985)

$(N_1)_{60}$	Potential Damage
0-20	High
20-30	Intermediate
>30	No significant damage

This method is qualitative due to inherent limitations of the SPT. These limitations include lack of repeatability, insensitivity to layering and unknown dynamic mechanisms (Scott, 1989).

2. Cone Penetration Tests (CPT)

The Cone Penetration Test (CPT) has advantages over the SPT that include repeatability and standardization. With the development of the electric cone, porewater pressure measurement can be obtained along with penetration resistance (q_c) and sleeve friction (f_s). CPT results can be correlated to SPT and liquefaction potential determined in terms of cyclic stress ratios (Robertson and Campanella, 1985). However, in addition to sharing some of the uncertainties of SPT correlation, the CPT is also limited by:

- Limited field correlation with liquefaction,
- No sample retrieved for additional laboratory testing,
- Unreliability in coarse grained soils.

3. Piezocone Evaluation

A standard or electric CPT equipped for measuring porewater pressure (piezocone) response during exploration has been used to evaluate liquefaction potential. Researchers have noted positive and negative porewater pressure responses during laboratory testing for loose and dense sands. However, in field tests the porewater pressure responses in both contractive and dilative soils have been less than the predicted. (Schmertmann, 1978 and Campanella et al., 1983). Further study of the complex contractive behavior due to cavity expansion and normal stresses at the tip on the porewater pressure response is required (Castro et al., 1982b). Other factors that influence porewater response are the location of the pressure transducer to measure porewater pressure response (Robertson, 1986), permeability (Castro et al., 1982b), and penetration rate (Canou et al., 1988). Evaluation of liquefaction potential is currently restricted to estimates of drainage, equilibrium groundwater conditions, and soil profiling. The evaluation by the piezocone is qualitative at this time (Scott, 1989).

4. Other Methods for Evaluation of Liquefaction Potential

Other methods used to evaluate liquefaction include flat plate dilatometer, and Geophysical methods. The flat plate dilatometer has been used with limited success by Marchetti (1982) and Robertson and Campanella (1985) for evaluating liquefaction potential. The interpretations have not been field tested and only used in clean sands. Geophysical testing using shear wave velocity of soil has been correlated with the potential for porewater pressure generation by Dobry et al., (1981). The potential for generating increased porewater pressure may not be a direct indication of liquefaction potentials since cyclic triaxial tests have shown that dense sands, which are not prone to liquefaction may generate increased porewater pressure (Castro et al., 1982b).

CHAPTER III

DEVELOPMENT OF THE PIEZOVANE AND TESTING APPARATUS

A. Determining Liquefaction Potential Using the Piezovane

Liquefaction is a physical phenomenon involving large uniaxial strains of the sand deposit. In order for a sand deposit to have liquefaction occur, the following conditions must exist.

1) The deposit must have contractive behavior, (loose enough to have a positive porewater response during shearing). When sand has contractive behavior, the undrained steady state strength of the deposit is less than the initial drained strength.

2) The driving shear stresses on the deposit must be greater than the undrained steady state strength.

3) A triggering mechanism occurs so that the mass is converted from a drained condition to an essentially undrained condition of shear (Castro et al., 1982b).

The first condition is often used when determining liquefaction potential. This condition must exist or a deposit cannot liquefy. A sand with the undrained steady state strength less than the initial drained strength (contractive behavior) has an initial state which plots above the steady state line. If the other two conditions occur, then the deposit will liquefy.

When a sand has an initial condition which is above the steady state line, it exhibits a volume decrease during shear in a drained condition, or porewater pressure increase in an undrained condition. If the sand has dilative behavior, then the sand state is below the steady state line and the undrained steady state strength is greater than the initial drained strength. This is assuming

that the steady state line is the approximate boundary in determining if a sand is susceptible to liquefaction.

To reach the large strains necessary for a sand to achieve steady state of deformation, it has been suggested that the vane test be utilized (Poulos, 1987; Casagrande, 1975). As previously discussed, there are two variables which the Piezovane can directly measure to analyze the susceptibility to liquefaction: (1) the porewater pressure response and (2) the measurement of the undrained steady state strength versus the initial drained strength.

B. Description of the Piezovane

The Piezovane was designed and constructed at Colorado State University in the summer of 1987. The Piezovane was designed to be used in conjunction with current state of the practice drilling techniques. The Piezovane vane consisted of four blades welded to a shaft. The dimensions of the Piezovane were designed to meet ASTM Specifications D-2573 for a conventional NX 5.08 cm (2 inch) casing size vane shear (ASTM, 1989). The diameter was 63.5 mm and the blades have a height of 127 mm and thickness of 3.2 mm. The Piezovane had an area ratio of 18%. Vickers (1983) recommended an area ratio to minimize disturbance to the shear zone of 10% to 25%.

Two of the blades had two 1.5 mm diameter pressure ports drilled into the shaft. The shaft was a 254 mm steel rod with OD of 19 mm. The center of the rod was drilled out to an ID of 6.35 mm to provide continuous fluid from the pressure ports to the transducer situated at the top of the vane shaft. The shaft extended 127 mm above the top of the blades. The center and pressure ports are filled with de-aired water and a plug is installed at the bottom of the Piezovane. The pressure transducer is sealed with a rubber O-ring to prevent leakage. A detailed drawing of the Piezovane is included on Figure 3.1 and is pictured in Figure 3.2.

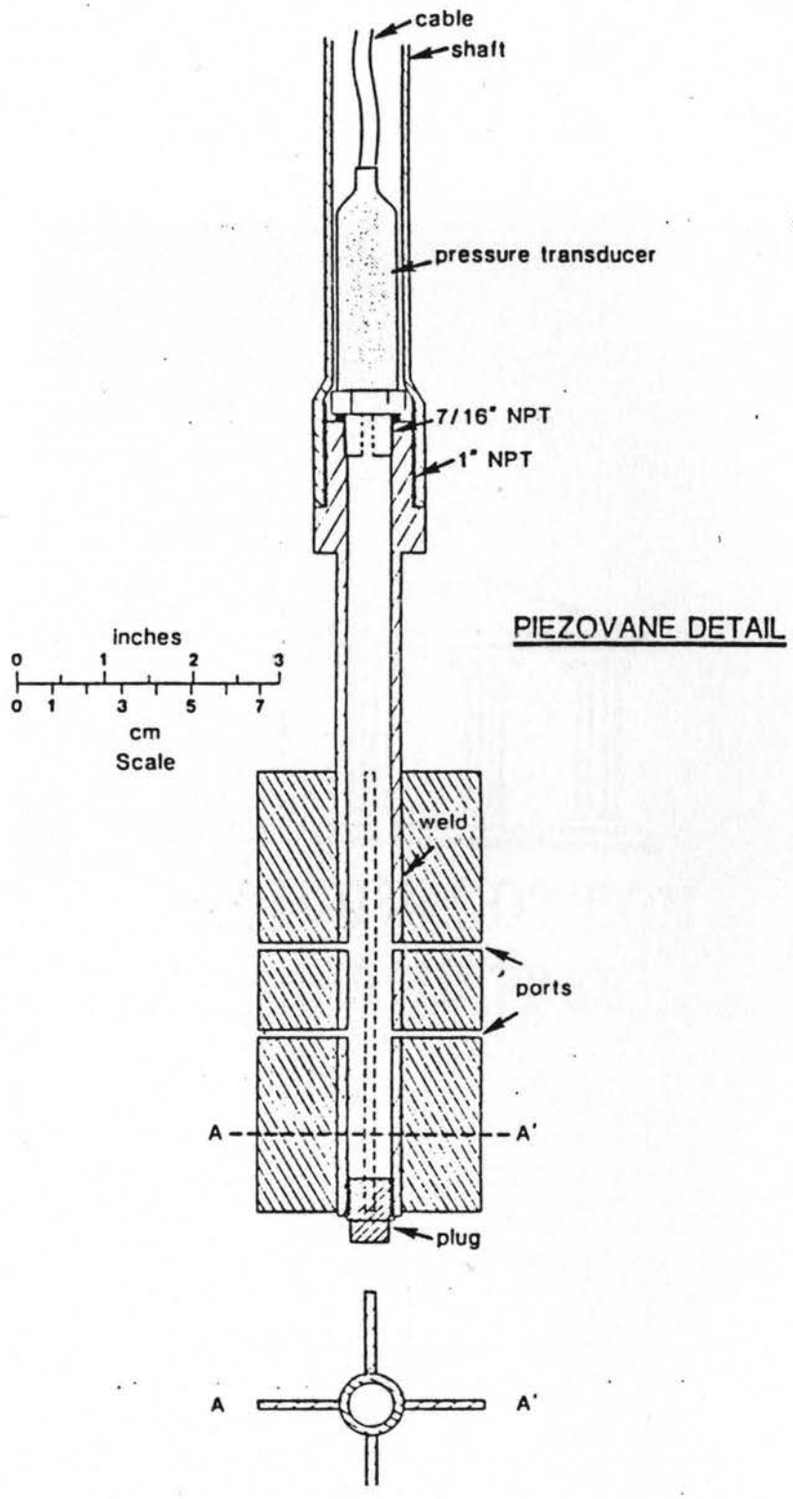

Figure 3.1 Detail of Piezovane (Scott, 1989)

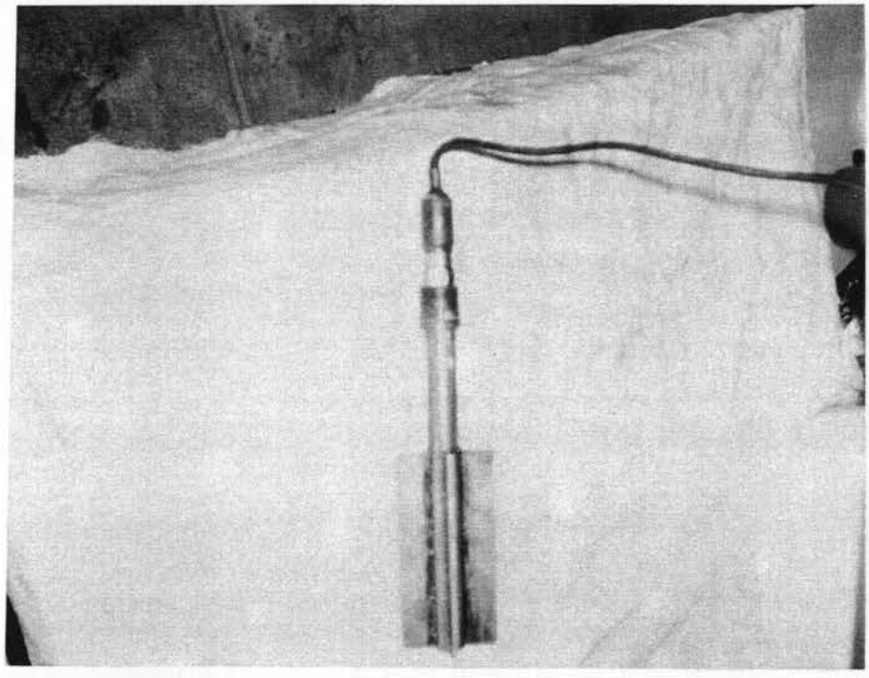

Figure 3.2 Piezovane and Porewater Pressure Transducer.

C. Calibration Chamber

Two types of calibration chambers have been used in previous studies of laboratory testing of in situ equipment. The more elaborate calibration chambers used in CPT testing include two membranes to provide lateral and vertical stress. The triaxial calibration chambers are more effective in controlling stress while the CPT penetrates into the chambers. (Been et al., 1988 and Bellotti et al., 1982, 1988 and Bunnell, 1978). The second chamber is a K_o (zero lateral strain) cell which applies only vertical stress from a membrane placed at the bottom of the cell. During testing no net volume displacement by the vane and shaft would occur. The K_o cell design was used for this research.

A 0.59 m diameter steel pipe (approximately 10 vane diameters) with a height of 0.78 m was selected for the chamber. The ends of the pipe were machined and a 6.35 mm groove cut for the placing of an O-ring at each end to seal the top and bottom plates to the chamber. A Thompson linear bearing was installed on the top plate to minimize shaft friction of the vane's rod. A more detailed description of K_o chamber is included in Scott (1989) and on Figure 3.3.

Carbon dioxide (CO_2) gas, de-aired water and back pressure was supplied to the sample by means of a diffuser placed at the bottom of the K_o chamber. The diffuser was connected to the control panel. Vertical pressure was applied under a membrane located at the bottom of the cell. Vertical pressure was controlled by the control panel. The control panel is described in Scott (1989) and is illustrated in Figure 3.4.

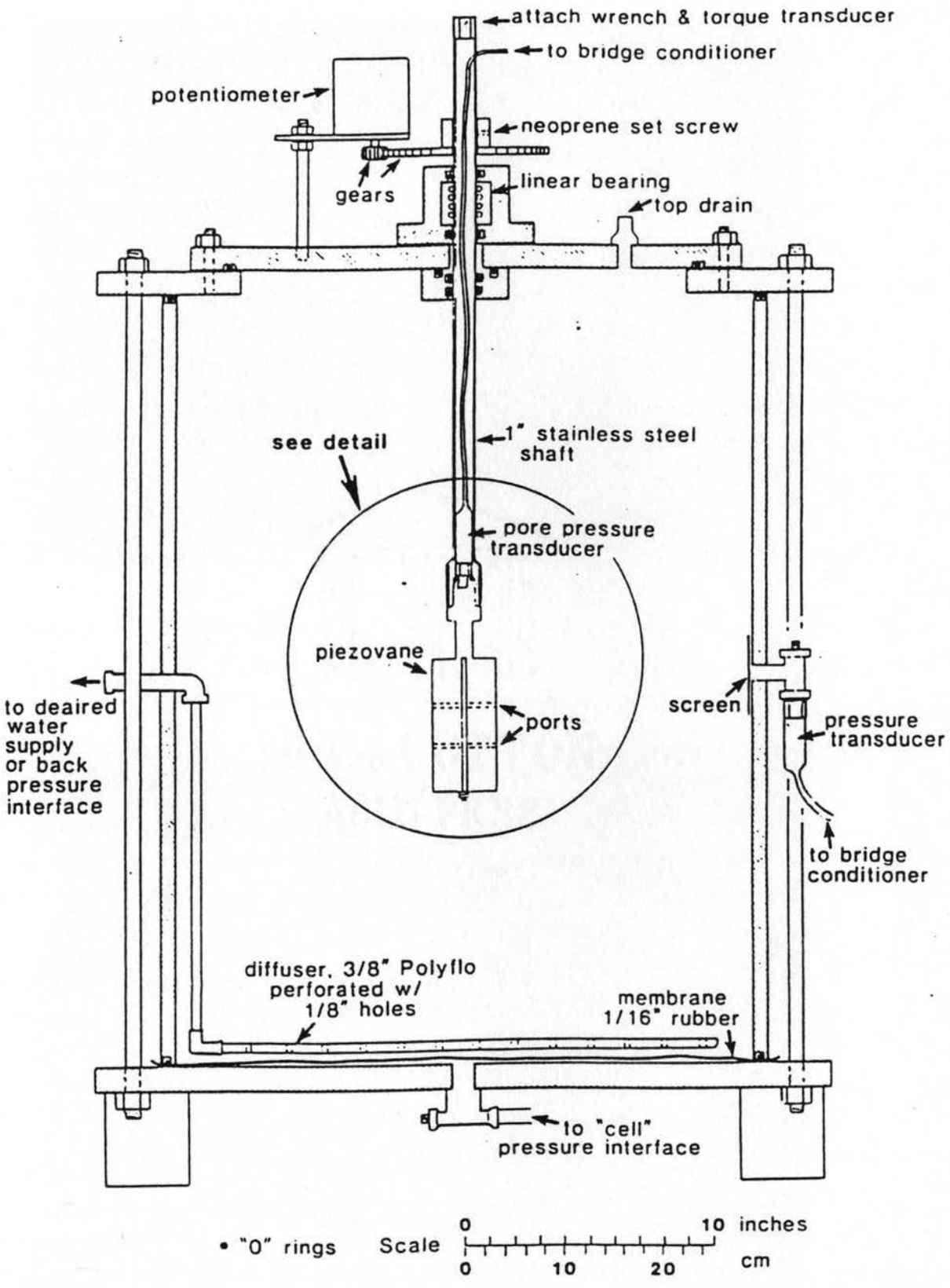

Figure 3.3 Diagram of Calibration Chamber (Scott, 1989)

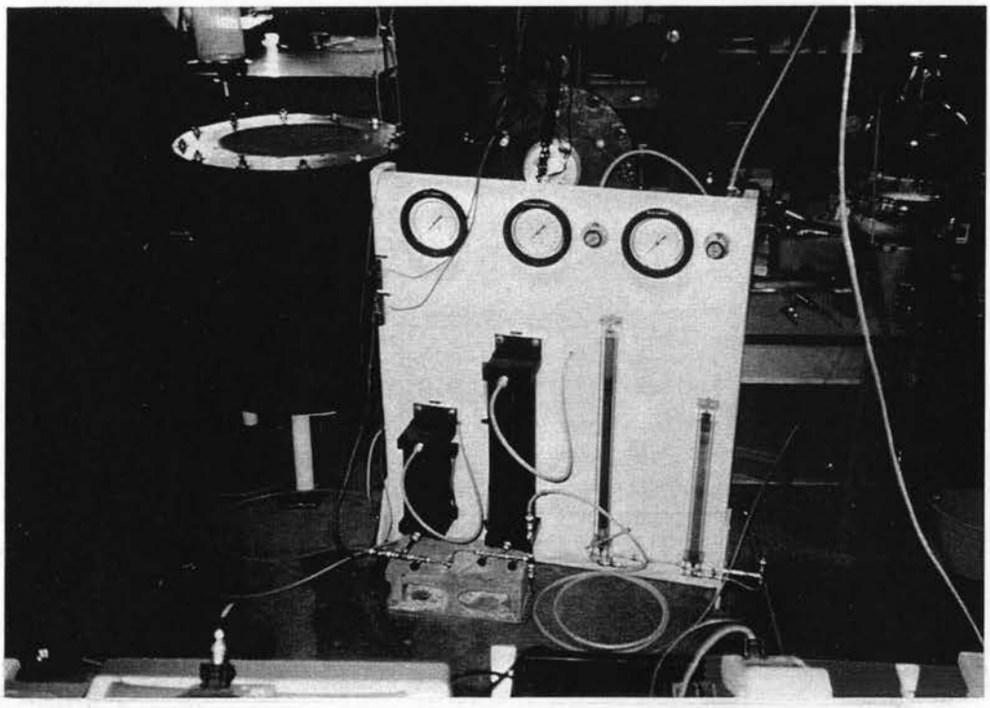

Figure 3.4 Calibration Chamber Control Panel

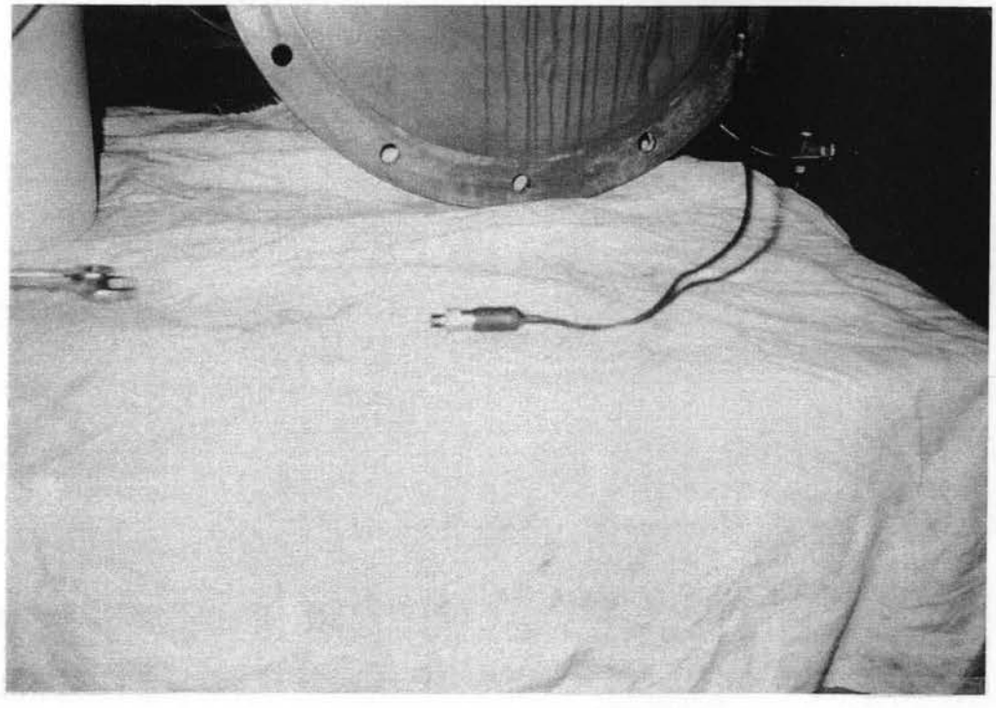

Figure 3.5 Druck Model PDCR 10 Porewater Pressure Transducer

D. Instrumentation

1. Porewater Transducers

Porewater pressure transducers Druck Model PDCR 10 were placed in the Piezovane and at the side of the K_o chamber. The transducers natural frequency is 28 kHz and can withstand a mechanical shock of 1000 g for 1 millisecond. A photo of the Druck Model PDCR 10 porewater pressure transducer is indicated on Figure 3.5. Other specifications are:

peak pressure	981.0 kPa
supply	10 volts
sensitivity	100 mV F.S.O
non-linearity and hysteresis	±0.1% B.S.L.
compensated temp range	0 to 50° C

Input voltage was supplied and the output signal amplified by Endevco 4470 signal conditioners and Endevco 4476.2A amplified Bridge conditions.

2. Rotation Potentiometer

A potentiometer was used to measure the rotational displacement of the shaft during shearing. The Model SB 1796 potentiometer was manufactured by Beckman Industrial Corporation. The potentiometer was designed for an output voltage change of 0.0 to 10 volts in 15 turns. The input voltage was a constant 10 volts from Hewlett-Packard 6212b power supply. The potentiometer is pictured on Figure 3.6.

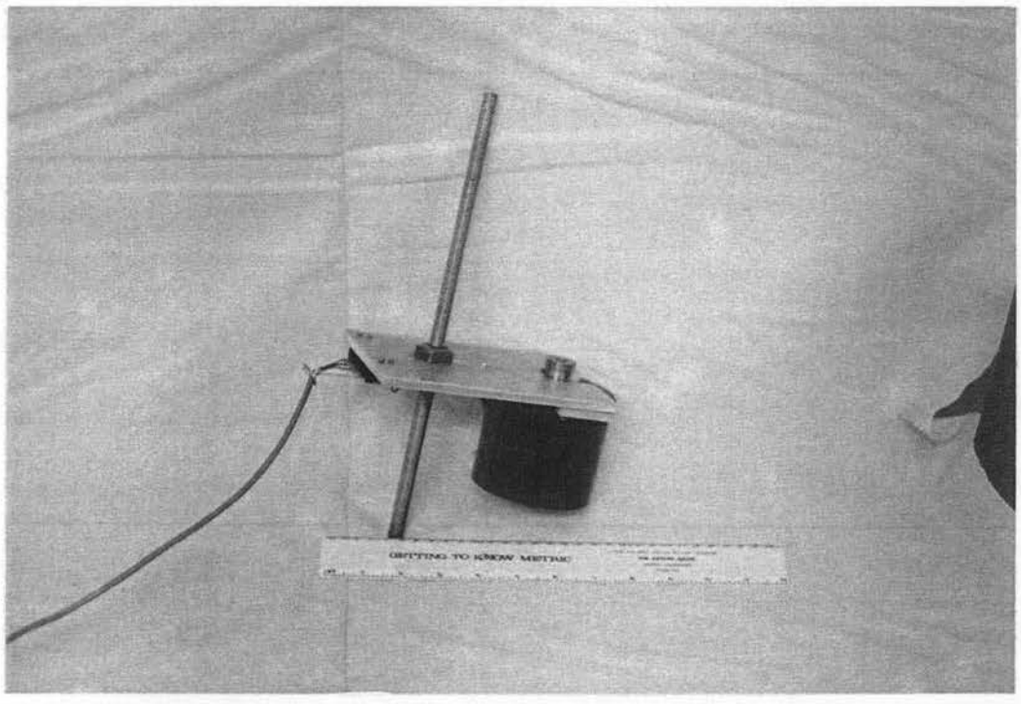

Figure 3.6 Rotational Potentiometer

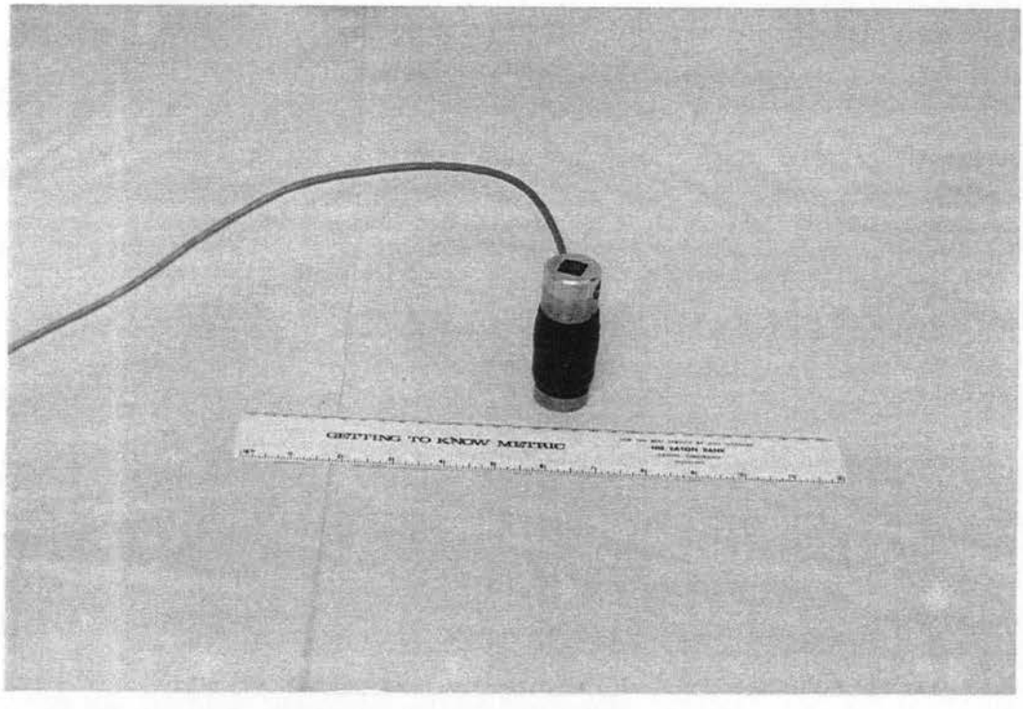

Figure 3.7 Torque Transducer

The shafts of the potentiometer and Piezovane were connected by gears and provided measurements of ±0.4 degrees. The potentiometer was held in place by a bracket, which could be adjusted on a threaded rod so that the two gear wheels would match. A 360° rotation of the Piezovane would produce 3 rotations of the potentiometer.

3. Torque Transducer

The Piezovane was rotated by hand using a torque wrench at the top of the vane. The socket of the torque wrench was modified to be a torsion cell. This was accomplished by mounting a full bridge strain gage to the socket. This had a resolution of 4mv per 1 N-m when a constant input voltage of 10 volts was supplied by the Endevco 4470 signal conditioners. The torque transducer is picture on Figure 3.7. The torque transducer was calibrated by connecting one end of a bar to the torsion cell and adding weight to a hanger connected to the other end of the bar as shown on Figure 3.8.

4. Data Acquisition

The output data from the porewater pressure transducers, potentiometer and torque transducer was in analog form. This data was digitized using Pacific Instruments Model 9820 transient data recorders. Data could be accessed by a IEEE-488 bus connection to a Compaq Computer. The porewater pressure transducers responses were monitored during testing using a Nicolet Oscilloscope. This system is discussed in more detail by Bretz (1989) and Hassen (1994). A diagram of instrumentation and data acquisition is indicated on Figure 3.9 and pictured on Figure 3.10. Data was later transferred to a VAX computer system and reduce using 20/20 ^{R} software. The data was also stored on magnetic tape for future use.

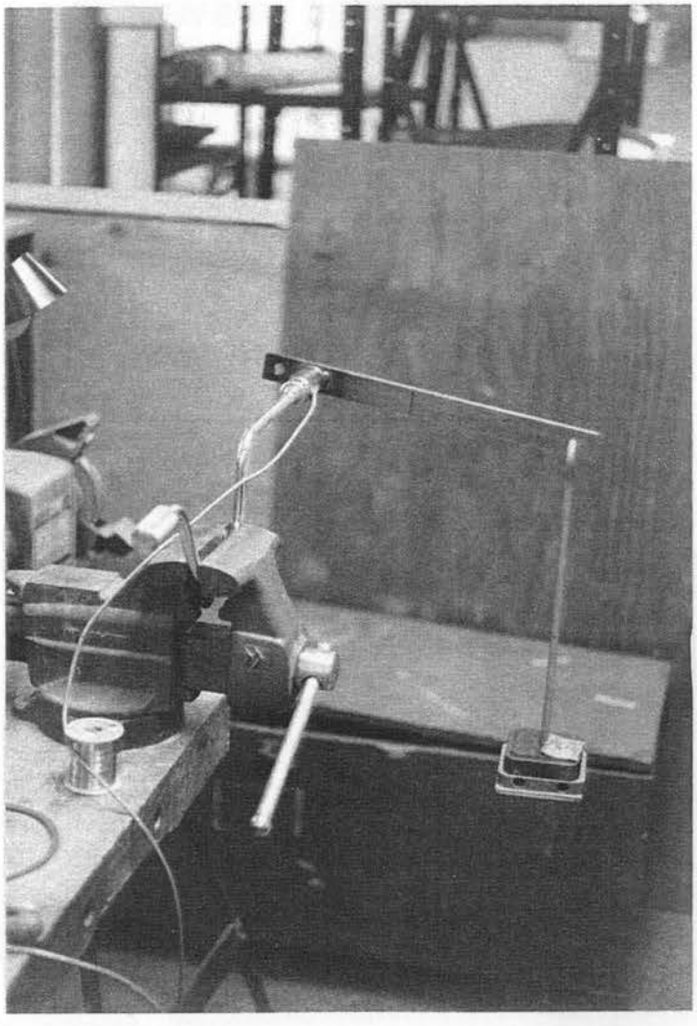

Figure 3.8 Calibrating the Torque Transducer

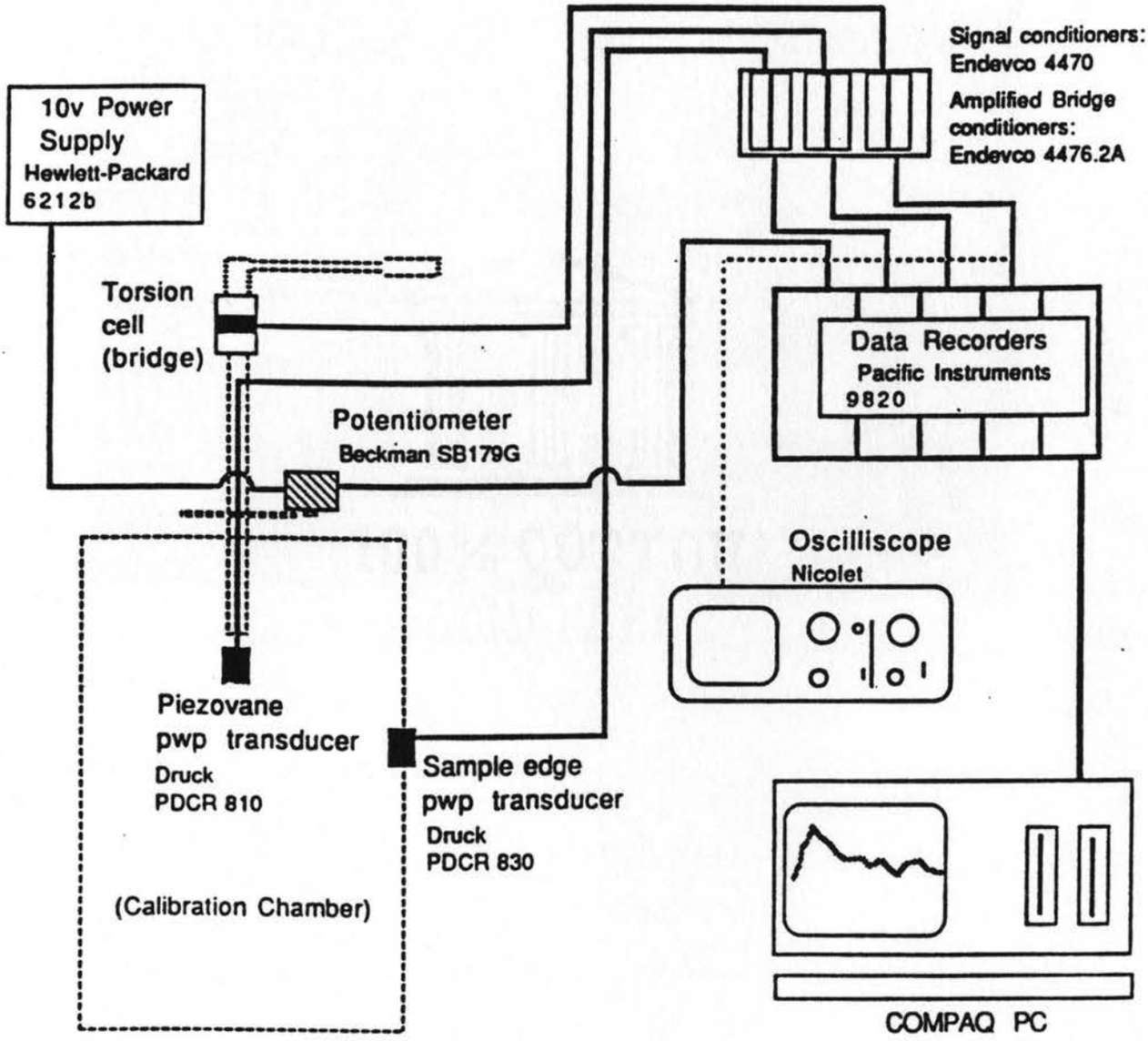

Figure 3.9 Diagram of Instrumentation and Data Recording System (Scott ,1989)

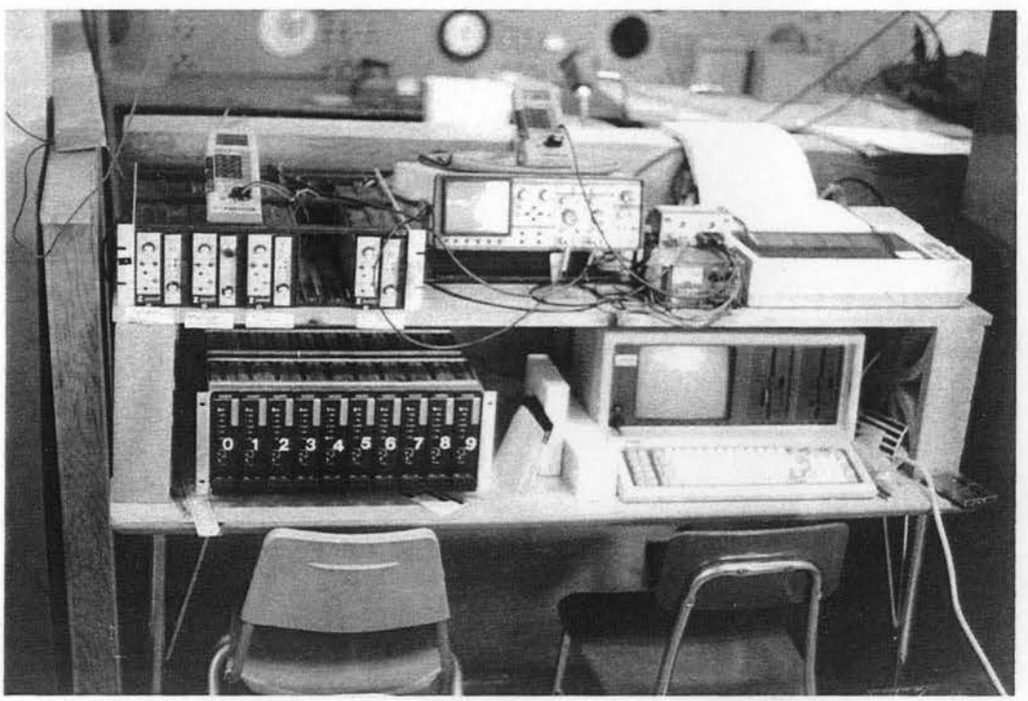

Figure 3.10 Computer and Data Acquistion System

CHAPTER IV

EXPERIMENTAL INVESTIGATION FOR DETERMINING THE STEADY STATE SOIL PARAMETERS

A. Poudre Valley Sand

The sand used in this study was produced by crushing cobbles obtained from the Poudre River near Fort Collins, Colorado, which will be referred to as Poudre Valley Sand (PVS). This sand was supplied by Sterling Sand and Gravel of Fort Collins, Colorado. The grain size distribution and selected index properties are shown in Figure 4.1 and Table 4.1, respectively. Results of permeability tests using the constant head test method is presented in Table 4.2. The linear regression best fit line for the permeability (k) is:

$$k = e\,(0.0260) - 0.009 \qquad \text{Eq. 4.1}$$

$$R^2 = 0.998$$

where e is the void ratio and k is the coefficient of permeability (cm/sec). A more detailed description of PVS is given in Bretz (1989) and Hassen (1994).

Table 4.1: Index Properties of Poudre Valley Sand

Unified Soil Classification (USCS) (ASTM D-2487-85)	SP
Specific Gravity (G_s) (ASTM D854-83)	2.68
Particle Size Distribution (ASTM D422-63)	
D_{10}	0.16 mm
D_{30}	0.25 mm
D_{50}	0.52 mm
D_{60}	0.65 mm
C_u	3.85
C_c	0.95
Relative Density (ASTM D4253-83)	
Dry mean Density (γ_d)	
maximum	1863 kg/m^3
minimum	1490 kg/m^3
Void Ratio (e)	
maximum	0.798
minimum	0.438
Grain Shape	Angular

Table 4.2: Permeability of Poudre Valley Sand

Relative Density (%)	Void Ratio, e	Permeability, k (m/sec)[1]
10	0.762	10.5×10^{-3}
40	0.654	8.10×10^{-3}
65	0.564	5.60×10^{-3}
85	0.492	3.50×10^{-3}

1 - Mean of 3 constant head tests performed at each relative density.

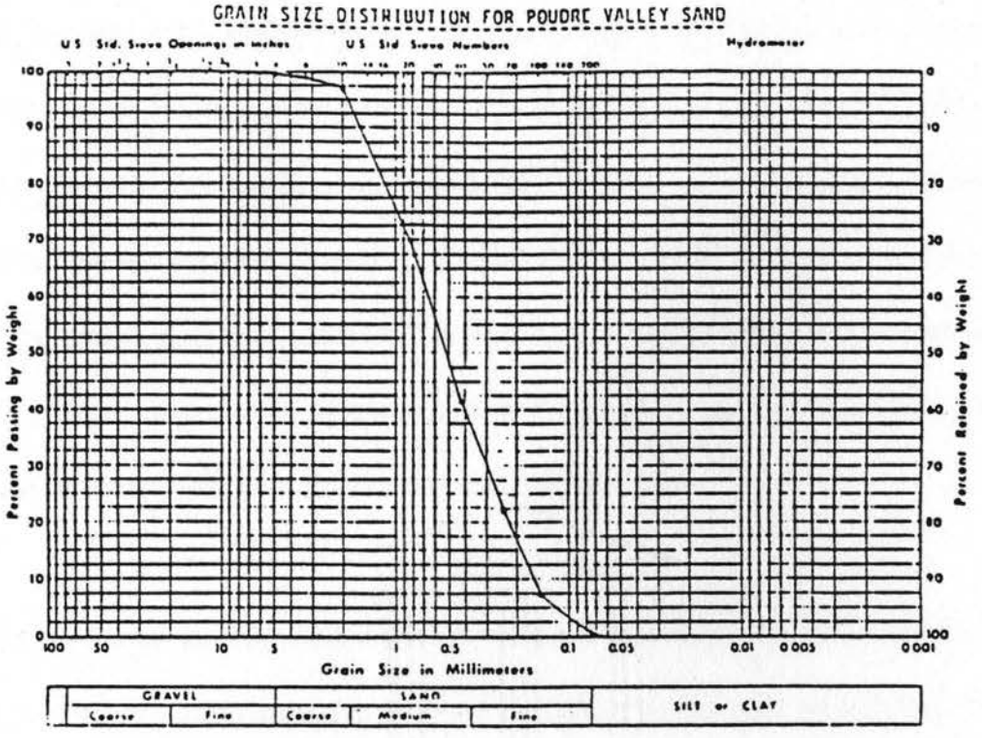

Figure 4.1 Grain Size Distribution for Poudre Valley Sand (PVS)

B. CD Direct Shear Tests

The steady state line for PVS was determined using CD direct shear tests. The method used follows the outline by Taylor (1939). The steady state condition occurs at the peak of the shear normal stress ratio when there is zero volume (thickness) change (Taylor, 1939). Several tests were conducted at a preselected initial void ratio with the variable being the normal stress of each test. The test results were plotted by normal displacement versus normal effective stress. A linear regression using Statgraphies ^{R} was performed on the data to determine the best fit line. The location of zero normal displacement at the peak shear stress determined the location of steady state normal effective stress at the void ratio tested.

The tests were performed on specimens prepared at void ratios of 0.600, 0.664, and 0.760. Results of steady state normal stress (σ'_f) and effective angle of internal friction (ϕ') are indicated in Tables 4.3 and 4.4 and plotted in Figure 4.2. The linear regression for the results presented in Table 4.4 indicates the equation of the best line for the steady state line is:

$$e = 1.948 - 0.488 \log (\sigma'_{fs}) \qquad \text{Eq. 4.2}$$

$$(R^2 = 0.951; s = 0.025)$$

Table 4.3: Summary of CD Direct Shear Results for Poudre Valley Sand

Test No.	Void Ratio	Normal Displacement at Shear Strength Peak (mm) (1)	Shear Strength(s) kPa	(psi)	Normal Effective Stress (σ_f') kPa	(psi)
1	0.760	0.038	113.0	(16.4)	137.8	(20.0)
2		0.098	116.0	(24.1)	206.7	(30.0)
3		0.028	244.6	(35.5)	275.6	(40.0)
4		-0.084	248.0	(36.0)	344.5	(50.0)
5		0.022	108.9	(15.8)	137.8	(20.0)
6	0.664	-0.106	395.5	(57.4)	516.8	(75.0)
7		-0.09	445.1	(64.6)	420.3	(61.0)
8		-0.145	560.8	(81.4)	689.0	(100.0)
9		0.043	248.6	(41.3)	344.5	(50.0)
10						
11	0.600	-0.024	598.7	(86.9)	689.0	(100.0)
12		-0.028	526.4	(76.4)	620.1	(90.0)
13		0.044	469.9	(68.2)	516.8	(75.0)

(1) (+) positive is dilative state
(-) negative is contractive state

Table 4.4: Summary of CD Direct Shear Tests

e_o	ϕ_s' (deg)	(σ'_{fs}) kPa
0.760	36.9	286.2
0.664	38.7	389.7
0.600	41.3	601.35

σ'_{fs} - steady state effective stress normal to the shear plane (determine from linear regression of displacement versus normal effective stress).

ϕ_s' - effective angle of internal friction

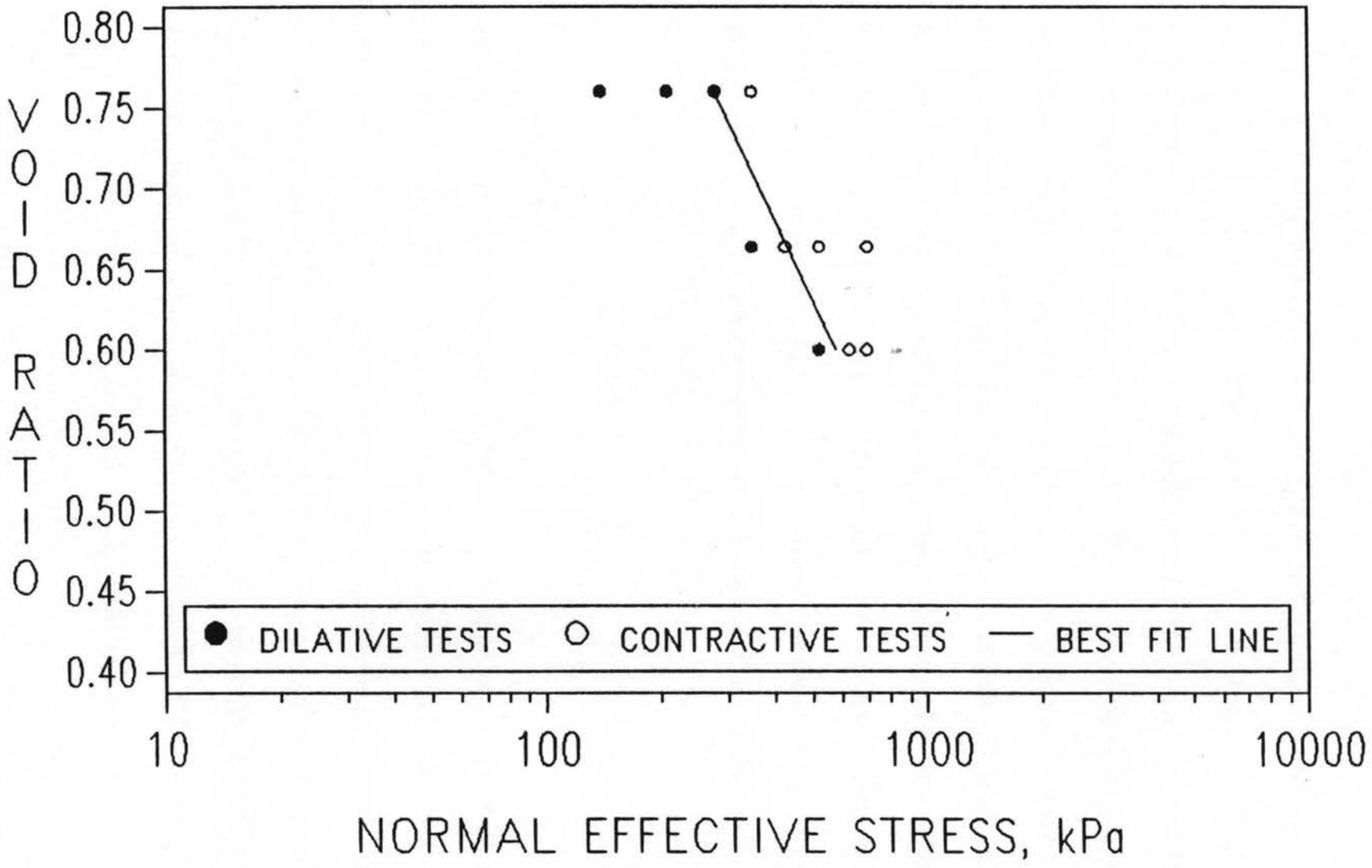

Figure 4.2 CD Direct Shear Results for Poudre Valley Sand (PVS).

C. Consolidation Undrained Triaxial Tests

1. Test Equipment

The equipment used in the triaxial tests was part of the Geotechnical Engineering Graduate Laboratory on the Colorado State University campus. The tests were conducted using Engineering Laboratory Equipment (ELE) 50 kN load frame, model No. EL25-284, with a Wykeham-Farrance proving ring model No. 14190. The capacity of the proving ring was 2000N with a sensitivity per division of 10.4N. The triaxial test equipment is pictured on Figures 4.3 and 4.4. The porewater pressure was measured utilizing a Druck pressure transducer, Model No. PDCR10, connected to a Vishay Strain Indicator Model P-350-A . The range of the transducer was 0.0 to 980.7 kPa with a sensitivity of 100 mV full scale. The base of the triaxial cell was modified so either vacuum or CO_2 could be introduced into the specimen. The porewater transducer was positioned so that the system could be purged of air. A diagram of the base is shown in Figure 4.5.

2. Preliminary Set-Up

The specimen was constructed in a 3.6 cm diameter by 7.3 cm in height split mold. A thin layer of vacuum grease was applied to the sides of the cap, base and the inside of the split mold to hold the membrane against sides of mold. A membrane having 0.0076 cm (0.003 inch) thickness was stretched over the base. Two O-rings were placed on the bottom groove of the base to support the split mold and to fasten the membrane to the base. The membrane was pulled through the split mold and stretched over the upper lip. A vacuum of 25.4 cm (10 inches) of Hg was applied to the split mold, which pulled the membrane snugly against the sides.

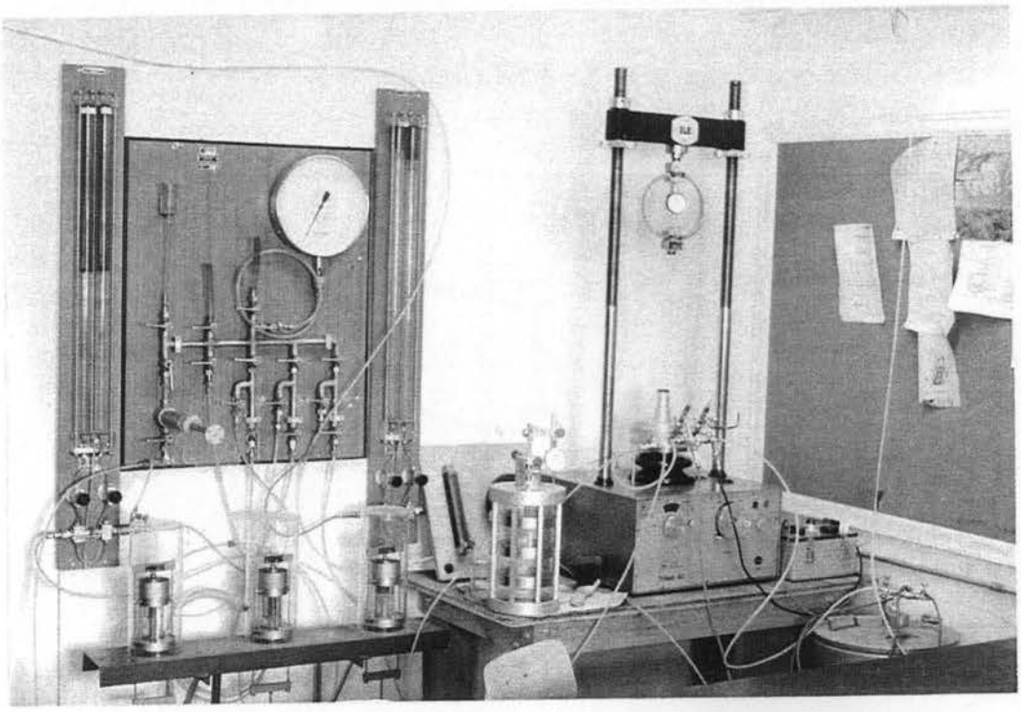

Figure 4.3 CSU Triaxial Equipment

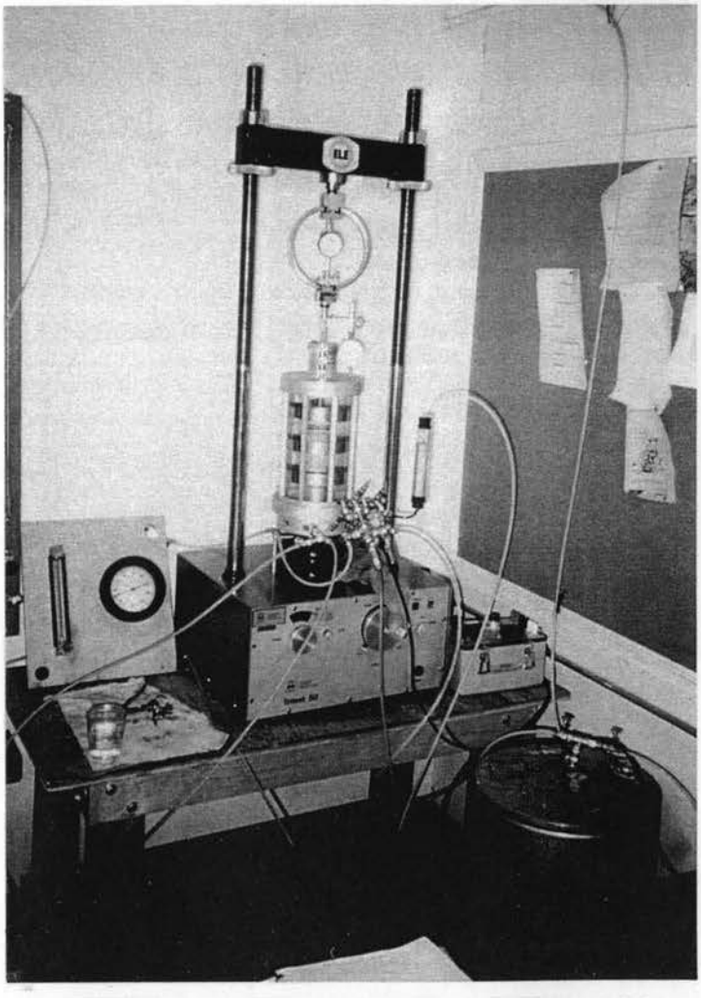

Figure 4.4 Triaxial Cell with CO_2 Bubble Tube

TRIAXIAL CELL

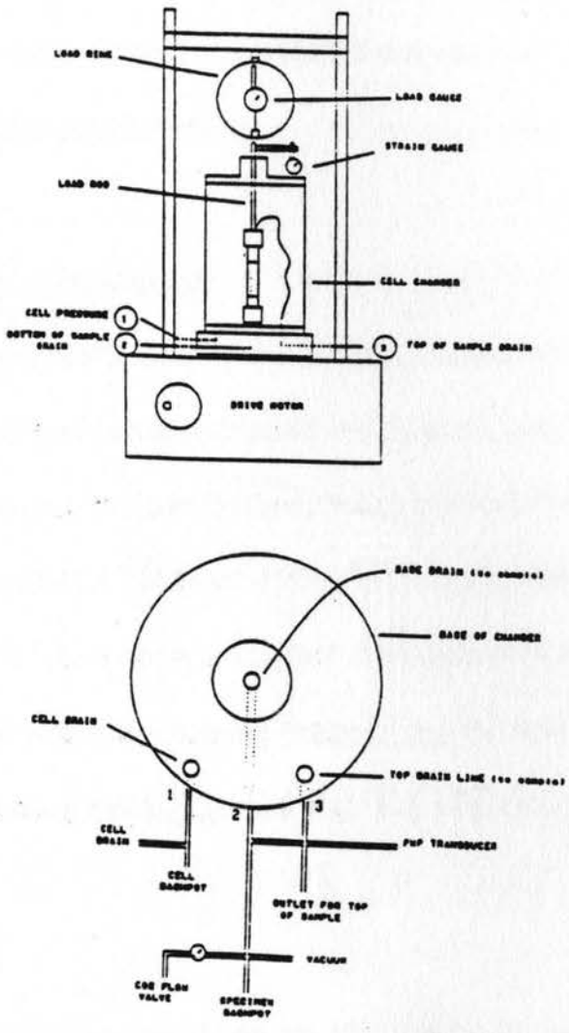

TRIAXIAL SAMPLE

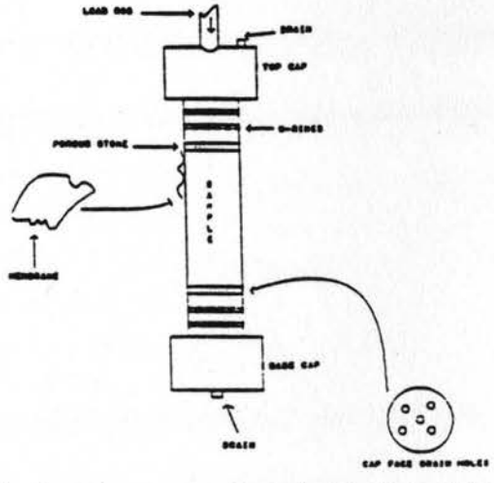

Figure 4.5 Diagram of Triaxial Cell Base

3. Specimen Placement

Specimens were placed with the split mold at a predetermined density using Ladd's (1978) undercompaction method. Ladd (1978) recommended that ten layers be used and the first layer be undercompacted by five percent. This method was used by Huberts (1986) in building samples using PVS for shock loading testing.

4. Height and Diameter Measurements

The diameter of the specimen is determined using a Pi tape, which is wrapped around the circumference of the specimen and directly reads the diameter. The Pi tape used was distributed by Pi tapes in Lemon Grove, California (Muzze, 1983), and read from 2.0 to 15.2 cm (0.8 to 6.0 inches) in diameter to the nearest 0.0254 cm (0.001 in). Measurements were taken at three points along the specimen. The diameter was measured at three points along the specimen. The membrane thickness was subtracted from the diameter and the three measurements averaged to obtain specimen average diameter (d_{ave}). The final height of the specimen was measured with the stand caliper.

Three samples of the sand being placed into the split mold were taken for determination of the water content. The water content was determined in general accordance with ASTM D-2216 "Laboratory Determination of Water (Moisture) Content of Soil, Rock, and Soil-Aggregate Mixtures." The average of the three moisture contents was used to determine the dry unit weight (γ_d) of the specimen.

5. Saturation

After the specimen was measured the triaxial cell was connected to the base and the cell was filled with de-aired water. The vacuum to the specimen was slowly decreased as the cell pressure was increased to 34.4 kPa (5 psi). After the specimen reached equilibrium, carbon

dioxide (CO_2) was injected into the bottom of the specimen at 34.4 kPa (5 psi) and allowed to flow through the sample for approximately 20 minutes. The cell pressure was increased to 51.7 kPa (7.5 psi).

Next, de-aired water was allowed to flow from the bottom of the specimen. The flow rate was adjusted so that the advancement of the wetting front was slower than the capillary rise of the sand; this minimizes the number of gas bubbles being trapped in the voids. After the wetting front reached the top of the specimen, the flow rate was increased and approximately 1000 ml of de-aired water was used to flush trapped bubbles of CO_2 out of the specimen. Any remaining gas bubbles would have to be forced into a solution using back pressure. The cell and specimen pressures were increased so that a maximum difference in pressure between the specimen and cell was 34.4 kPa (5 psi).

The Skempton's B-parameter method was used to determine if the sample was saturated (Skempton, 1954; Head, 1986). Silver (1977) states that for B-parameters greater than 0.95, the specimen can be assumed to be saturated. If the specimen had a B-parameter lower than 0.95, then the back pressure was increased.

6. Consolidation

After the specimen was considered to be saturated, the consolidation portion of the test was started. Specimens were isotropically consolidated by increasing the confining stress and holding the back pressure constant. The confining stress was increased in increments of 68.9 kPa (10 psi) so as not to shock the specimen. During consolidation, the following parameters were monitored: porewater pressure, volume change, and cell pressure. Increments were increased every ten minutes, until the desired confining stress was reached. The specimen was allowed to consolidate for 8 to 12 hours after the last increment.

7. Shearing

All tests were undrained with porewater pressure measurements (CU). The strain rate was determined using the procedure described in Head (1986). Initial readings for load, strain, porewater pressure, and cell pressure were recorded. Readings were recorded at one minute intervals for the initial 10% strain after which readings were recorded every two minutes during the test. The test was terminated when:

1. 20% vertical strain was reached;
2. porewater pressure decreased to below zero; or
3. specimen tilts or part of the sample slides out from under the loading ends.

8. Test Results

A total of 11 tests were performed on the PVS. Tests 1, 2, and 5 were terminated due to membrane leaks or porewater pressure decreases below zero. Test results are included in the Appendix on the Triaxial Test Results Diagrams.

Four distinctive stress-strain type curves have been observed by Castro et al., (1982). These curves are shown in Figure 4.6. Curves A and B are completely contractive while curves D and C exhibited dilated tendencies at large strains. The location of peak and steady state strengths are easiest to determine in Type A and B curves. Peak and steady state are more difficult to identify in dilated curves such as Type C or D. Slightly dilated soils reach the steady state deformation at actual strains greater than contractive specimens. At large strains the effects of boundary and redistribution of the void ratio become significant.

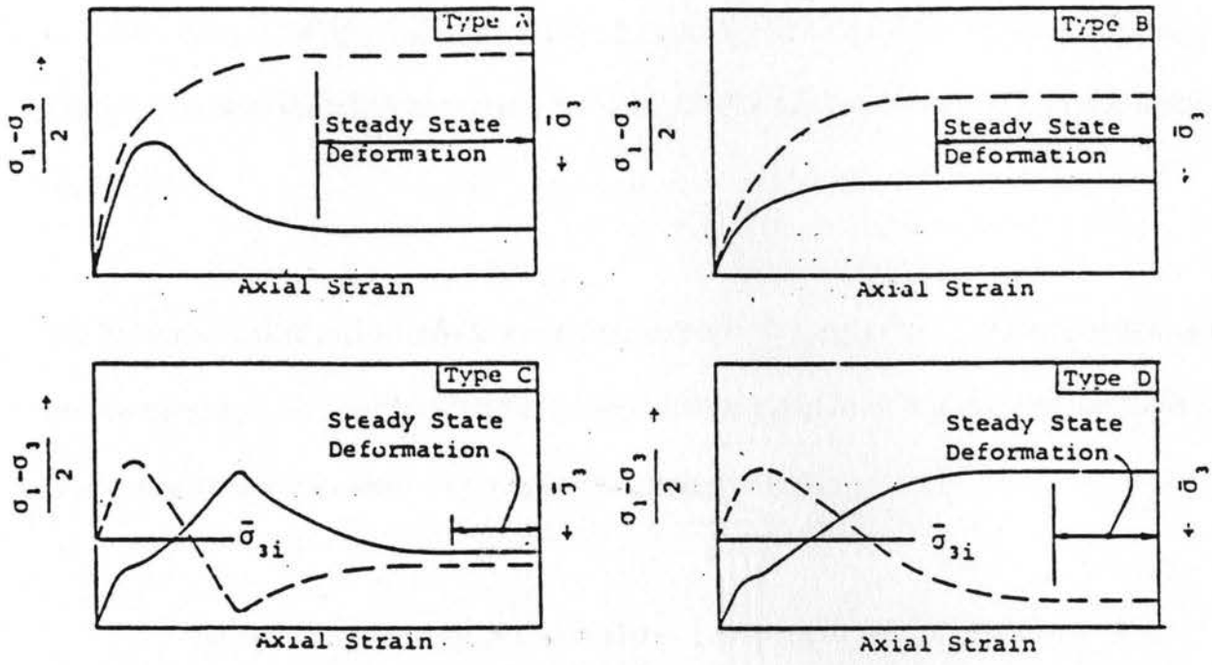

Figure 4.6 Types of Steady State Curves (Castro et al., 1982a)

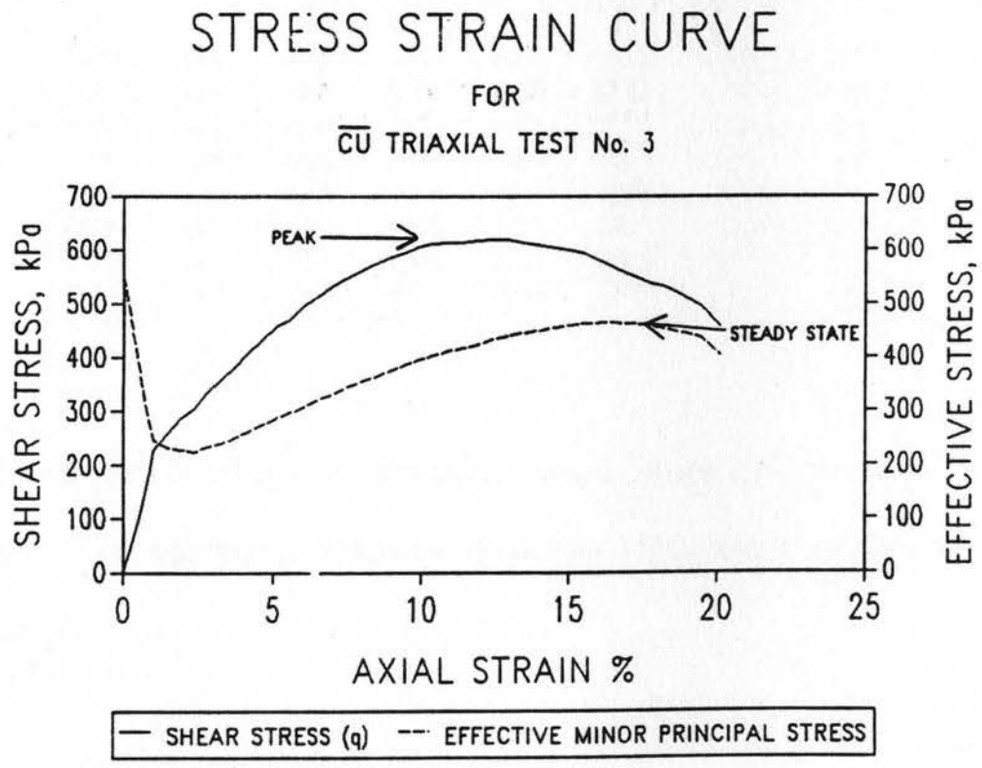

Figure 4.7 Example of $\overline{CU}$ Triaxial Test Type BD Curve from PVS 3.

The tests conducted on the PVS were similar to Type D curves but the effective stress (σ_3') remained positive. Scott (1989) refers to this type of curve as BD. Type BD curves are the result of being consolidated to a state near the steady state line. This type of curve also was observed by Castro et al., (1982a). It has been noted by both authors that Type BD curves exhibit larger scatter in the data than A or B curves. An example of a BD curve from PVS Test 3 is shown on Figure 4.7.

The location of the steady states were determined when: (1) the effective confining stress becomes constant (i.e. stabilized induced porewater pressure) or (2) the slope of the stress point q versus strain curve was zero. Test results are summarized on Table 4.5.

Table 4.5: Summary of CU Triaxial Test Results for Poudre Valley Sand

Test No.	Strain %	e_o	e_c	σ'_{3s} (kPa)	q_s (kPa)	p'_s (kPa)	ϕ'_s (deg)	S_{su} (kPa)
PVS3	16.1	0.635	0.592	465.4	578.0	1042.5	33.7	481.0
PVS4	15.4	0.610	0.552	587.8	859.2	1447.1	36.4	492.9
PVS6	18.8	0.699	0.654	519.3	590.8	1116.9	31.9	501.4
PVS7	16.6	0.691	0.642	293.9	323.3	617.2	31.6	275.4
PVS8	14.5	0.678	0.622	323.3	440.9	754.4	35.8	357.8
PVS9	15.9	0.672	0.657	159.9	207.7	367.4	34.4	171.4
PVS10	18.3	0.695	0.644	391.9	520.3	913.1	34.7	427.6
PVS11	16.7	0.695	0.607	339.9	305.7	645.7	28.3	269.3

Figures 4.8 plots void ratio (e) versus the effective minor principal stress (σ'_{3s}). A linear regression was performed to determine the location of the steady state line for all of the data. This equation is:

$$e = 0.928 - 0.12 \log \sigma'_{3s} \qquad \text{Eq. 4.3}$$

$$(R = -0.59; s = 0.031)$$

Also depicted on Figure 4.8 are the results of the linear regression with the exception of Tests PVS 6 and PVS 9. These tests were omitted as possible outliers. The equation of the best fit line from the linear regression is:

$$e = 1.29 - 0.261 \log \sigma'_{3s} \qquad \text{Eq. 4.3a}$$

$$(R = -0.85, s = 0.02)$$

From the stress points q and p_s, the steady state shear strength (S_{su}) was determined using the following equation:

$$S_{su} = q_s \text{ Cos } [\text{Sin}^{-1} (q_s/p_s)] \qquad \text{Eq. 4.4}$$

Where, q_s and p_s were determined from the results of the stress paths from the triaxial tests. Results of the steady state shear strength are included in Table 4.5 and are illustrated on Figure 4.9. The equation of the best fit line from the linear regression for all the data is:

$$e = 0.867 - 0.097 \log S_{su} \qquad \text{Eq. 4.5}$$

$$(R = -0.45, s = 0.03)$$

The equation of the best fit line of the linear regression without Tests PVS 6 and PVS 9 is:

$$e = 1.03 - 0.162 \log S_{su} \qquad \text{Eq. 4.5a}$$

$$(R = -0.54, s = 0.03)$$

The internal friction angle was calculated from the stress path q-p relationship. The steady state effective stress normal to the plane of shear, σ'_{fs} was calculated using:

$$\sigma'_{fs} = S_{su} * (\tan \phi_s)^{-1} \qquad \text{Eq. 4.6}$$

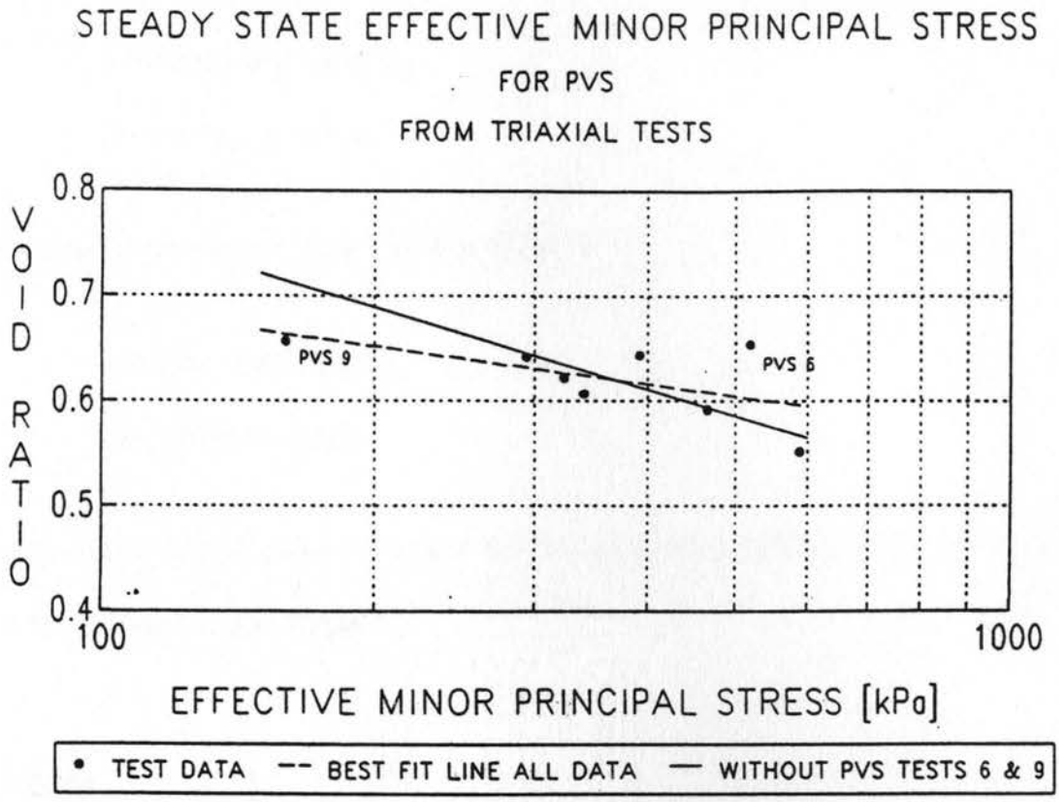

Figure 4.8 Steady State Line for Effective Minor Principal Stress.

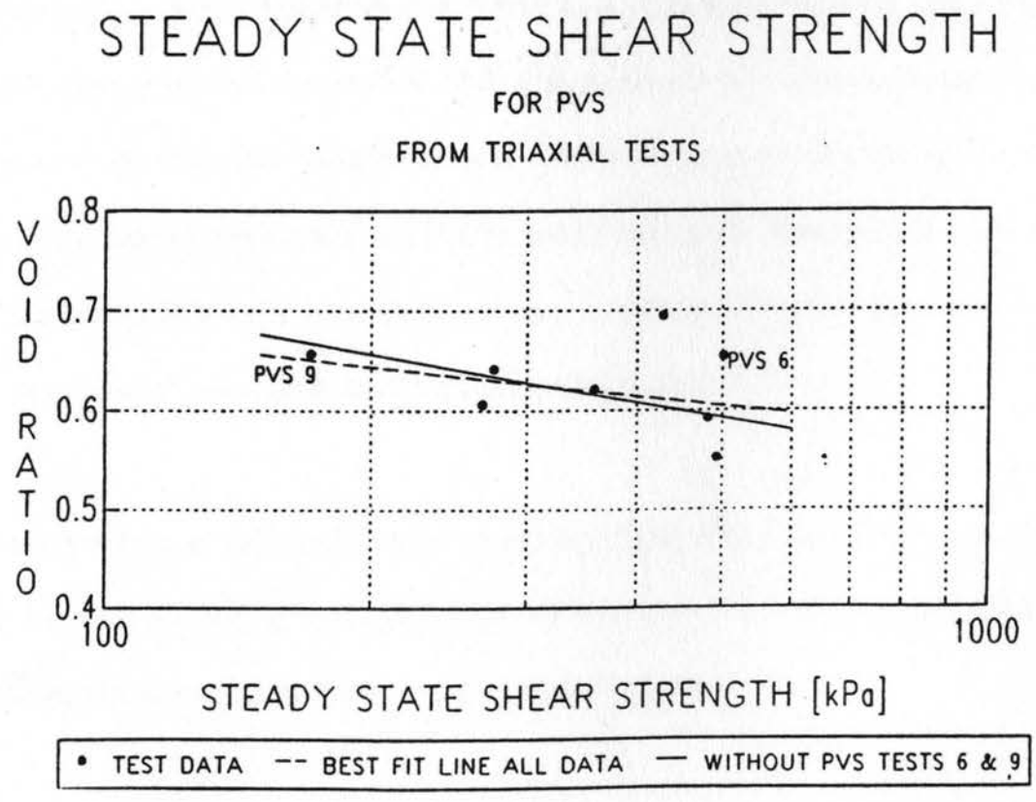

Figure 4.9 Steady State Line for Shear Strength.

The linear regression of all the data indicated that the best fit line is:

$$e = 0.871 - 0.091 \log \sigma_{fs} \qquad \text{Eq. 4.7}$$

$(R = -0.40, s = 0.04)$

The linear regression without Tests PVS 6 and PVS 9 is:

$$e = 1.34 - 0.265 \log \sigma_{fs} \qquad \text{Eq. 4.7a}$$

$(R = -0.62, s = 0.03)$

The steady state effective stress normal to the failure plane is plotted versus the void ratio in Figure 4.10 and also listed in Table 4.5.

D. Summary

The best fit line of void ratio versus normal effective stress for both direct shear and triaxial tests is plotted on Figure 4.11. Also plotted on Figure 4.11 is the steady state line from Poulos et al., (1985) for angular sand similar to PVS. This line appears to be parallel and slightly above the direct shear steady state line. The triaxial steady state line appears to be positioned lower and has a flatter slope than the direct shear and Poulos steady state lines. The actual position of the line could be affected by having the majority of the triaxial test being BD type curves. BD type curves, as previously mentioned, do exhibit larger data scatter.

However, the slope of the steady state line without Tests PVS 6 and PVS 9 appears to more closely resemble the Poulos et al., (1985) steady state line. Tests PVS 6 and PVS 9 could be possible data outliers due to specimen setup or equipment error.

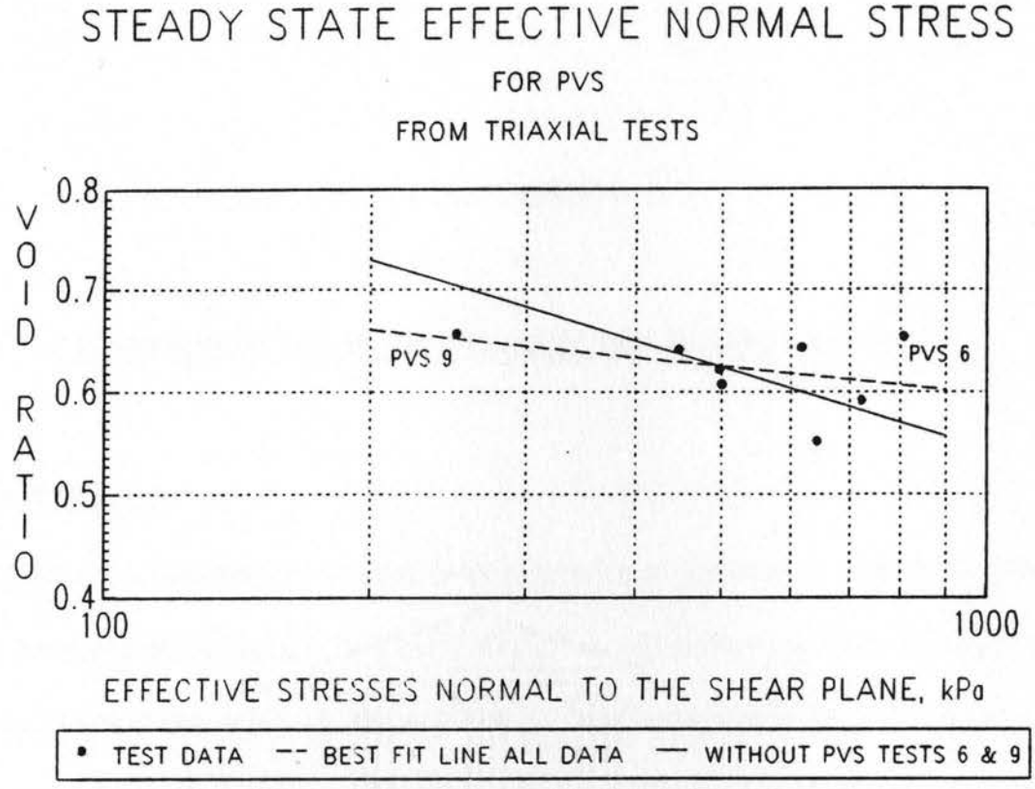

Figure 4.10 Steady State Line for Normal Effective Stress.

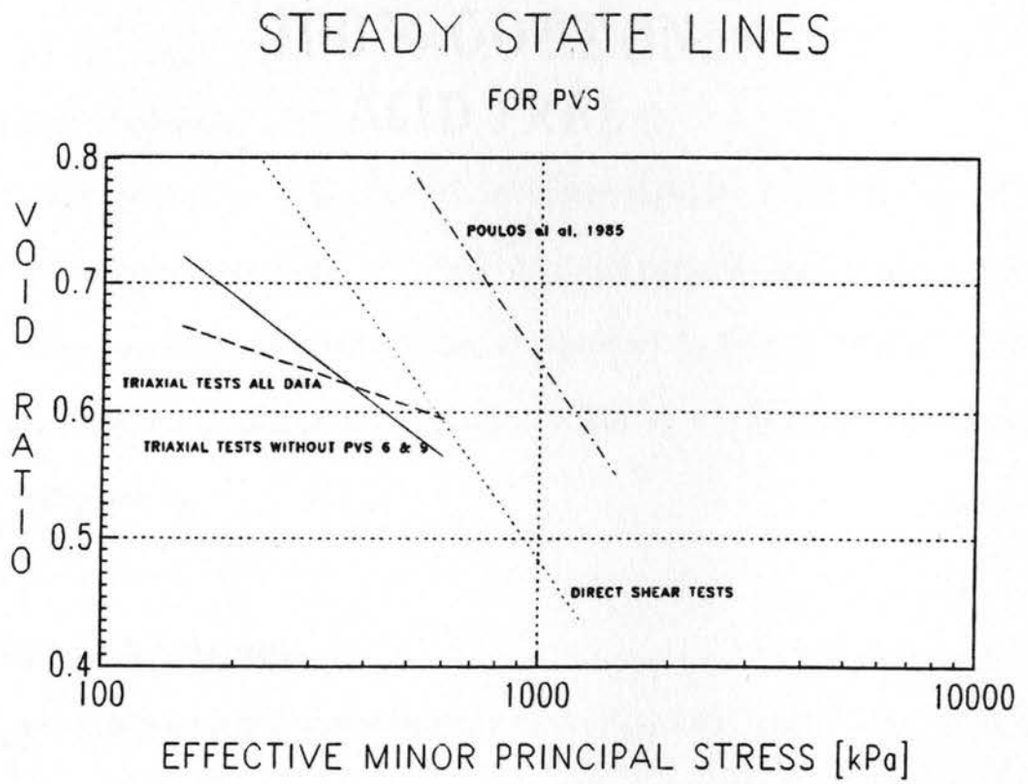

Figure 4.11 Steady State Lines for Direct Shear Tests, Triaxial Tests (With and Without PVS Tests 6 and 9) and Poulos et al., (1985).

CHAPTER V

EXPERIMENTAL INVESTIGATION OF THE PIEZOVANE

A. Test Procedure

The following is a summary of the Piezovane test procedures used in this study. The testing program consisted of setting up 7 specimens within the calibration tank from which 12 tests were performed. During saturation of Specimen 3 a leak in the membrane occurred and the test was aborted. Scott (1989) used the same Piezovane, calibration tank, specimen preparation techniques and testing procedures developed for this research.

1. Specimen Placement

PVS was placed within the calibration tank using a modification to the dry plaviation method outlined by Rad and Tumay (1987). A funnel and plastic tube were used to place the sand within the tank. Changes in density could be achieved by adjusting the drop height of the end of the plastic tube. After testing, the sand was removed and allowed to air dry to water content of less than 5% before reusing.

2. Assembling the Piezovane

The unassembled Piezovane was submerged in de-aired water along with the end plug and porewater pressure transducer. The Piezovane was assembled within the de-aired water to prevent air bubbles from being trapped within the pressure ports and center of the vane. Air bubbles reduce the porewater pressure response measured by the transducer. A hypodermic

needle filled with de-aired water was inserted into each pressure port, and de-aired water was injected to displace any trapped air bubbles within the pressure ports. De-aired water was then flushed through the center of the vane and at the end of the porewater pressure transducer. The porewater pressure transducer was then connected to the Piezovane while still under water. The end plug was fastened to the end of the vane. Inserting the end plug forced water out of the center of the vane through the pressure taps, displacing any remaining air bubbles.

The shaft was connected to the vane and a plastic bag filled with de-aired water was fastened around the vane. This way, the vane could be transferred to the tank without being exposed to air, reducing the chance that air bubbles could enter the Piezovane.

3. Saturation of Specimen

Following placement of the sand in the calibration tank, carbon dioxide (CO_2) was injected into the specimen through the defuser located at the bottom of the tank. Carbon dioxide was flushed through the specimen until a candle at the top of the specimen was extinguished. Then de-aired water was slowly allowed to flow upward into the specimen similar to the wetting procedure used in the triaxial test.

After the wetting front reached the top of the tank the Piezovane was inserted. The plastic bag around the vane was broken during insertion into the water-saturated sand specimen. The Piezovane was lower approximately 0.3 meters into the specimen, and the tank was sealed. Approximately 2 to 3 pore volumes of de-aired water were flushed through the specimen. A predetermined back pressure and confining stress was then applied to the specimen. The specimen was allowed to saturate under the back pressure for 12 to 24 hours before determining the degree of saturation.

The degree of saturation was determined using the "C" parameter pore pressure response as outlined by Veyera (1985). This is the ratio of the specimen porewater pressure to response to increase in vertical confining pressure. It is generally assumed that a "C" parameter of 1.0 indicates that the specimen was saturated or the specimen has a stiff soil skeleton. Saturation data for the tests are presented in Table 5-1.

Table 5-1: "C" Parameter Test Results

Sample No.	Test No.	Initial Void Ratio (e_i)	Initial Vertical Confining Stress kPa	(psi)	Back Pressure kPa	(psi)	"C" Parameter
1	1,2,3	0.769	137.8	(20)	68.9	(10)	0.60
2	4,5	0.691	103.4	(15)	68.9	(10)	0.60
3(1)	--	--	--	--	--	--	--
4	6,7	0.661	172.3	(25)	137.8	(20)	0.84
5	8	0.773	172.3	(25)	137.8	(20)	0.55
6	9,10	0.766	103.4	(15)	68.9	(10)	0.60
7	11,12	0.617	137.8	(20)	103.4	(15)	0.63

(1) Membrane leak

The "C" parameter ranged from 0.55 to 0.84. In some of the specimens the back pressure was applied up to 5 days with no increase in the "C" parameter. Veyera (1985) noted that "C" parameter is a function of effective stress and relative density. The response of the tank and vane transducer were approximately the same when the "C" parameter reached 0.5. The soil skeleton and size of specimen should be taken into consideration when using the "C" parameter response. Therefore all specimens were considered to be saturated.

4. Consolidation of Specimen

Specimens were consolidated by increasing the effective stress in 34.5 kPa (5 psi) increments similar to the triaxial tests consolidation method. When the desired effective stress was reached the specimen was allowed to completely consolidate by waiting 8 to 12 hours after the last increment was added before commencing with the Piezovane tests. Some collapse of the specimen occurred during wetting of the specimen. This volume change was taken into account when the initial volume was calculated. Change in volume during consolidation ranged from 0.0 to 3.1 liters which corresponds to change in void ratios of 0 to 0.029. Consolidation results are summarized in Table 5.2.

Table 5.2: Consolidation of Specimens for Piezovane Tests

Specimen No.	Initial Void Ratio (e_i)	Test No.	Change Volume		Void Ratio After Consolidation (e_c)	Vertical Effective Stress (σ'_{vc}) After Consolidation	
			Liters	(ft^3)		kPa	(psi)
1	0.769	1,2,3	1.4	(0.05)	0.757	345	(50)
2	0.691	4,5	2.3	(0.08)	0.671	241	(35)
3 (1)							
4	0.661	6,7	1.1	(0.04)	0.65	172	(25)
5	0.773	8	3.1	(0.11)	0.744	482	(70)
6	0.766	9,10	0.0	(0)	0.766	34	(5)
7	0.612	11,12	1.7	(0.06)	0.599	207	(30)

(1) Membrane leak

5. Shearing

Upon completion of the consolidation portion of the test, instrumentation was hooked up to the shaft which included installing the rotation potentiometer and torque transducer. Shearing of the vane was done by hand with the assistance of two people to maintain a constant velocity. However, a constant velocity was not always maintained. The vane was rotated 360° in 4.4 to 11.3 seconds. Angular velocities ranged from 87 to 203.9 degrees/sec with velocities at the edge of the vane ranging from 3.7 to 11.3 centimeters per second (cps). The velocity at the edge of the blade and angular velocity for the Piezovane tests are presented in Table 5.3. After the initial test of each specimen, the Piezovane was lowered approximately 0.3 meter by placing a jack at the top of the shaft and using an overhead I-beam to provide support to jack against. While lowering the Piezovane, porewater pressure was monitored and the second test was not conducted until the porewater pressure had dissipated. Results of time versus displacement for each test are included in Appendix A. Test 3 was sheared at the same position as Test 2, however the Vertical effective Stress was decreased to 34.4 kPa.

Table 5.3: Rate of Shearing During Piezovane Tests

Specimen	Test No.	Position[1]	Tests Shearing Time Sec	Velocity at Edge of vane (cm/sec)	Angular Velocity (Deg/sec)
1	1	T	6.32	4.4	79.4
1	2	B	4.4	5.0	90.2
1	3	B[2]	4.3	4.8	86.6
2	4	T	6.2	4.9	88.4
2	5	B	2.8	8.3	149.8
4	6	T	2.2	8.2	148.0
4	7	B	5.7	3.7	66.8
5	8	T	4.4	5.9	106.5
6	9	T	2.6	8.9	160.6
6	10	B	2.0	11.3	203.9
7	11	T	3.4	7.5	135.3
7	12	B	5.2	5.2	93.8
		Mean		6.5	117.4
		Standard Deviation		2.3	41.4

(1) T - Top vane position
B - Bottom vane position

(2) The tested at the same position as Test 2, however vertical effective stress was decreased to 34.4 kPa.

6. Data Processing

Test data was recorded using the transient data recorders. Test data was then transferred to 5 1/4-inch disks and later downloaded to a VAX computer and stored on magnetic tape. The data was reduced using 20/20 ^{R} Spreadsheet software. The data suffered a tremendous amount of electrical noise, especially during the initial testing. Noise was filtered out by use of a moving average. Data which experienced the most noise was the porewater pressure transducers. The torque and rotation potentiometer data did not require smoothing.

B. Piezovane Test Results

1. Calibration Chamber's Drainage Conditions

The majority of the tests were conducted under drained conditions where porewater was allowed to flow in or out of the chamber. For the drained tests porewater pressures could increased or decreased with vane rotation and dissipated after shearing ceased. The actual rate of dissipation of porewater pressure is a function of the diffuser at the bottom of the chamber.

However, in Test 2, the valve to the chamber was closed during the test allowing no drainage to occur. Therefore, Test 2 was considered to be an undrained test. During Test 2, the porewater pressure increased with the vane rotation with no dissipation occurring after completion of shearing. This was consistent with findings observed by Castro (1982b).

2. Porewater Pressure Response

During shearing both positive and negative porewater pressures were observed. Negative porewater pressure was defined by the writer as porewater pressure less than the initial at rest porewater pressure. Likewise, a positive response is the resulting pressure greater than the initial at rest porewater pressure.

Three phases of porewater pressure responses were observed. The first phase was the initial shearing response; the second was the shearing response; and the third phase was the drainage response after the completion of shearing. Within the majority of the tests, the initial pressure response was negative spike. The peak of the negative spike ranged between 0.1 to 3 kPa. Generally, the initial response occurred between 0.0 to 1.0 centimeter of rotation at the edge of the vane (0 to 18° of rotation). This initial response is most likely due to dilation of the particles at the edge of the blade at the beginning of shearing.

During the shearing, two types of porewater pressure responses were observed. The first type was a slightly positive with gradual increase or decrease in porewater pressure. Porewater pressure changes ranged from 0.5 to 2.0 kPa. This slight porewater pressure decrease indicated that dilative behavior of the shear zone was occurring, as indicated with Tests 9 and 4 on Figure 5.1, Steady State Line and Porewater Pressure Response. The amount of pressure change was proportional to the distance to the steady state line. The second response was a positive pressure response that can be associated to contractive behavior as indicated with Test 8 shown in Figure 5.1.

The drainage portion of the test occurred upon completion of the shearing phase. Generally, the porewater pressure returned to zero. However, in three tests, negative porewater pressures were observed and in two tests, substantial porewater pressure still remained at the end of recording of data at 140 seconds. After shearing, the porewater pressure response was most likely determined by the amount of drainage through the diffuser at the bottom of the specimen.

Pressure response at the edge of the tank was also measured. The measured vane porewater pressure was generally greater than the porewater pressure measured at the side of the tank, with the exception of Test 6. This suggests that the tests were not completely drained shear tests and that the edge of the tank could have induced some edge effects on the tests. However, in Test 6, the vane peak porewater pressure was approximately 4.9 kPa and the tank transducer indicated 6.7 kPa. A comparison of the peak porewater pressure measured at the vane and edge of tank is indicated on Figure 5.2 and in Table 5.4.

3. Shear Strength Response of Piezovane

The shear strength response varied from 11.5 to 165 kPa. The majority of the peak responses occurred within the first centimeter of shearing (18° of rotation). Residual shear strength responses ranged from 6 to 60 kPa and occurred at 9 to 24 centimeters of shearing (162.4 to 433.1 degrees). Results of the shear strength from the Piezovane tests are indicated on Table 5.4.

4. Rate of Shearing

The rate of shearing ranged from 67 to 204 degrees/sec and appears to have very little effect on the porewater pressure as shown in Figure 5.3, Angular Velocity verus Residual Porewater Pressure Response. The rate also has little effect on shear strength. However, stopping during the shearing operation did have a significant effect, as indicated in Tests 4, 6, 7, 8, and 12 shown in the Appendix. Abrupt stopping of the test created lower or negative porewater pressure and increased shear strength when shearing continued. Test 8, a contractive sample, had an increase in porewater pressure during the pause. This is also noted by Castro (1982b).

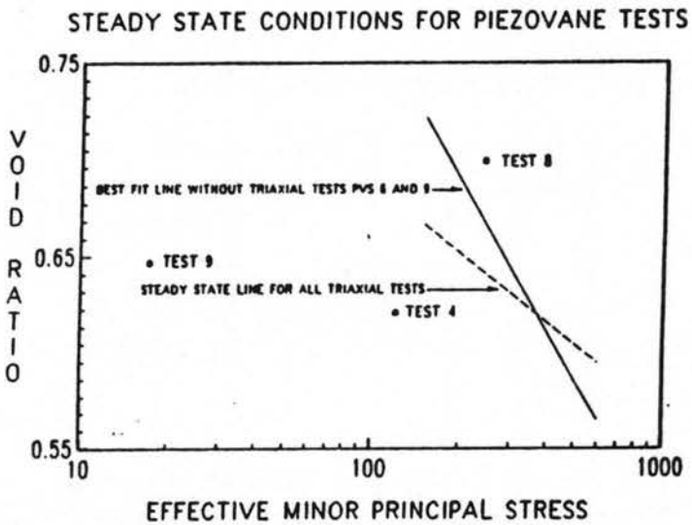

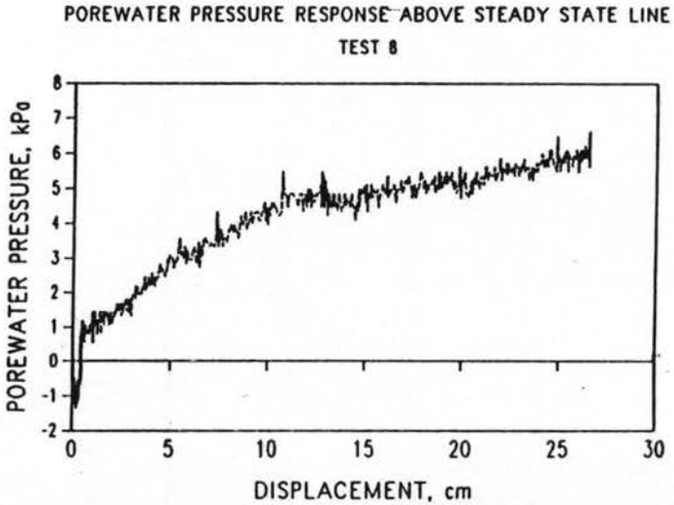

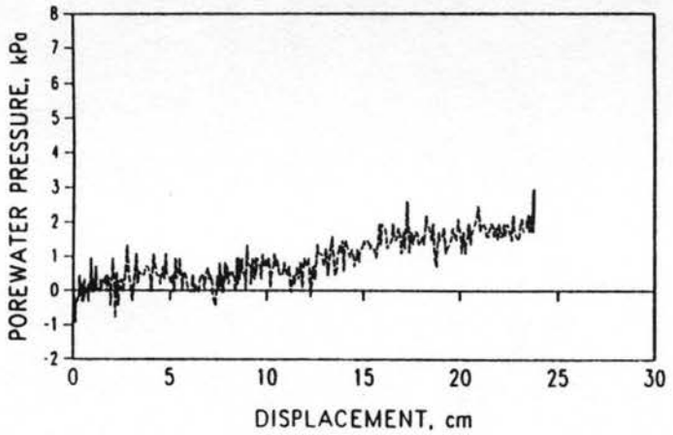

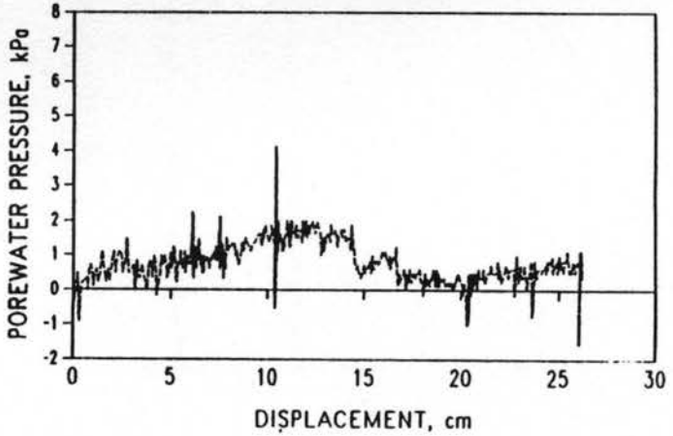

Figure 5.1 Steady State Line and Porewater Response

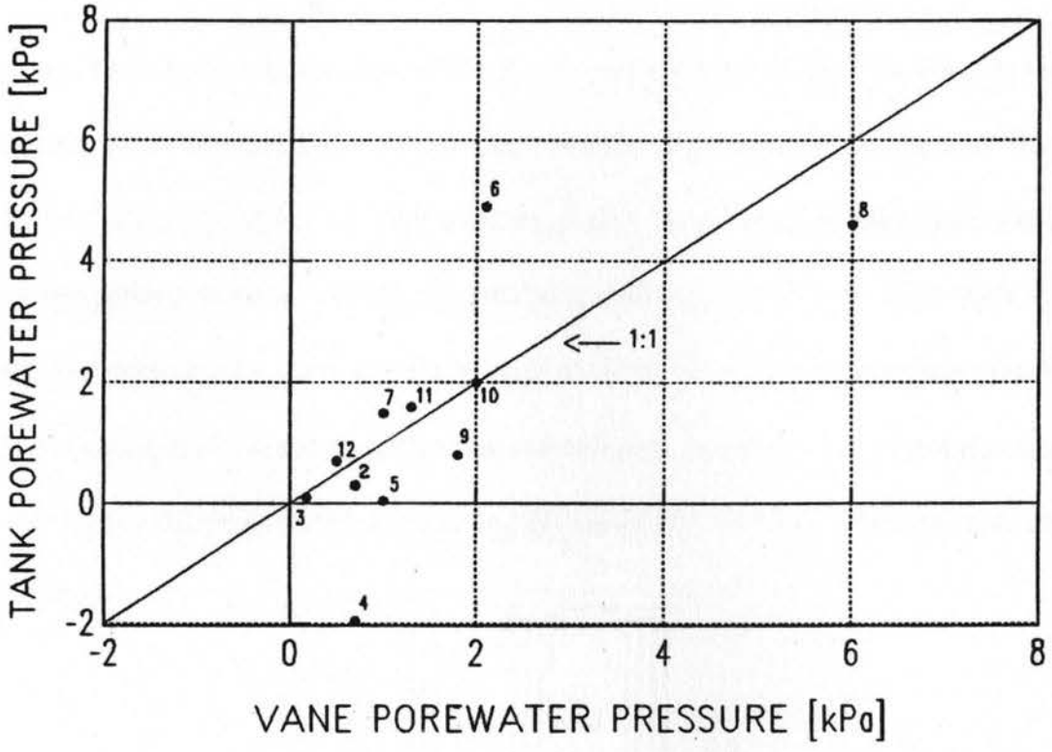

Figure 5.2 Comparison of the Vane and Edge of Calibration Chamber's Peak Porewater Pressure Response.

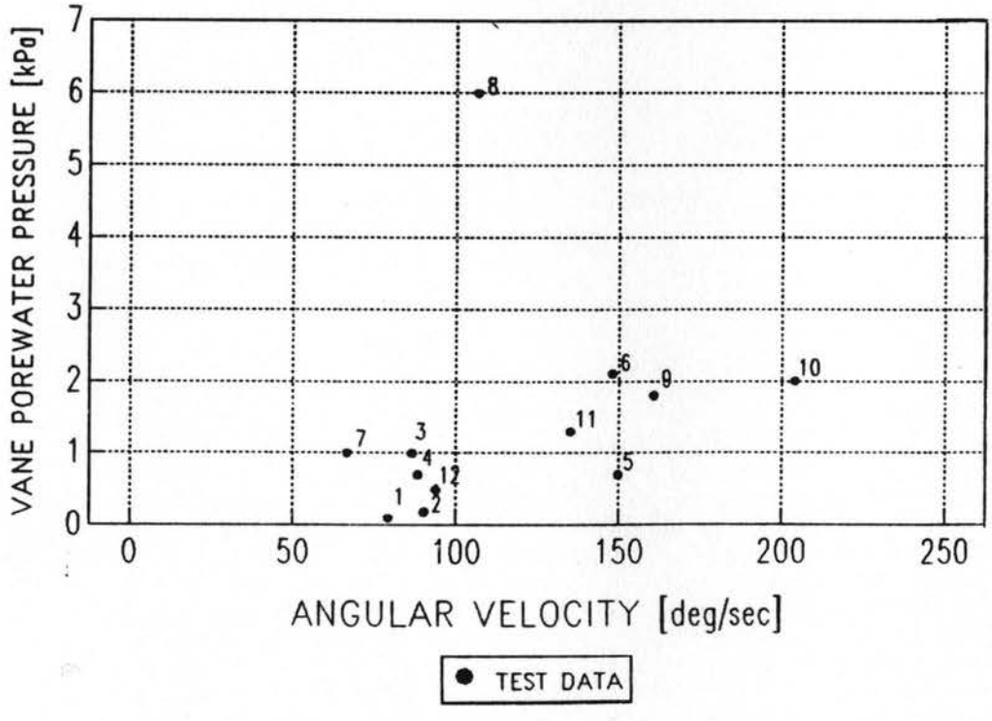

Figure 5.3 Angular Velocity vs. Residual Porewater Pressure Response

5. Effects of Insertion of Piezovane in Chamber

Piezovane Tests 3, 4, 6, 8, and 9 were the initial tests conduct on the Chamber specimens. For these tests, the vane was inserted to the test position before consolidation of the specimen. Piezovane Tests 5, 7, 10 and 12 were conducted after the initial tests. The vane was lowered to the second (lower) position within the specimen after the initial tests. The tests at the lower position had consistently greater shear strength than the test at an initial (upper) position. This was attributed to an increase in the normal effective stress caused by volumetric displacement from the advancement of the Piezovane and increased rod friction. This was also observed by Scott (1989).

Table 5.4 Piezovane Test Results

Test No.	Position	σ_h' (kPa)	Porewater Pressure at Piezovane, kPa		Porewater Pressure at Edge of tank, kPa		Shear Strength, kPa	
			Peak	Residual	Peak	Residual	Peak	Residual
1	T	172.3	0.17	0.10	--	--	--	--
2	B	172.3	0.01	0.18	0.0	0.1	--	--
3	B(1)	34.4	0.5	1.0	0.04	0.04	52	63
4	T	120.6	-0.4	0.7	-0.3	1.96	38	52
5	B	120.6	0.5	0.7	0.0	0.3	11	5
6	T	120.6	0.3	2.1	0.0	4.9	80	28
7	B	86.1	-0.4	1.0	0.6	1.5	117	40
8	T	86.1	-1.25	6.0	-1.0	4.6	105	15
9	T	241.1	-0.3	1.8	0.0	0.8	25	7
10	B	17.2	-3.0	2.0	-2.3	2.0	51	8
11	T	103.3	-0.6	1.3	0.0	1.6	100	20
12	B	103.3	-0.8	0.5	0.3	0.7	165	60

(1) Same test position as Test 2 however effective σ_v' stress decrease from 172.3 to 34.4 kPa.

CHAPTER VI

ANALYSIS OF RESULTS

A. Comparison of Results of Triaxial Tests

There are two dependent steady state variables which can be determined from triaxial tests and Piezovane tests. The two variables are shear strength (S_v) and effective normal stress to the shear plane (σ_f'). To obtain these variables from the Piezovane requires an assumption that the shear surface is uniform and cylindrical. It was also assumed that the radial effective stress (σ_h') controls the shear strength (Scott, 1989). Generally, all tests were conducted on dilative specimens except for Tests 1, 2, and 8 which were conducted on contractive specimens as indicated on Figure 6.1. Also included on Figure 6.1 are steady state lines determined by direct shear tests; triaxial tests with and without PVS Tests 6 and 9; and Poulos et al., (1985).

1. Peak and Steady State Shear Strength Comparison

The Piezovane shear strength was calculated from the shear vane torque using the Cadling equation presented in Chapter 2 (Eq. 2.4). The peak shear strength was calculated using the peak torque during the initial shear stages. The steady state shear strength was selected where the torque remained relatively constant at large strain.

The peak reference shear strength was also predicted using the effective internal friction angle (ϕ_s') from triaxial tests and the peak normal effective stress on the failure plane ($\sigma'_{f\ peak}$). The peak reference shear strength can be expressed as:

$$S_{refpeak} = \sigma'_{f\,peak} \tan \phi'_s \qquad \text{Eq. 6.1a}$$

The steady state reference shear strength was also predicted using the steady state normal effective stress on the failure plane ($\sigma'_{f\,ss}$) and the effective internal friction angle (ϕ_s'). The steady state shear reference strength can be expressed as:

$$S_{refss} = \sigma'_{f\,ss} \tan \phi_s' \qquad \text{Eq. 6.1b}$$

The peak normal effective stress along the Piezovane failure surface (σ'_f) was estimated using the horizontal effective stress (σ'_{hc}) reduced by the change in pore pressure (Δu_{peak}) at the peak shear stress.

$$\sigma'_{f\,peak} = \sigma'_{hc} - \Delta u_{peak} \qquad \text{Eq 6.2a}$$

The steady state normal effective stress along the failure surface was calculated using the horizontal effective stress (σ'_{hc}) reduced by the change in pore pressure (Δu_{ss}) at steady state deformation.

$$\sigma'_{f\,ss} = \sigma'_{hc} - \Delta u_{ss} \qquad \text{Eq 6.2a}$$

The horizontal effective stress (σ'_{hc}) was a function of the vertical effective stress (σ'_{vc}) after consolidation and the coefficient of lateral stress (K_o):

$$\sigma'_{hc} = K_o \sigma'_{vc} \qquad \text{Eq 6.3}$$

where a vertical effective stress (σ'_{vc}) is the stress condition applied to the bottom of the calibration chamber. K_o had been previously assumed by Castro (1985b) to be $K_o = 0.5$ and Scott (1989) used $K_o = 1 - \sin\phi_s'$. For the purpose of this study, $K_o = 0.5$ was used.

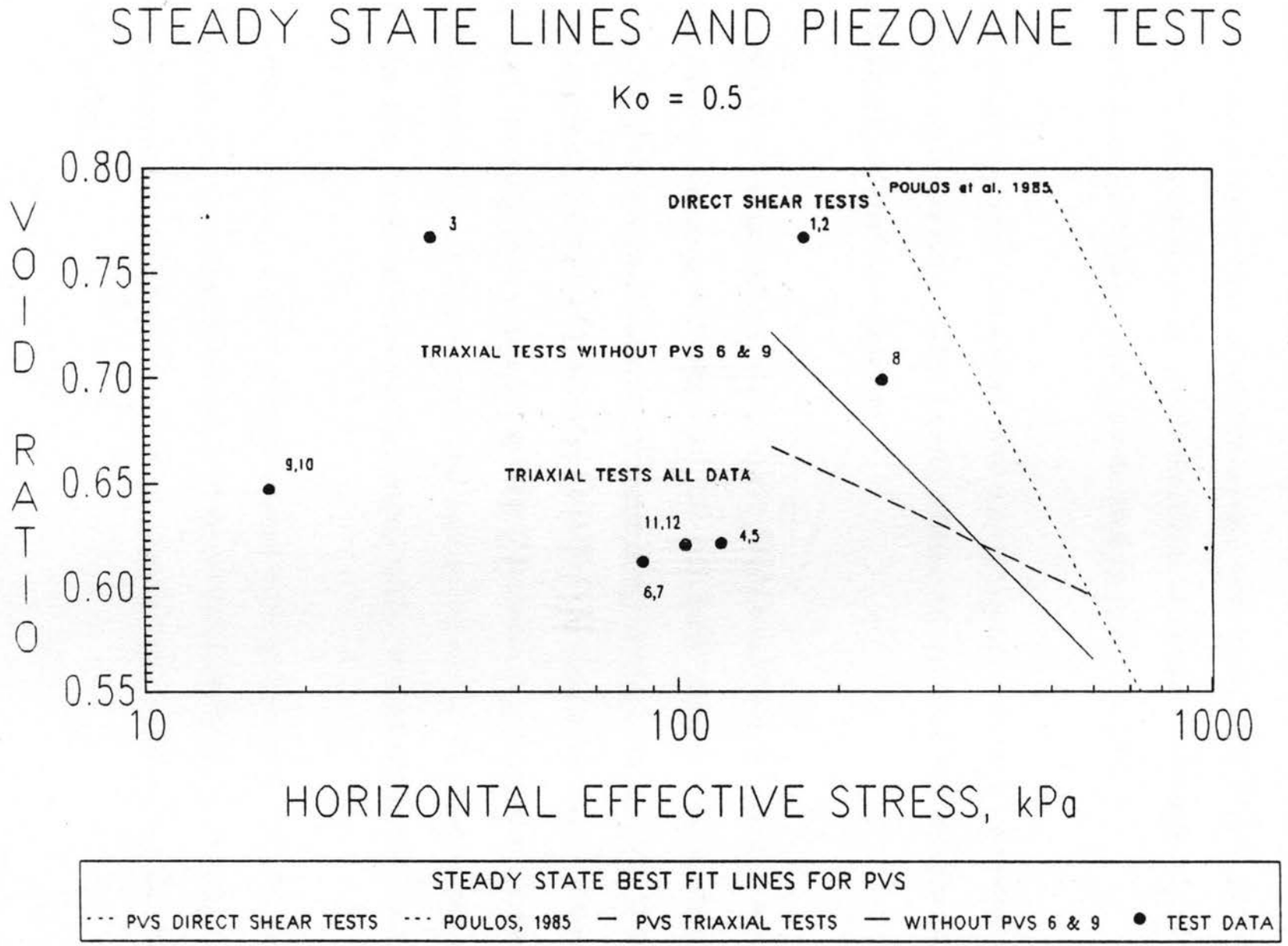

Figure 6.1 Piezovane Tests and Steady State Lines

Equation 6.1 also assumes that during shearing of the Piezovane, no void ratio change occurred within the specimen and that the vertical effective stress remained constant. There was a large amount of data scatter with void ratio versus steady state friction angle (ϕ'_s), as depicted in Figure 6.2. Therefore, an average value for the effective steady state friction angle (ϕ'_s) of 34.0° (standard deviation 1.8°) was obtained from the triaxial tests that were used.

Both the peak and steady state normal effective stress to the shear plane (σ_f') are presented in Table 6.1. Also presented in Table 6.1 are the reference and measured shear strengths (S_v) for both the peak and steady state conditions.

The peak reference shear strengths computed using Eq. 6.1a and measured peak shear strengths from Piezovane tests are plotted in Figure 6.3. Generally, for the dilated tests, the measured peak shear strengths were greater than the calculated peak reference shear strength. This was attributed to an increase in effective stress along the shear plane due to dilation of the sand particles. The contractive specimen in Test 8 had a lower measured peak shear strength than the calculated peak reference shear strength. This probably indicates that the effective stress along the shear plane was reduced due to positive porewater pressure from contraction of the sand.

The steady state reference shear strength and measured steady state shear strengths from the Piezovane were plotted on Figure 6.4. With the exception of Test 3, the measured shear strengths were less than the calculated reference shear strengths. This was also observed by Scott (1989).

Table 6.1 Effective Normal Stress and Shear Stress From Piezovane Tests

Test No.	e_c	σ'_{vc} (kPa)	σ'_{hc} (kPa)	Δu (kP)A Peak (1)	SS (2)	σ'_f (kPa) Peak	SS	S_v (kPa) Peak (1)	SS (2)	S_{ref} (kPa) Peak (1)	SS (2)
1	0.767	344.5	172.3	0.2	0.2	172.1	172.1	--	--	--	--
2	0.767	344.5	172.3	0.0	0.3	172.3	172.0	--	--	--	--
3	0.767	68.9	34.4	-0.5	1.0	33.9	33.4	52	63	22	22
4	0.621	241.1	120.6	0.5	0.7	121.1	121.3	38	52	79	79
5	0.621	241.1	120.6	0.5	0.7	121.1	121.3	11.5	50	79	79
6	0.612	172.3	86.1	0.3	2.1	85.8	84.0	80.0	27	56	55
7	0.612	172.3	86.1	-0.4	1.0	86.5	85.1	117.0	40	56	55
8	0.699	482.3	241.1	-1.3	6.0	242.4	235.1	105.0	15	157	153
9	0.647	34.4	17.2	-0.3	1.8	17.5	15.4	25.0	7	11	10
10	0.647	34.4	17.2	-3.0	2.0	20.2	15.2	51.0	8	13.1	10
11	0.620	206.7	103.3	-0.6	1.3	102.7	104.6	100.0	20	67	68
12	0.620	206.7	103.3	-0.8	0.5	104.1	102.8	165.0	60	68	67

e_c - void ratio after consolidation

σ_{vc} - effective vertical stress

σ_{hc} - effective horizontal stress (K_o = 0.5)

Δu - change in porewater pressure

σ'_f - effective normal stress

(1) at peak shear strength

(2) at large strains

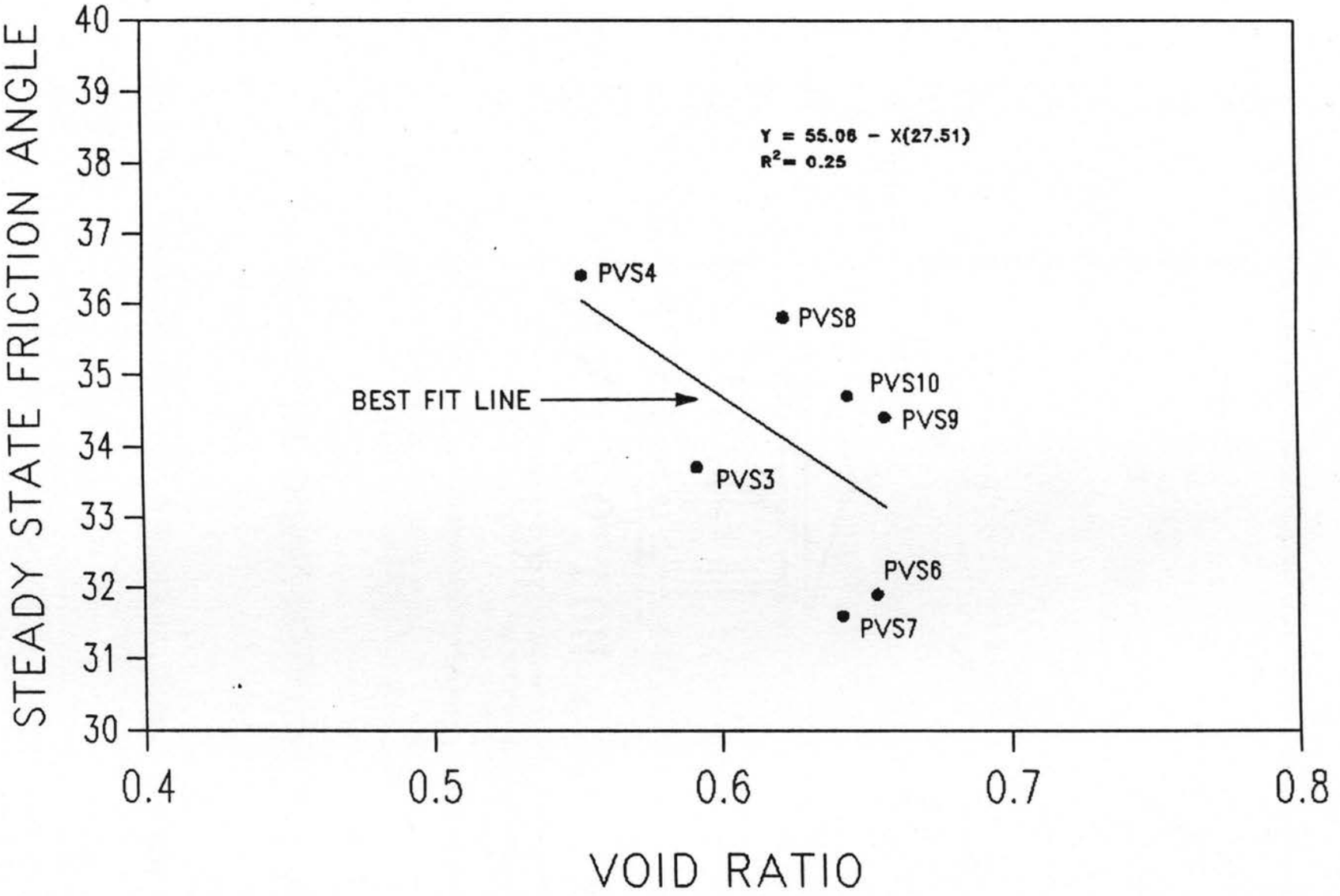

Figure 6.2 Effective Steady State Friction Angles vs. Void Ratio

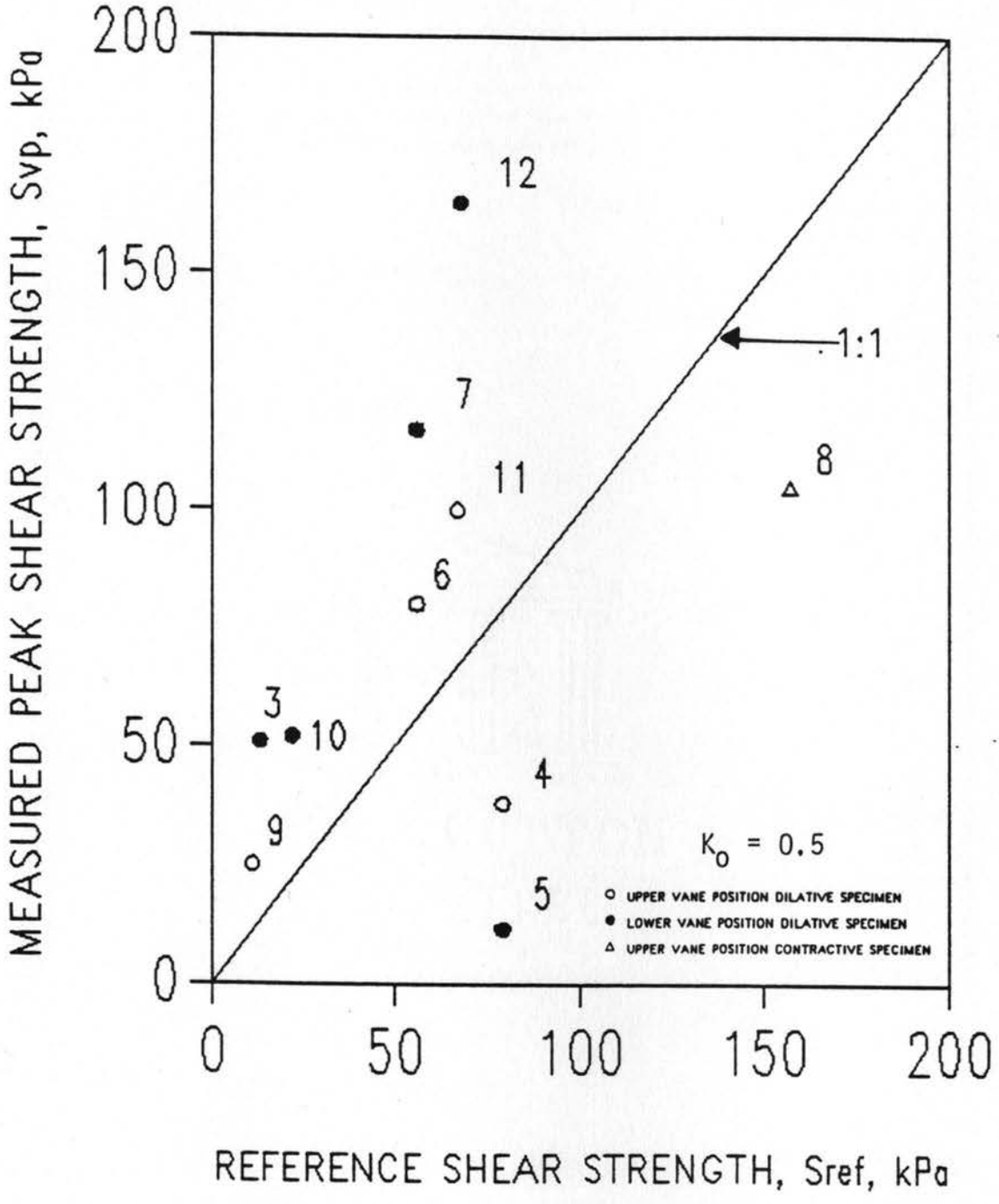

Figure 6.3 Measured Peak Shear Strength vs. Reference Shear Strength.

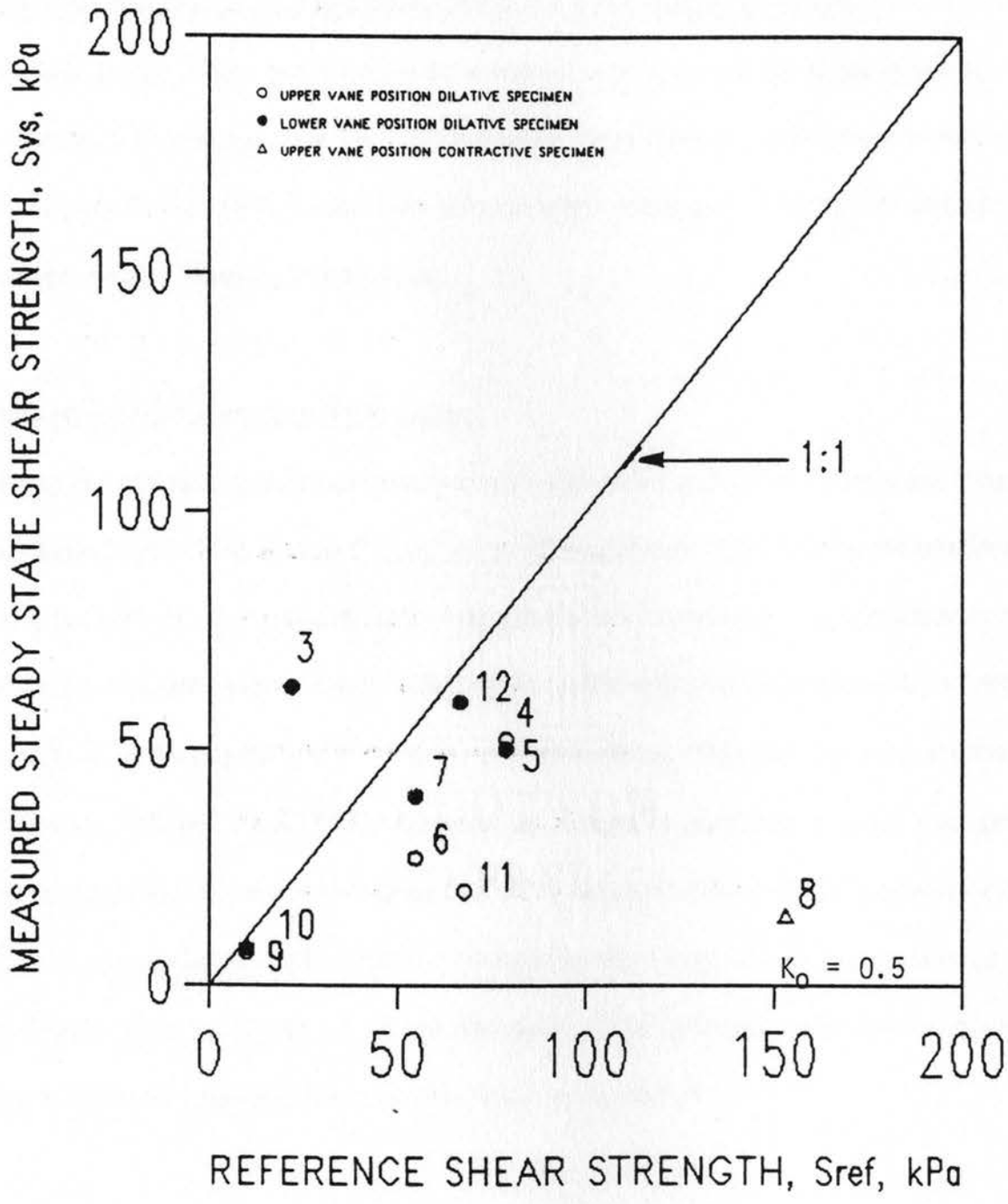

Figure 6.4 Measured Steady State Shear Strength vs. Reference Shear Strength.

B. Determining Contractive or Dilating Behavior from Piezovane Results

Based on the steady state line developed from triaxial tests, the majority of the Piezovane tests were conducted on specimens having a dilative state. Only Tests 1, 2 and 8 were conducted on contractive specimens. Tests 1 and 2 were plagued with instrumentation and noise problems; the results were omitted from the final analysis.

1. Analysis of Porewater Pressure Response

Two types of porewater pressure responses were observed for the Piezovane tests. The two responses can be classified as a dilative and contractive response. The initial porewater pressure response for both dilative and contractive samples was a negative porewater pressure spike during the initial shearing of the vane. This initial negative spike was most likely due to dilation of the particles at the edge of the blade at the start of shearing. This response was observed by others (Castro, 1982 and Scott, 1988). After the initial negative porewater pressure response, the dilative samples had slight positive (less than 2.5 kPa) porewater pressure responses during shearing. Some specimens had negative porewater pressure responses at large strains such as seen on Test 4, shown on Figure 5.1. It was also observed that at higher strains there was a slight increase in porewater pressure shown on Test 9 also on Figure 5.1.

The contractive specimen's porewater pressure response was similar to the porewater pressure response of the triaxial tests, a constant increase in porewater pressure to the steady state condition where it stabilized was observed. In contrast to the slight porewater pressure response observed within the dilative specimens, the contractive specimen response was much greater, as depicted for Test 8 in Figure 5.1.

Tests where the Piezovane stopped during shearing had a noticeable effect on the porewater pressure response. Dilative specimens would have a negative porewater pressure response during the pause. A positive porewater response would occur with the commencement of shearing as observed in Figure 6.5. The contractive specimen had a positive porewater pressure during a pause in the shearing. The contractive response is shown in Figure 6.6. This response of porewater during pauses in shearing could be used as an indication of contractive or dilative states.

2. Analysis of Porewater Pressure Dissipation and Rate of Shearing

The amount of drainage which occurred during shearing was estimated using Blights Equation (Eq. 2.7). The coefficient of compressibility, m_v, was determined from the consolidation phase of the Piezovane test. The coefficient of compressibility was used to obtain coefficient of consolidation, C_v:

$$C_v = \frac{k}{\gamma_w m_v} \qquad \text{Eq. 6.4}$$

The time to failure was estimated from vane tests to occur when the peak stress was reached. The range of coefficient of compressibility (m_v), coefficient of permeability (k), coefficient of consolidation C_v), and time to failure (t) are listed in Table 6.2.

Table 6.2: Estimation of Porewater Pressure Dissipation

	Best Case	Worst Case
Coefficient of Compressibility, m_v, (m^2/kN)	4.76×10^{-5}	2.53×10^{-5}
Coefficient of Permeability, k, (m/s)	6.4×10^{-3}	1.05×10^{-2}
Coefficient of Consolidation, C_v, (m^2/s)	13.9	42.3
Time to Failure, t, (sec)	0.05	3.0
Sphere of Influence, a, (m)	0.0935	0.0635
Dissipation, U (%)	99.0	99.0

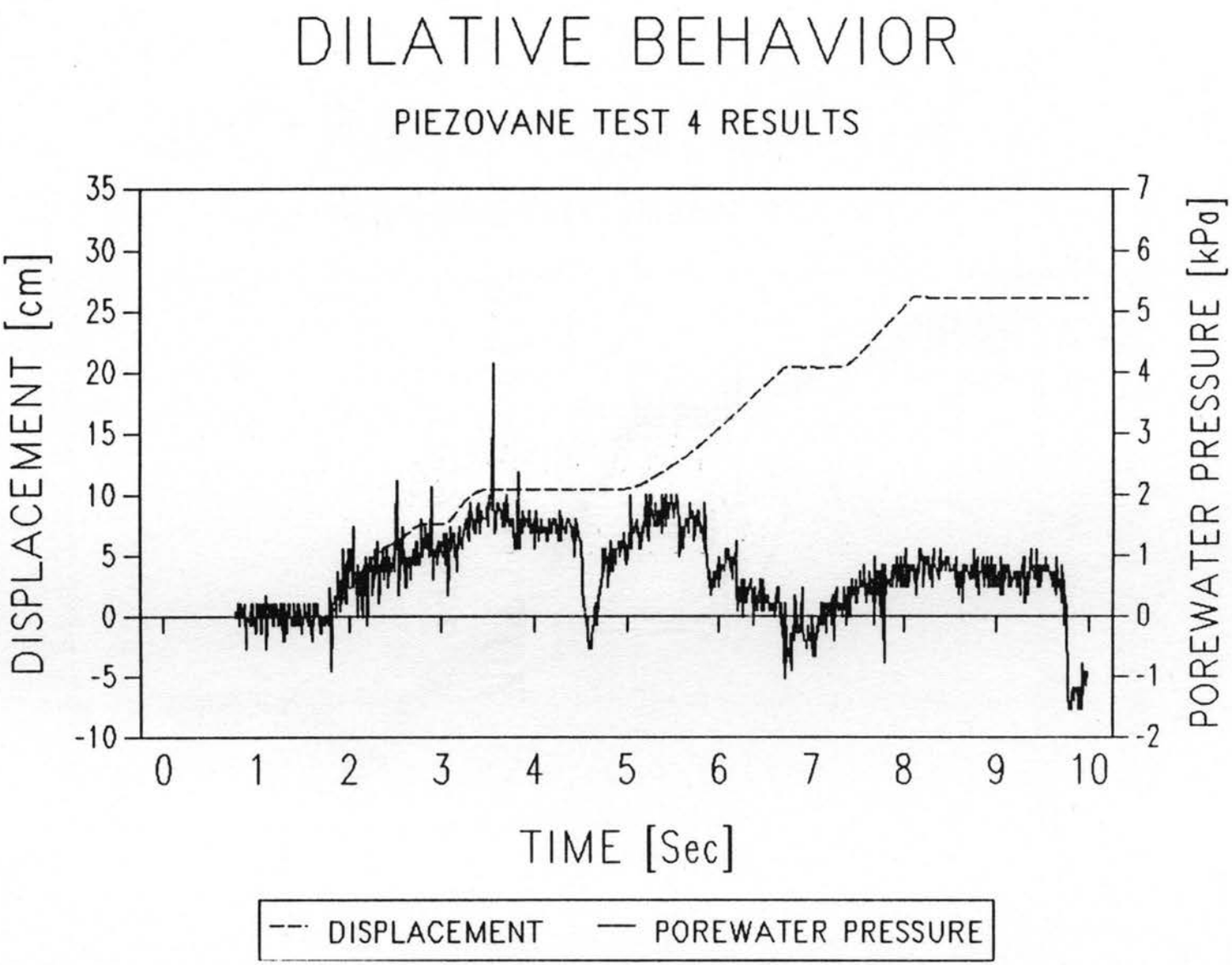

Figure 6.5 Dilative Porewater Pressure Response

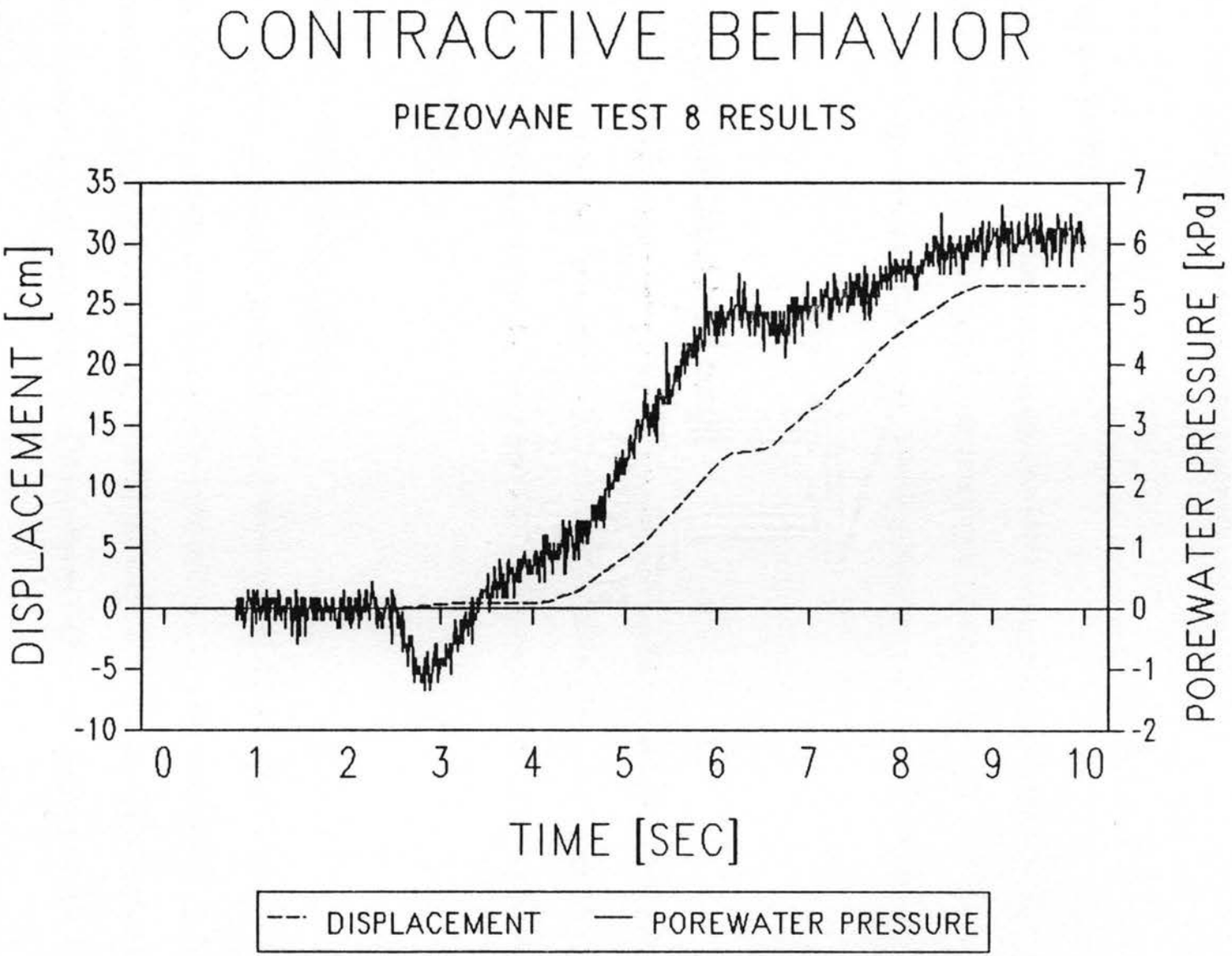

Figure 6.6 Contractive Porewater Pressure Response

Blight (1967) estimated that the sphere of influence would range from a = Diameter of vane (D) to 3D/2. The estimation of dissipation indicates that all test were drained tests. However,the drainage of the chamber may have caused the tests to be partially drained.

3. Steady State Shear Response

The responses of the steady state shear strength in relation to the location to the steady state line is indicated on Figure 6.7. The data indicates that no noticeable difference in shape occurs between dilative and contractive specimens. However, the author is aware of the limitations of the data.

C. Factors Affecting Experimental Results

There were three major factors affecting the experimental results of laboratory testing of the Piezovane. These include the estimate of the normal effective stress on the failure plane; measuring the void ratio of the soil near the Piezovane; and increased torque from friction along the Piezovane shaft.

1. Estimate of the Normal Effective Stress

There is a question on the actual lateral effective stresses applied within the calibration chamber. Results indicate that the K_o at the vane location may be larger than the estimated ($K_o = 0.5$). The increase K_o value could result from some stress concentration due to side friction and boundary effects of the calibration chamber or stress changes induced by shearing the soil when the vane is rotated.

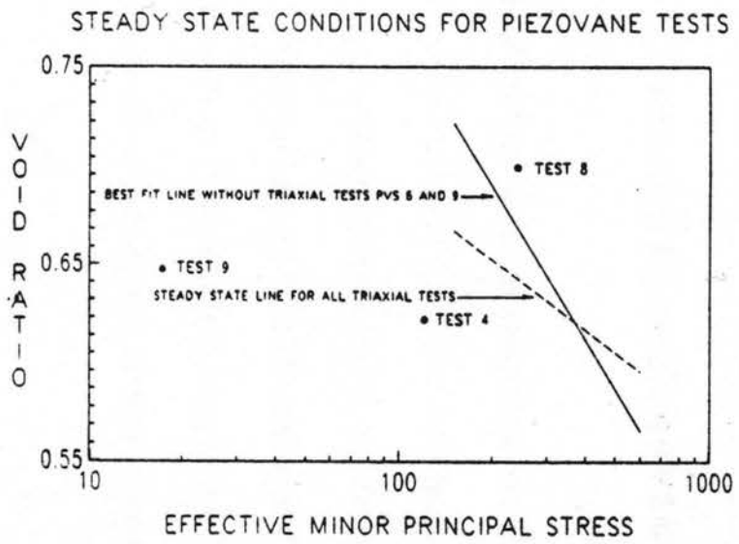

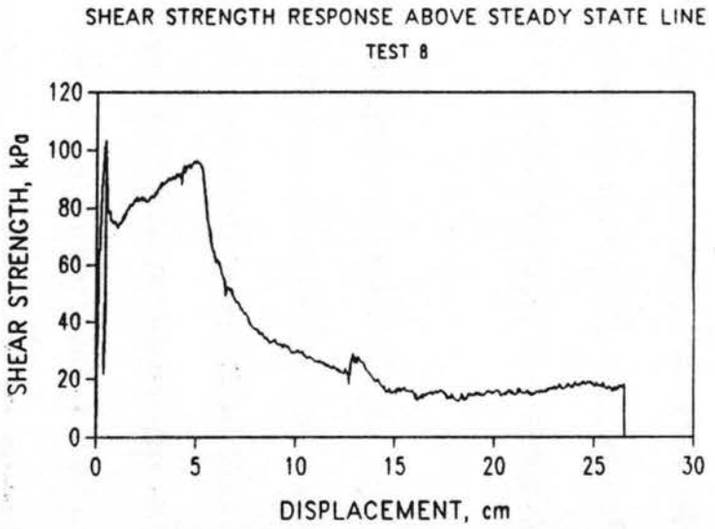

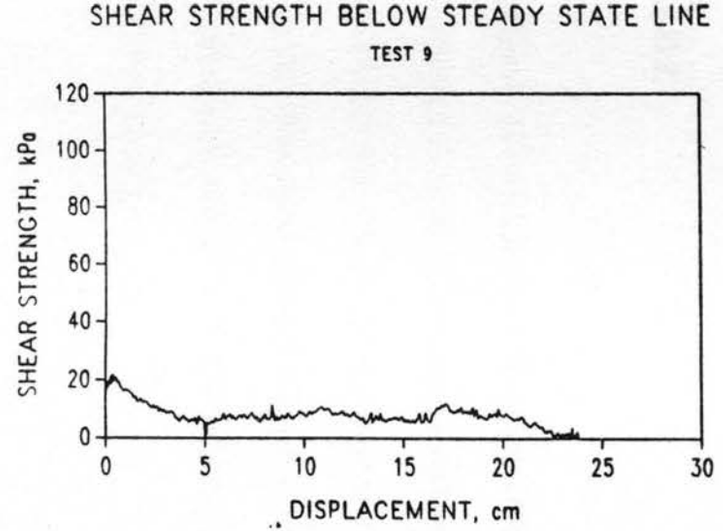

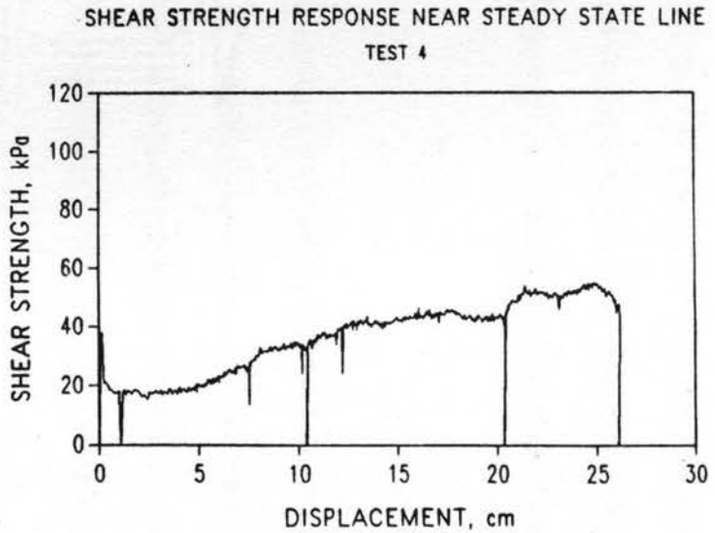

Figure 6.7 Steady State Line and Shear Strength for Piezovane Tests

Also, soil arching from the one dimensional loading applied at the bottom of the specimen could occur at large effective stresses. The arching of the membrane may have imposed an non-uniform stress distribution across the specimen. The non-uniform stress distribution may have increased the stress concentration at the center of the specimen where the Piezovane was located. The uncertainty in the actual K_o could have effected the estimate of the normal effective stress on the failure surface. This would also change the position of the test specimen to the steady state line.

2. Estimation of the Void Ratio

The determination of the void ratio was an average void ratio within the sample based upon the total volume and amount of sand placed within the chamber. Collapse of the specimen during wetting also limited testing at higher void ratios where less effective stress would be required. The uncertainty in the actual void ratio at the vane location could affect the estimate of the specimen's relationship to the steady state line.

3. The Effects of Friction Along the Piezovane Shaft

Side friction along the Piezovane could have influenced the measured shear strength. The amount of torque which can be attributed to the side friction could not be measured since the torque gauge was located at the top of the shaft. Within the calibration chamber test this is probably not as significant, as the depth of the embedment is less than 0.3 to 0.6 meter. However, in future in situ testing, the amount of side friction along the shaft will be significant and should be taken into account when determining shear strength.

CHAPTER VII

SUMMARY, CONCLUSIONS AND RECOMMENDATIONS

A. Summary

The purpose of this study was to develop and evaluate the Piezovane, a new in situ device for determining liquefaction potential. The scope of this study was limited to the design, construction and preliminary testing of the Piezovane. Current methods of in situ evaluation of liquefaction potential are empirical, based on correlation of SPT, CPT or shear wave velocity analysis. Based upon the steady state liquefaction analysis, the liquefaction potential can be determined by ascertaining the contractive/dilative behavior of the in situ soils.

The Piezovane was developed so that porewater pressure and shear strength could be measured in situ during testing. The changes in porewater pressure were measured along the shear zone by pressure ports placed at the edge of the blade of the Piezovane. Torque and rotation of the Piezovane were recorded to determine stress and strain conditions during testing. Steady state normal effective stress and shear strength was determined for a poorly graded angular sand (PVS) by CU triaxial tests. The Piezovane was tested within the laboratory using a large one-dimensional calibration chamber developed for this study.

Piezovane test results indicate that both positive and negative porewater pressure responses could be measured. Constant and/or negative porewater pressure responses were observed for dilative

samples and a large positive porewater pressure response was observed for the contractive sample. Tests were conducted under drained conditions.

Shear strength measured by the Piezovane had significant scatter. The general trend observed was that steady state shear strengths were lower than the CU triaxial steady state shear strengths. The peak shear strengths for dilative samples were higher than the CU triaxial tests. The contractive sample had a lower peak shear strength than the CU triaxial test. This could be attributed to the partially drained conditions and the porewater pressure response of the sample. Generally, these observations were also made by Scott (1989).

B. Conclusions

Based on this study, distinct porewater pressure trends can be observed from the Piezovane. Dilative samples exhibited negative and/or little positive porewater pressure response. The contractive sample porewater pressure response was positive. The pressure response is more pronounced during pauses in shearing. Steady state shear strength (large strains) determined by the Piezovane are generally less than calculated assuming undrained conditions. However, due to the high permeability of the sand, undrained steady state shear strengths may approach the steady state shear strength for drained conditions. In its present form the Piezovane can be used as an index tool for determining liquefaction potential.

C. Recommendations

Results of the literature review and laboratory testing suggest that additional studies are required to evaluate the Piezovane as a device for determining liquefaction potential of soils. Based upon this investigation, the following recommendations for modification to the Piezovane and calibration chamber are suggested before additional testing commences. The following recommendations for additional field and laboratory testing are presented.

1. Modifications to Piezovane and Calibration Chamber

a. Modifications to Piezovane

The existing Piezovane should be modified to limit the effects of trapped air and shaft friction. The modification should include placing the porewater pressure transducer near the edge of the blade. The cavity of the transducer should be filled with glycerin or silicone oil prior to placement within the blade. A porous stone also saturated with glycerin or silicon oil should be placed between the transducer and the soil to prevent soil particles from becoming trapped within the transducer cavity and damaging the transducer. To reduce the effects of side friction along the shaft, it is recommended that the strain gage be placed on the shaft just above the Piezovane to measure the torque required for the vane to shear the soil. The effects of side friction will become more significant as the Piezovane is used in the field at greater depths than tested in this study. To provide more accurate rotation data, it is also recommended that an accelerometer or velocity transducer be placed within the blade of the Piezovane. This will reduce cumbersome equipment at the surface and limit errors associated with tightening of connections and elastic strain of shaft under large shear stresses.

b. Modifications to Calibration Chamber

Due to the complex stress distribution of the calibration chamber, the chamber should be modified so that horizontal stresses can be applied to the specimen. This can be accomplished by adding a second tubular membrane around the sides of the chamber. Actual stresses within the specimen should then be measured using total stress cells placed within the specimen near the Piezovane. Total stress cells should be situated to measure both vertical and horizontal stresses.

2. Additional Testing Recommendations

Additional research needs to be conducted after the above-recommended modification to the Piezovane and calibration chamber are made. Testing on various gradations and angularities of soils should be conducted to determine the overall ability of the Piezovane to evaluate liquefaction potential. Tests should be conducted on samples that can be tested in the calibration chamber and in the field where the steady state conditions have already been determined. Testing should include the effect of the Piezovane at higher strains such as two to three rotations (720° to 1080°).

CHAPTER VIII

REFERENCES

Al-Mukhtar, M., Robinet, J. C., and Shahrour, I., (1988), "Monotonic and Cyclic Penetration Tests in Calibrated Chamber." Proceedings, First International Symposium on Penetration Testing, Orlando, FL, March, A. A. Balkema, Rotterdam, Vol. 2, pp. 621-633.

ASTM, (1989), Annual Book of ASTM Standards, "Soil and Rock; Building Stone", Vol. 04.08, Philadelphia, PA.

Arman, A., Poplin, J. K., and Ahmad, N., (1975), "Study of the Vane Shear." Proceedings, In Situ Measurement of Soil Properties, ASCE Speciality Conference, Raleigh, North Carolina, June, Vol. 1, pp. 93-120.

Barros, P. L. A., and Barros, C. L. A., (1989), "Vane Shear Test Application on Cohesionless Soils." Proceedings of the Twelfth International Conference on Soil Mechanics and Foundation Engineering, ISCMFE, Rio De Janeiro, Brazil, Vol. 1, Aug 13-18, pp. 171-174.

Been, K., Crooks, J. H. A., and Rothenburg, L., (1988), "A Critical Appraisal of CPT Calibration Chamber Tests." Proceedings, First International Symposium of Penetration Testing, Orlando, FL, March, A. A. Balkema, Rotterdam, Vol. 2, pp. 651-660.

Bellotti, R., Bizzi, G., and Ghionna, V. N., (1982), "Design, Construction and Use of a Calibration Chamber." Proceedings, Second European Symposium of Penetration Testing, Amsterdam, May, A. A. Balkema, Rotterdam, Vol. 2, pp. 439-466.

Bellotti, R., Crippa, V., Ghionna, V. N., and Pedroni, S., (1988), "Saturation of Sand Specimen for Calibration Chamber Tests." Proceedings, First International Symposium of Penetration Testing, Orlando, FL, March, A. A. Balkema, Rotterdam, Vol. 2, pp. 661-679.

Blight, G. E., (1968), "A Note on Field Vane Testing of Silty Soils." Canadian Geotechnical Journal, Vol. 5, No. 3, pp. 142-149.

Bretz, T. E. (1989), Soil Liquefaction resulting from Blast-Induced Spherical Stress Waves, Ph.D. Dissertation, Colorado State University, Fort Collins, Colorado, Fall 1989.

Bunnell, D. B., (1978), "A Study of Excess Pore Pressures Generated by a Penetrating Probe in Granular Soils," Masters Thesis, Dept. of Civil Engineering, University of Florida, pp. 23-25.

Cadling, L., and Odenstad, S., (1950), "The Vane Borer." Proceedings No. 2, Royal Swedish Geotechnical Institute, Stockholm, 87p.

Campanella, R. G., Robertson, P. K., Gillespie, D. G., (1983), "Cone Penetration Testing in Deltaic Soils, " Canadian Geotechnical Testing Journal, Vol. 20, No. 1, pp. 23-35.

Canou, J., El Hachem, M., Kattan, A., and Juran, I, (1988), "Mini Piezocone Investigation Related to Sand Liquefaction Analysis." Proceedings, First International Symposium on Penetration Testing, Orlando, Florida, March, A. A. Balkema, Rotterdam, Vol. 2, pp. 699-706.

Casagrande A., and Watson J. D. (1938), Appendix BII Of: "Compaction Tests and Critical Density Investigations of Cohesionless Materials for Franklin Fall's Dam, " Report for U.S. Engineer Corps, Boston, 1938.

Casagrande, A., (1940), "Characteristics of Cohesionless Soils Affecting the Stability of Slopes and Earth Fills." Boston Society of Civil Engineers, January, pp. 257-276.

Casagrande, A., (1975), "Liquefaction and Cyclic Deformation of Sands, a Critical Review." Harvard Soil Mechanics Series No. 88, Pierce Hall, Cambridge, MA., 27p.

Castro, G., and Poulos, S. J., (1977), "Factors Affecting Liquefaction and Cyclic Mobility." Journal of Geotechnical Engineering Division, ASCE, Vol. 103, No. 6, pp. 501-515.

Castro, G., Enos, J. L., France, J. W., and Poulos, S. J., (1982a), "Liquefaction Induced Cyclic Loading." Final Report, NSF/CEE-82018, National Science Foundation, Geotechnical Engineering Inc., March, 325p.

Castro, G., France, J. W., and Shields D. R., (1982b), "Field Index Test for Estimating Liquefaction Potential." Final Report, Award No. CEE-8114111, SBIR Phase I, National Science Foundation, Geotechnical Engineering Inc., March, 23p.

Castro, G. (1969), "Liquefaction of Sands" Ph.D. Thesis, Harvard Soil Mechanics Series, No. 81, Pierce Hall, Harvard University, 112p.

Charlie, W. A. and Butler, L. W. (1990), "A Method for Determining Liquefaction Potential of Cohesionless Soils," Air Force Invention No. 18,634, Declaration for Patent Application, U.S Patent and Trademark Office, Washington, D.C.

Charlie, W. A.; Veyera, G. E., Doehring, D. O., and Abt, S. R., (1985b), "Blast Induced Liquefaction Potential and Transient Porewater Pressure Response of Saturated Sands." Final Report, Grant No. AFOSR-80-0260, Air Force Office of Scientific Research, Colorado State University, Dept. of Civil Engineering, Fort Collins, Co., 198p.

Dobry, R., Stokoe, K. H. Ladd, R. S., and Youd, T. L., (1981), "Liquefaction Susceptibility from S-Wave Velocity." In Situ Testing to Evaluate Liquefaction Susceptibility Proceedings, Session 24, ASCE National Convention, St. Louis, pp. 55-64.

Hassen, H. A., (1994), Saturated Sand Response and Liquefaction Under Planar Explosive Loading, Ph. D. Dissertation, Colorado State University, Fort Collins, Colorado.

Hazen, A. (1920), "Hydraulic Fill Dams," ASCE Transactions, Vol. 83, pp. 1713-1745.

Head, K. H. (1986), Manual of Soil Laboratory Testing, Vol. 3, Effective Stress Tests, Wiley, New York.

Housner, G.W., Chmn., (1985), Liquefaction of Soils During Earthquakes, Commission on Engineering and Technical Systems, National Research Council, National Academy Press, Washington, D.C., 240p.

Huberts, M.E., (1986), Shock Loading of Water Saturated Eniwtok Coral Sand, M.S. Thesis, Colorado State University, Dept. of Civil Engineering, Fort Collins, Colorado, Summer.

Ladd, R., S., (1978), "Preparing Test Specimens using Undercompaction." Geotechnical Testing Journal, ASTM, GTJODJ, Vol. 1, No. 1, pp. 16-23.

Marchetti, S., (1982), "Detection of Liquefiable Sand Layers by Means of Quasi-static Penetration Tests." Proceedings, Second European Symposium on Penetration Testing, Amsterdam, May, A. A. Balkema, Rotterdam, Vol. 2, pp. 689-695.

Marcuson, William F., III,Chmn., (1978), "Definition of Terms Related to Liquefaction," Journal of the Geotechnical Engineering Division, ASCE, Vol. 104, No. GT9 pp. 1197-1200.

Muzze, M. W., (1983), Cyclic Triaxial Behavior of Monterey No. 0 and No. 0/30 Sands, M. S. Thesis, Colorado State University, Dept. of Civil Engineering, Fort Collins, Colorado, May.

Osterberg, J. D. (1956) "Symposium on Vane Shear Testing of Soils", STP 193, American Society for Testing and Materials, Philadelphia, Penn., pp. 1-7.

Peck, R. B., (1979), "Liquefaction Potential: Science Versus Practice." Journal of Geotechnical Engineering Division, ASCE, Vol. 105, No. 3, pp. 393-398.

Perlow, M., and Richards, A. F., (1977), "Influence of Shear Velocity on Vane Shear Strength." Geotechnical Testing Journal, ASTM, Vol. 103, No. GT1, pp. 20-32.

Poulos, S. J. (1971), "The Stress-Strain Curves of Soil," Geotechnical Engineers Inc. Winchester, MA, pp. 1-80.

Poulos, S. J., (1981), "The Steady State of Deformation." Journal of Geotechnical Engineering Division, ASCE, Vol. 107, No. 5., pp. 553-561.

Poulos, S. J., (1988), "Strength of Static and Dynamic Stability Analysis." Hydraulic Fill Structures, Specialty Conference, Geotechnical Division, ASCE, Fort Collins, CO., pp. 452-474.

Poulos, S. J., Castro, G., and France, J. W., (1985), "Liquefaction Evaluation Procedure." Journal of the Geotechnical Engineering Division, ASCE, Vol. 111, No. 6, pp. 772-792.

Poulos, S. J.; Robinsky, E. I. and Keller, T. O., (1985), "Liquefaction Resistance of Thickened Tailings", Journal of Geotechnical Engineering Division, ASCE, Vol. 111, No. 12, pp. 1380-1385.

Rad, N. S., and Tumay, M. T., (1987), "Factors Affecting Sand Specimen Preparation by Raining." Geotechnical Testing Journal, ASTM, Vol. 10, No. 1, pp. 31-37.

Robertson, P. K., and Campanella, R. G., (1985), "Liquefaction Potential of Sands using the CPT." Journal of the Geotechnical Engineering Division, ASCE, Vol. 111 No. 3, pp. 384-403.

Roscoe, K. H., (1953), "An Apparatus for the Application of Simple Shear to Soil Sample." Proceedings, 3rd International Conference on Soil Mechanics and Foundation Engineering, Vol. 1, Switzerland, pp. 186-191.

Roscoe, K. H., Schofield, A. N., and Wroth, C. P., (1958), "On Yielding of Soils." Geotechnique, Vol. 8, pp. 22-53.

Schmertmann, J. H., (1978), "Study of Feasibility of Using Wissa-Type Piezometer Probe to Identify Liquefaction Potential of Saturated Fine Sands," Technical Report S-78-2, U.S. Army Engineer Waterways Experiment Station, University of Florida, 73 p.

Scott, C. E., (1989), "Estimating Liquefaction Potential of Sands Using the Piezovane," M.S. Thesis, Colorado State University, Department of Civil Engineering, Ft. Collins, CO., Summer.

Seed, H. B., and Lee, K. L., (1966), "Liquefaction of Saturated Sands during Cyclic Loading." Journal of the Soil Mechanics and Foundations Division, ASCE, Vol. 92, No. 6, pp. 105-134.

Seed, (1976), "Evaluation of Soil Liquefaction Effects on Level Ground During Earthquakes," Liquefaction Problems in Geotechnical Engineering ASCE Annual Convention and Exposition, Philadelphia, Penn., pp. 1-104.

Seed, H. B., (1979), "Soil Liquefaction and Cyclic Mobility Evaluation for Level Ground During Earthquakes," Journal of the Geotechnical Engineering Division, ASCE, Vol. 105, No. 6T2, pp. 201-255.

Seed, H. B.; (1985), "Influence of SPT Procedures in Soil Liquefaction Resistance Evaluations." Journal of the Soil Mechanics and Foundations Division, ASCE, Vol. 111, No. 12, pp. 1425-1445.

Seed, H. B. (1987), "Design Problems in Soil Liquefaction," Journal of the Geotechnical Engineering Division, ASCE, Vol. 113, No. 8, August, pp. 827-845.

Seed, R. B.; Dickenson, S. E.; Riemer, M. F.; Bray, J. D.; Sitar, J.; Mitchell, J. K.; Idriss, I. M.; Kayern, R. E.; Kropp, A.; Harder, L. F. and Power, M. S.; Preliminary Report on the Geotechnical Aspects of the October 17, 1989 Loma Prieta Earthquake, (1990), Earthquake Engineering Research Center, University of California at Berkeley, Berkeley, California, 137p.

Seed, R. B. and Harder, L. F., (1990), "SPT-Based Analysis of Cyclic Pore Pressure Generation and Undrained Residual Strength." Memorial Symposium Proceeding for H. Bolton Seed, Vol. 2, B; Tech Publishers, Ltd., pp. 351-376.

Silver, M. L., (1977), "Laboratory Triaxial Testing Procedures to Determine the Cyclic Strength of Soils," Report NUREG-0031, United States Nuclear Regulatory Commission, 129p.

Skempton, A. W.; (1948), "Vane Tests in Alluvial Plain of the River Forth, Near Grangemouth, " Geotechnique, Vol. 1, pp. 111-124.

Skempton, A. W. (1954), "The Pore-Pressure Coefficients A and C," Geotechnique, Vol. 4, 143-147.

Taylor, D. W., (1939), "A Comparison of Results of Direct Shear and Cylindrical Compression Tests." Proceedings, 42nd Annual Meeting, American Society for Testing Materials, Technical Papers, Volume 39, pp. 1058-1070.

Terzaghi, K., (1943), Theoretical Soil Mechanics, John Wiley and Sons, New York, 510p.

Veyera, G. E., (1985), Transient Porewater Pressure Response and Liquefaction in a Saturated Sand, Ph.D. Dissertation, Colorado State University, Dept. of Civil Engineering, Fort Collins, Colorado, Fall.

Vickers, B., (1983), Laboratory Work in Soil Mechanics, Granda, New York, NY, 168p.

Wilson, N. E., (1963), "Laboratory Vane Shear Tests and the Influence of Pore-water Stresses." Symposium on Laboratory Testing of Soils, ASTM, STP No. 361, pp. 377-385.

Woods, R., and Henke, R., (1981), "Seismic Techniques in the Laboratory." Journal of Geotechnical Engineering Division, ASCE Vol. 107, No. 10, pp. 1309-1325.

APPENDIX

Piezovane Test Results
Figures A.1 through A.12

Triaxial Test Results
Figures A.13 through A.20

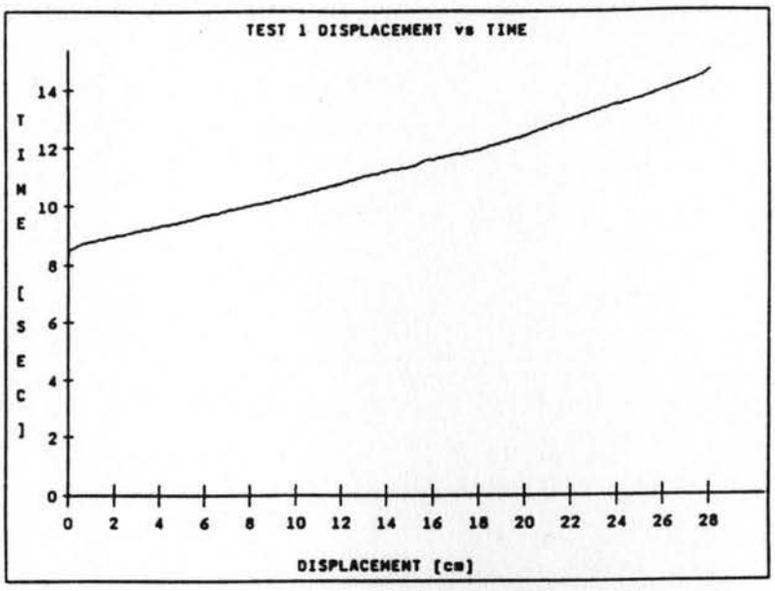

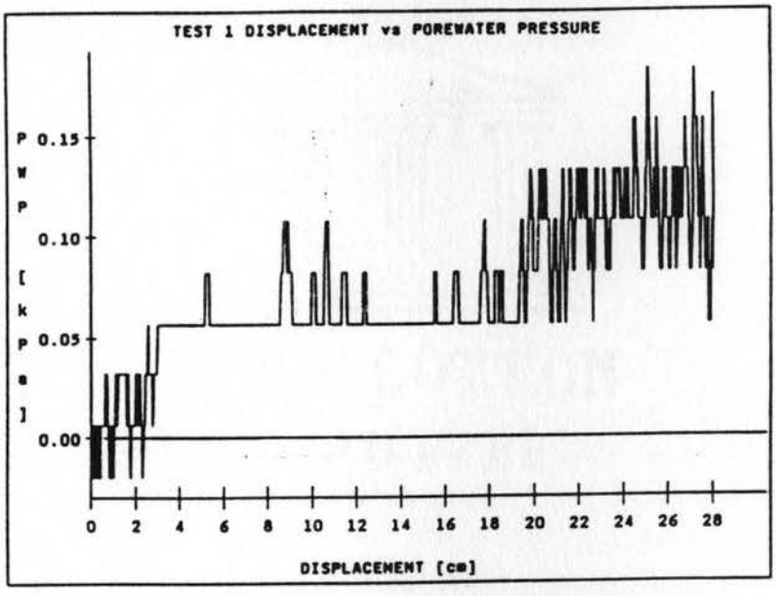

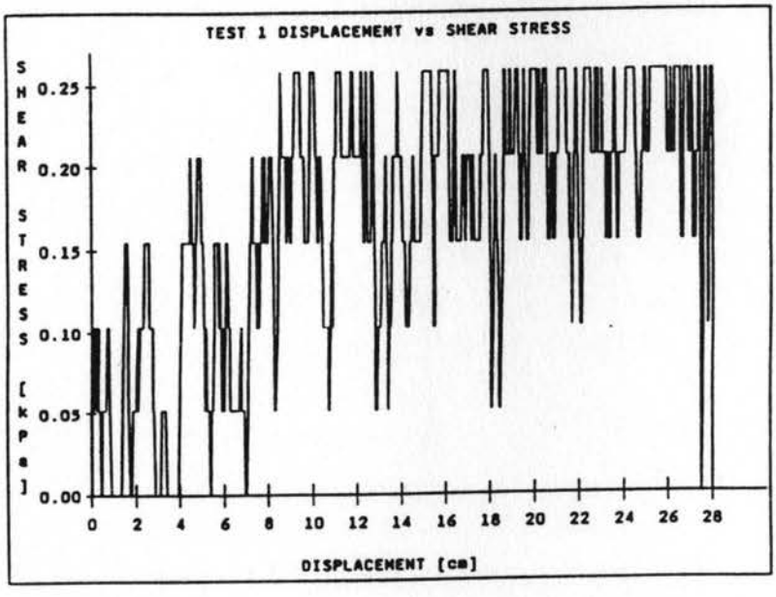

Figure A.1 Piezovane Test No. 1

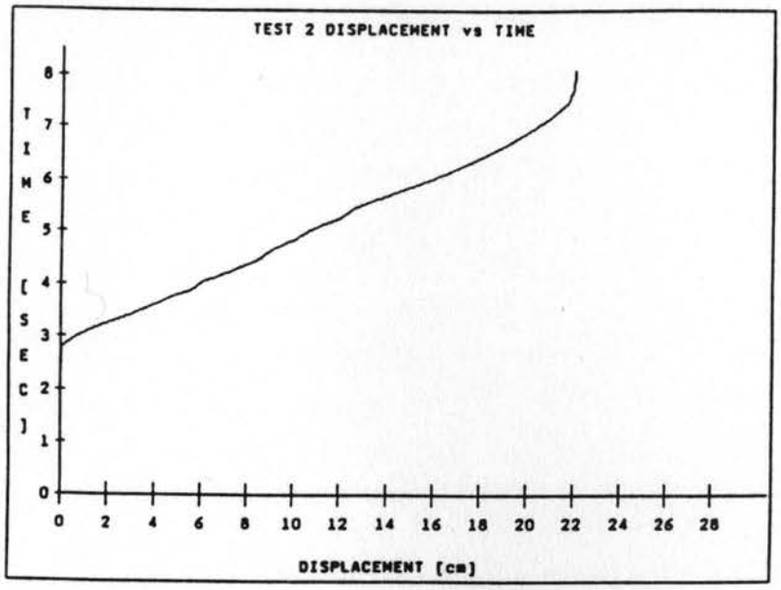

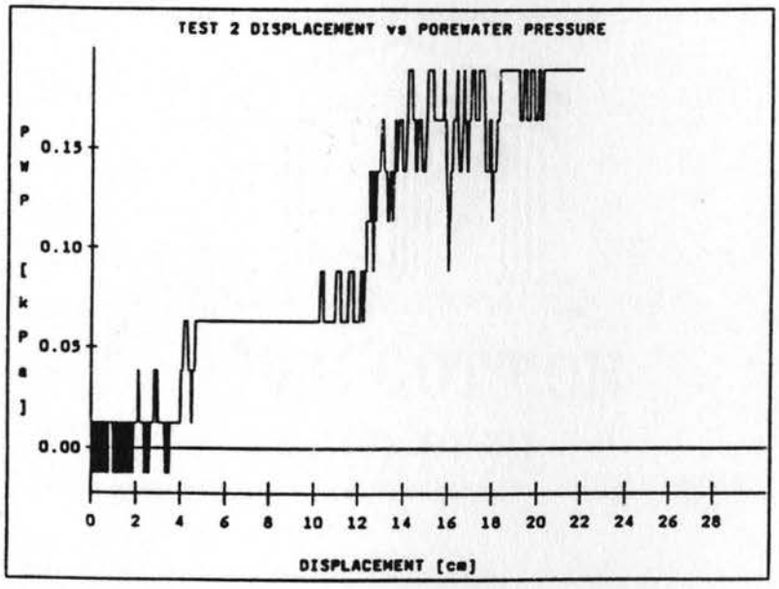

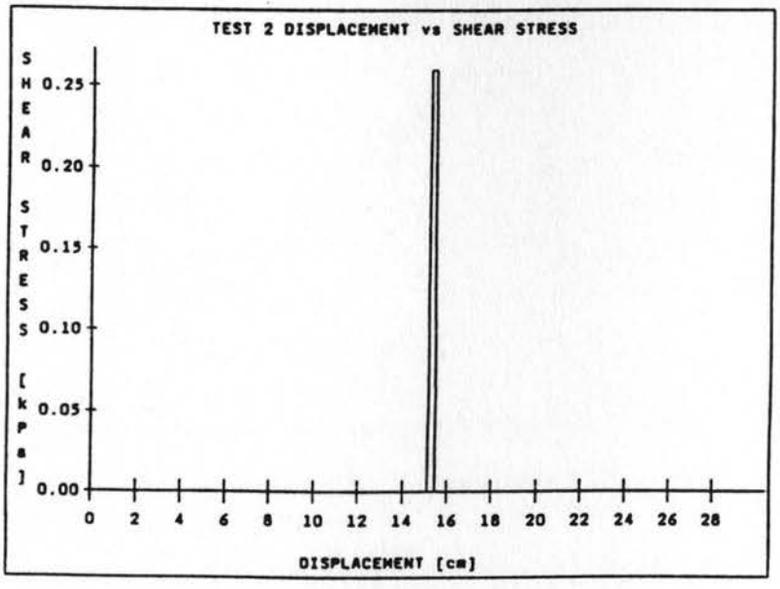

Figure A.2 Piezovane Test No. 2

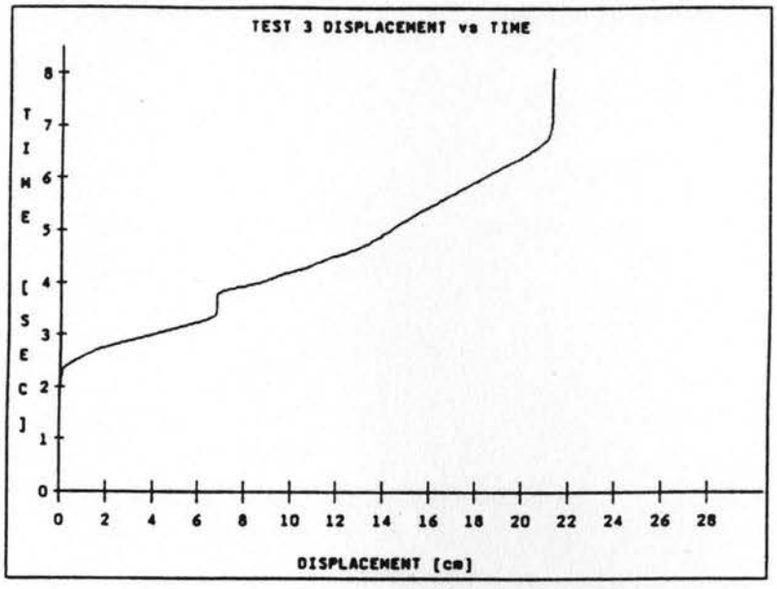

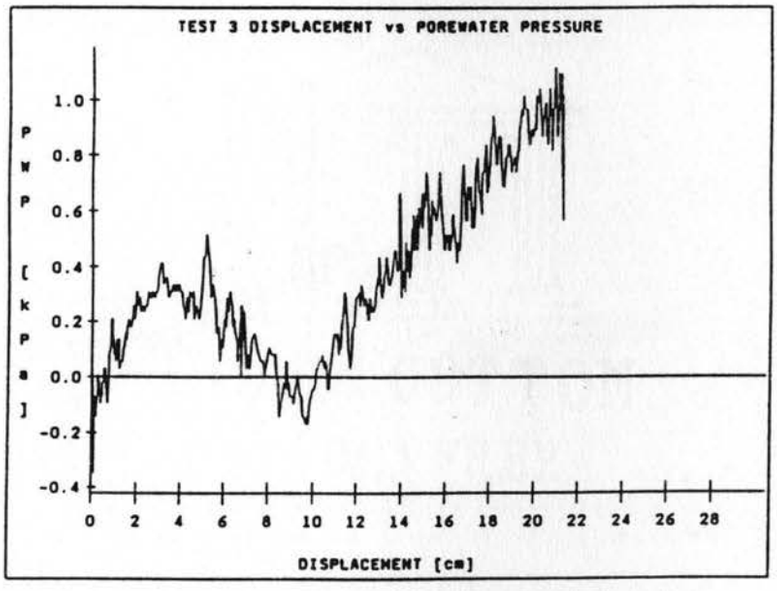

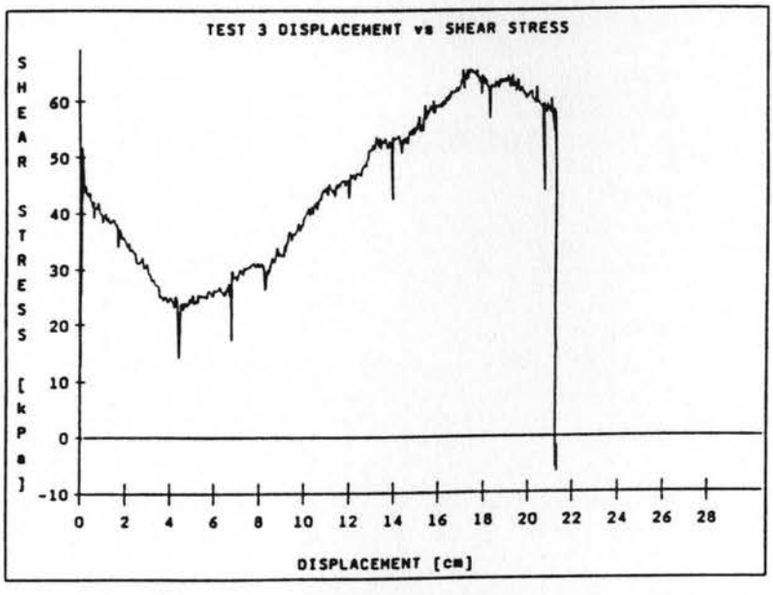

Figure A.3 Piezovane Test No. 3

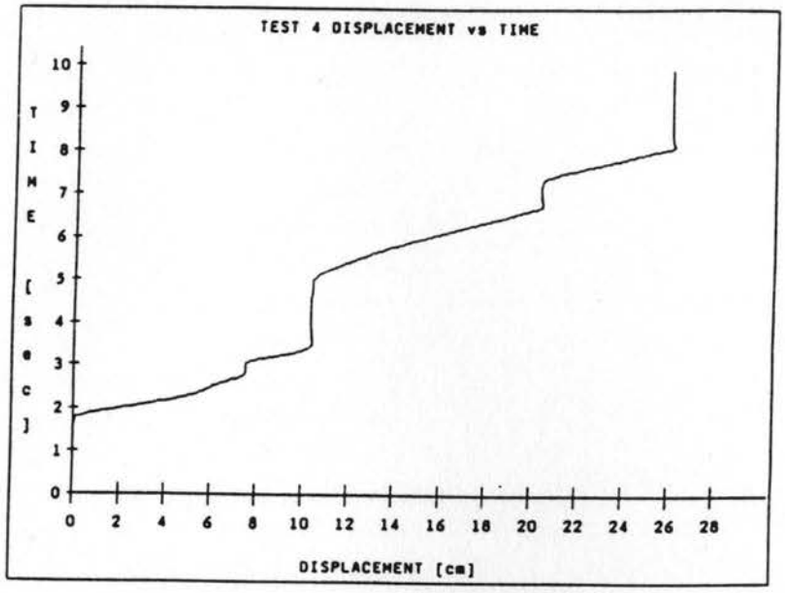

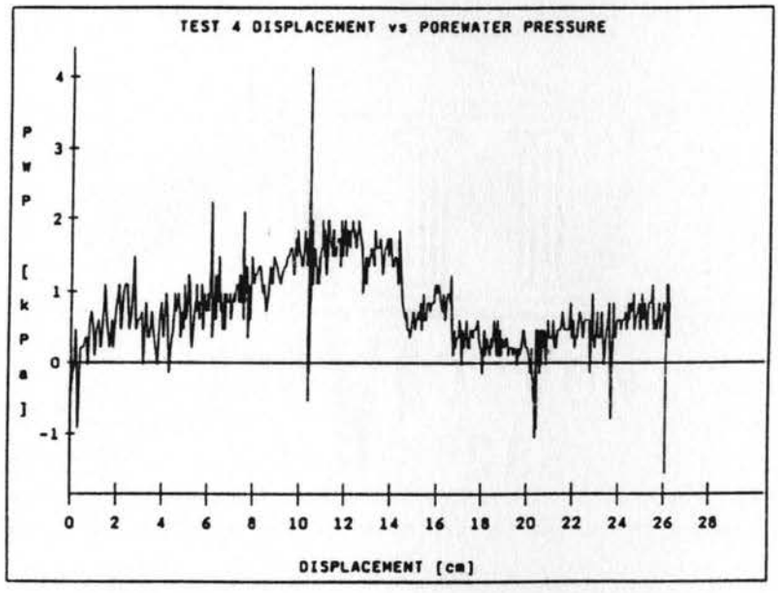

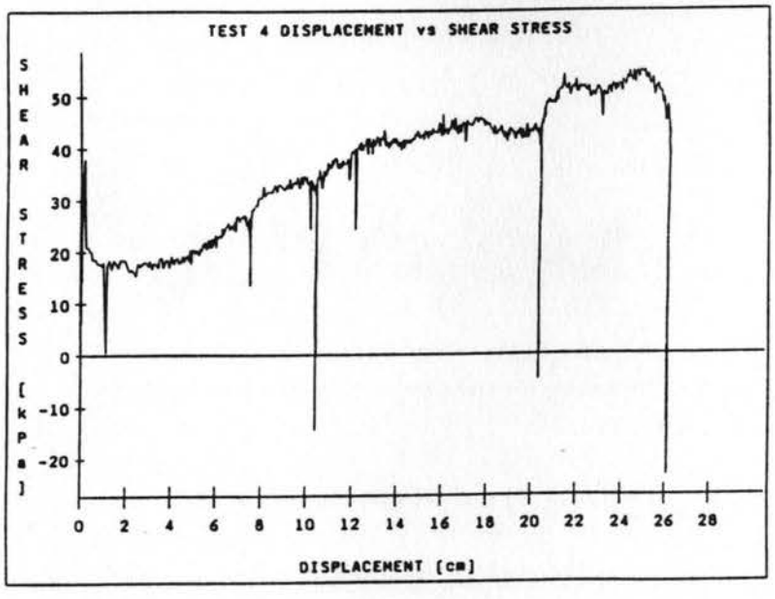

Figure A.4 Piezovane Test No. 4

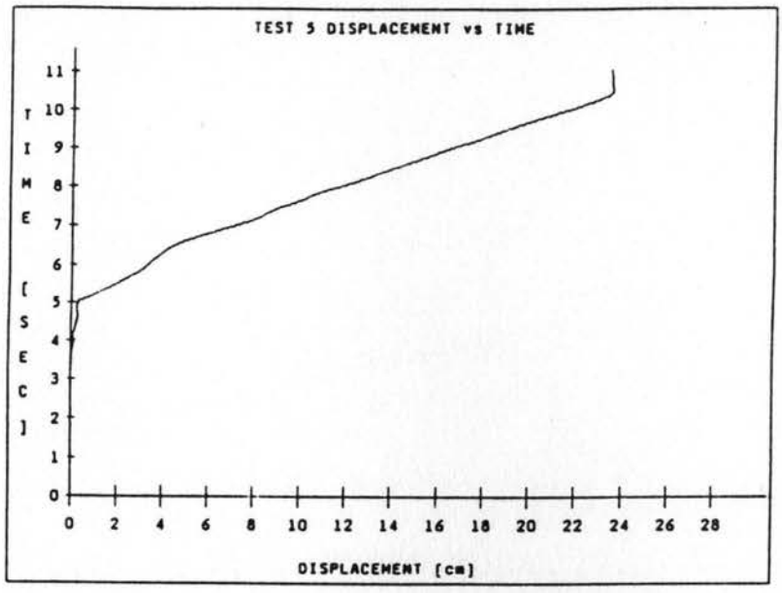

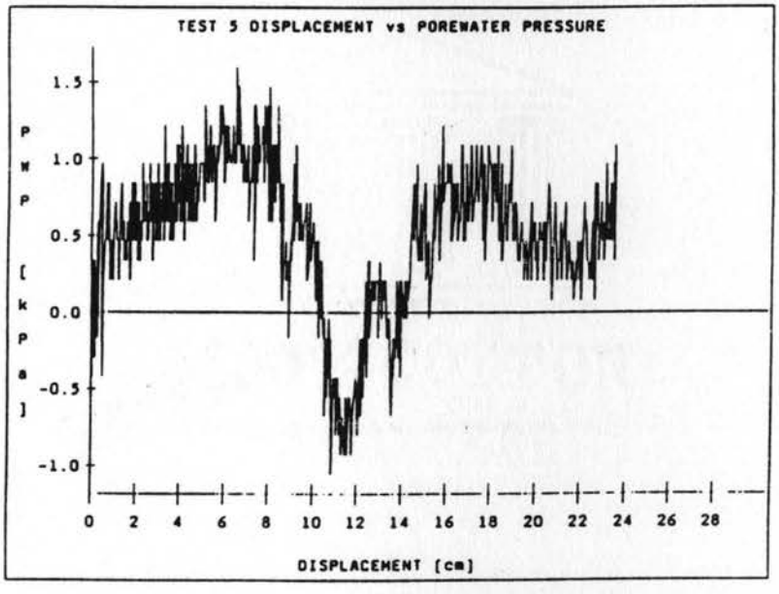

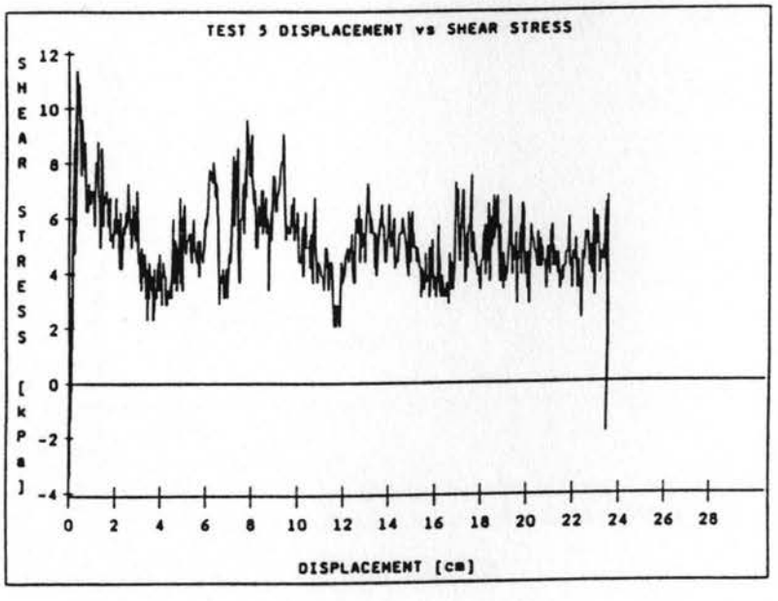

Figure A.5 Piezovane Test No. 5

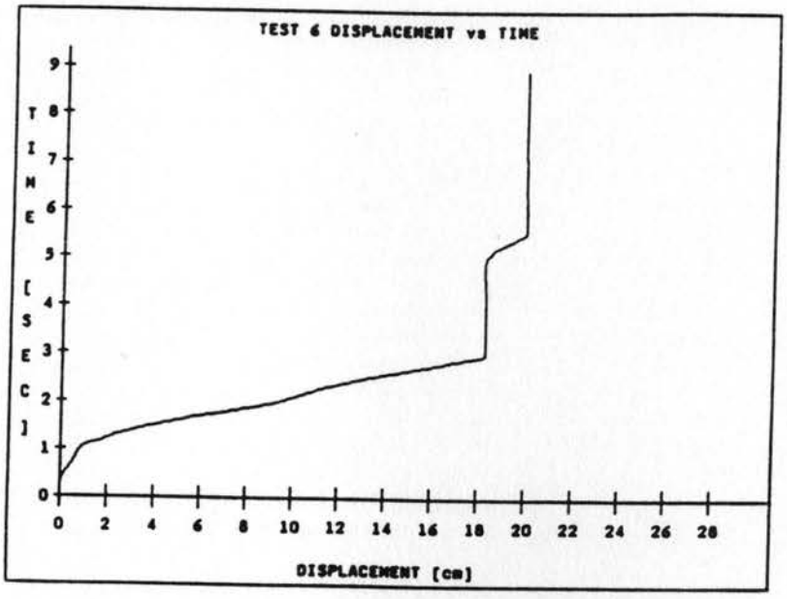

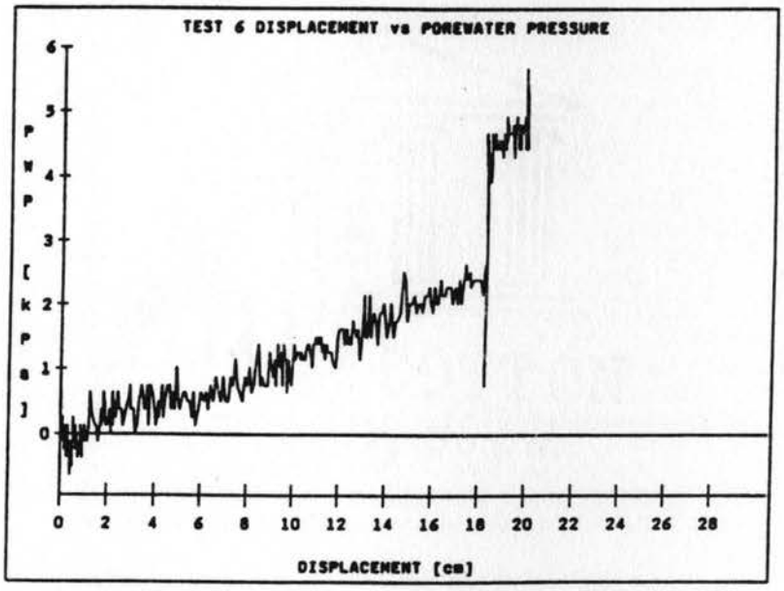

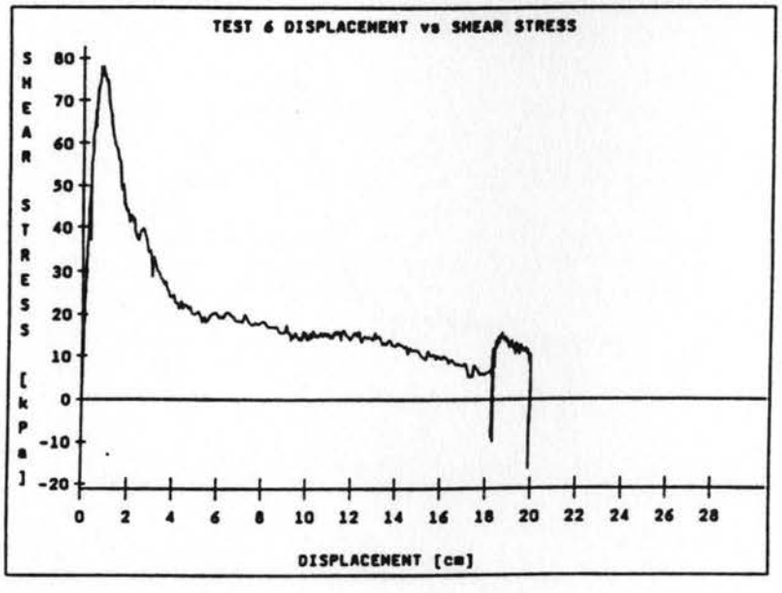

Figure A.6 Piezovane Test No. 6

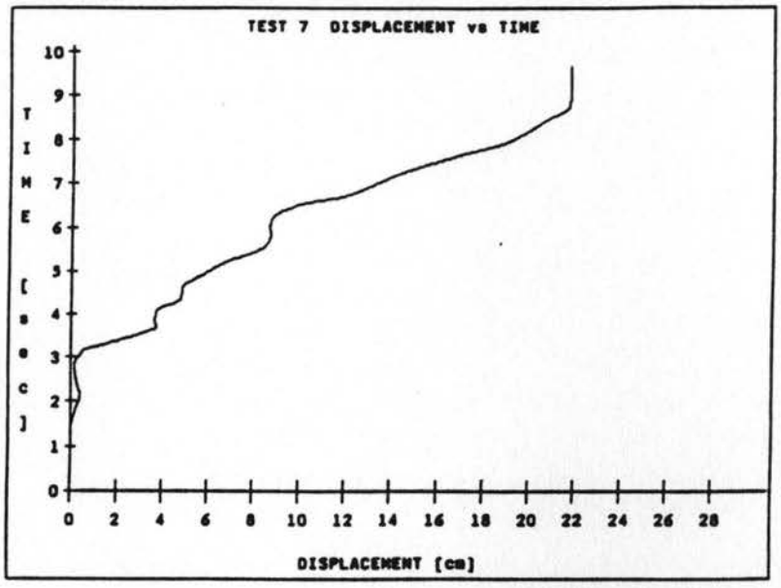

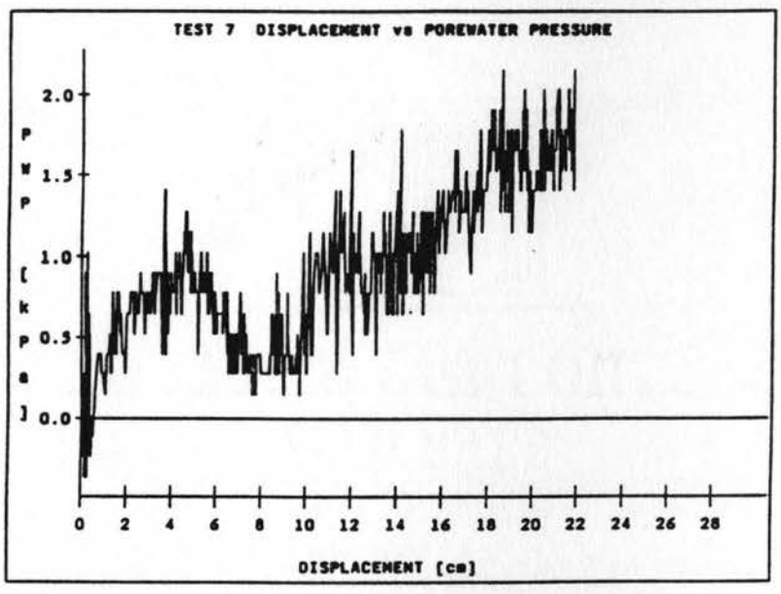

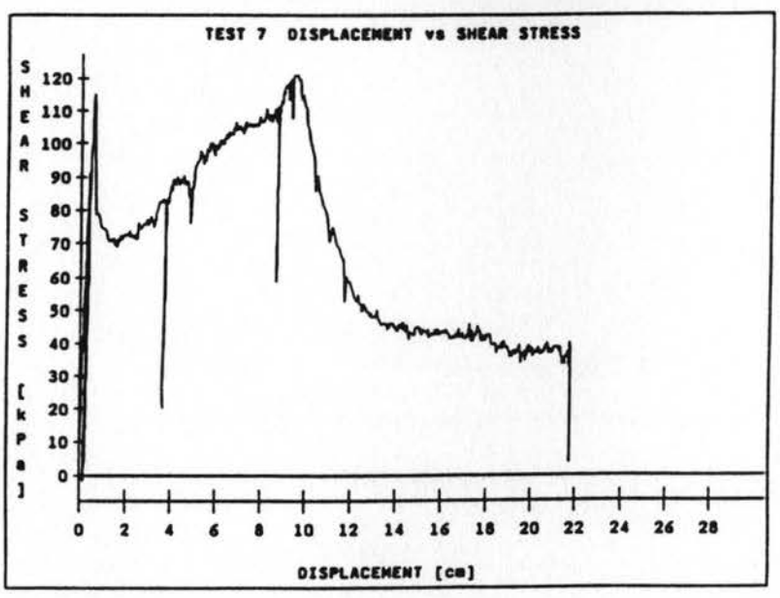

Figure A.7 Piezovane Test No. 7

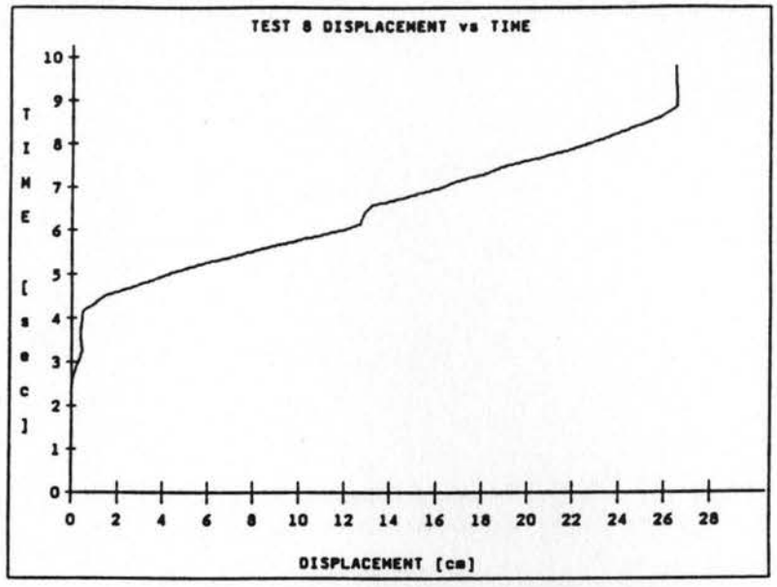

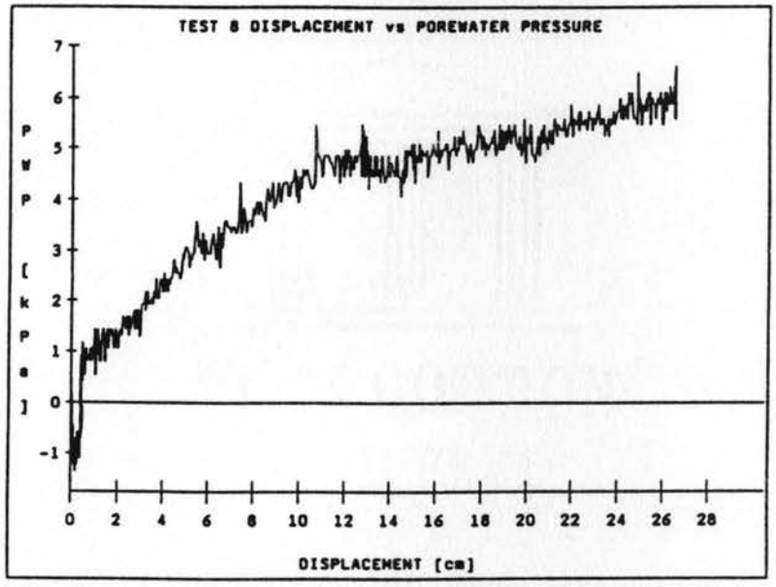

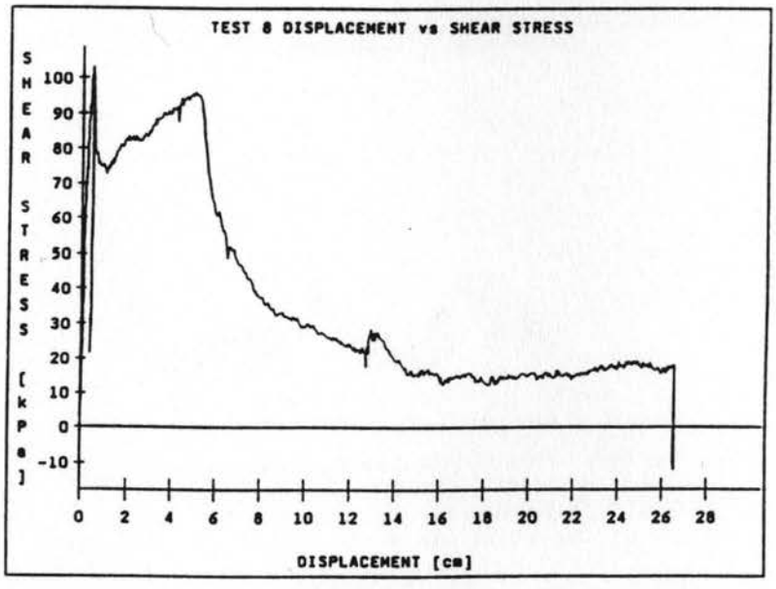

Figure A.8 Piezovane Test No. 8

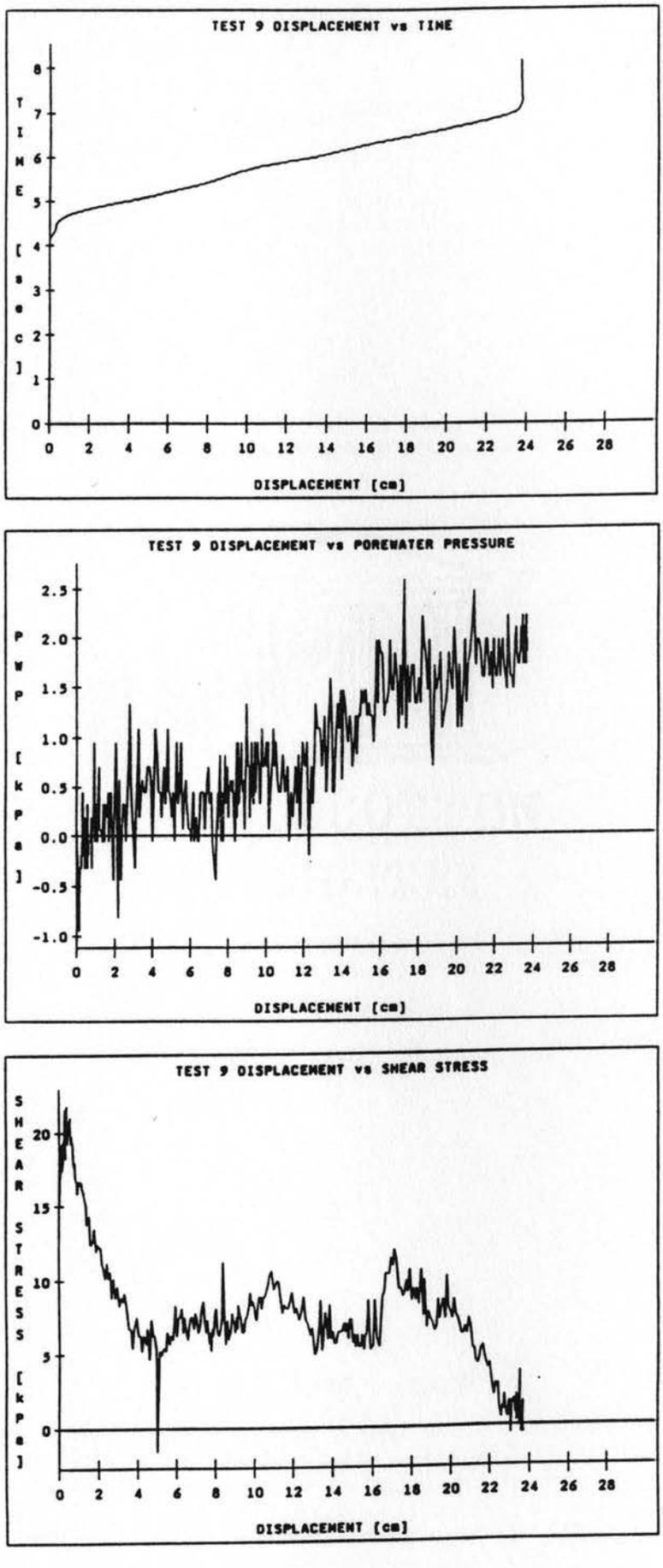

Figure A.9 Piezovane Test No. 9

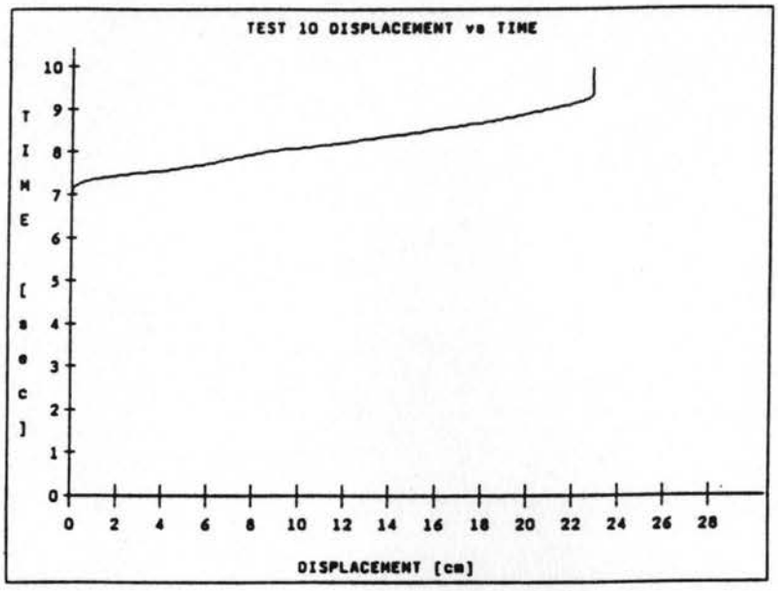

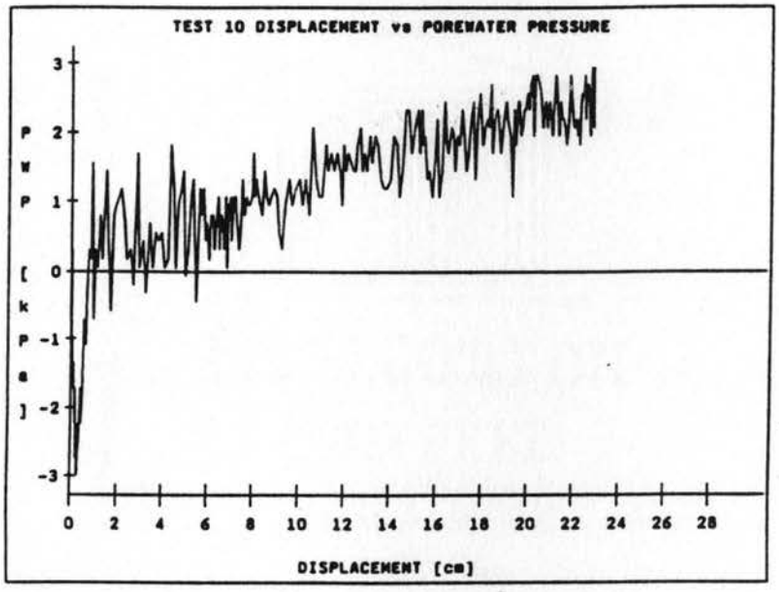

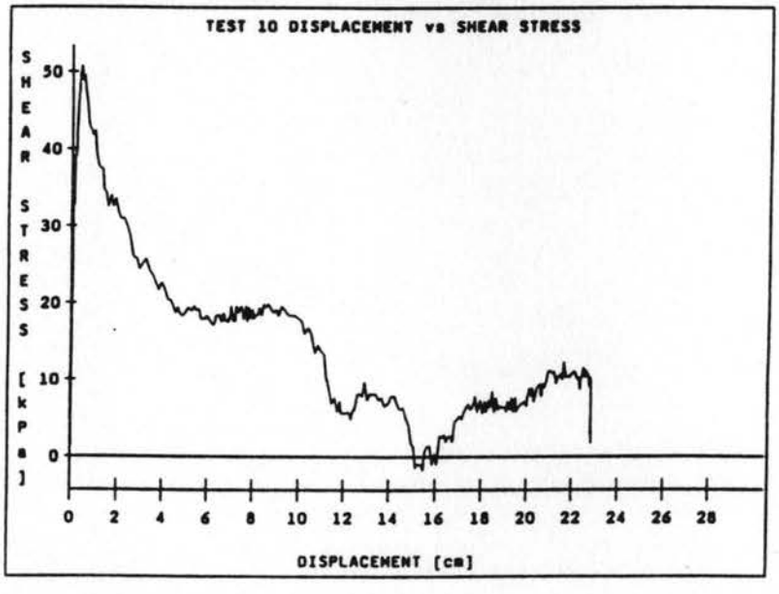

Figure A.10 Piezovane Test No. 10

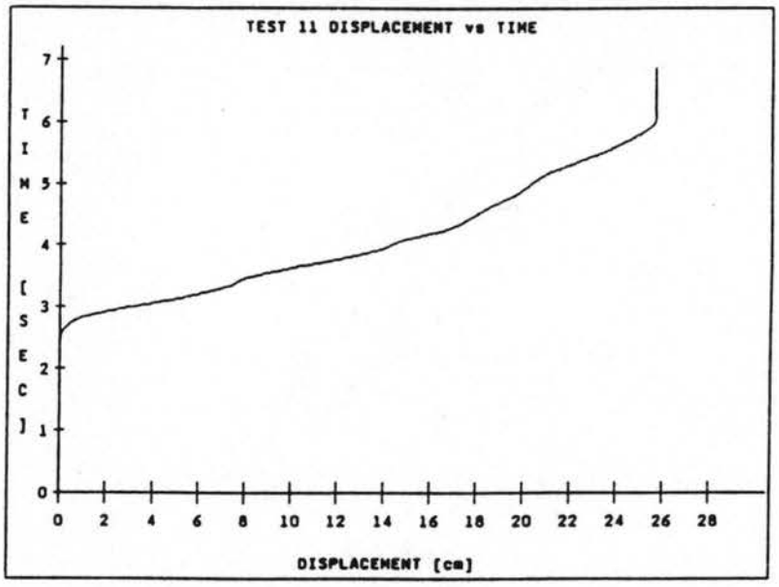

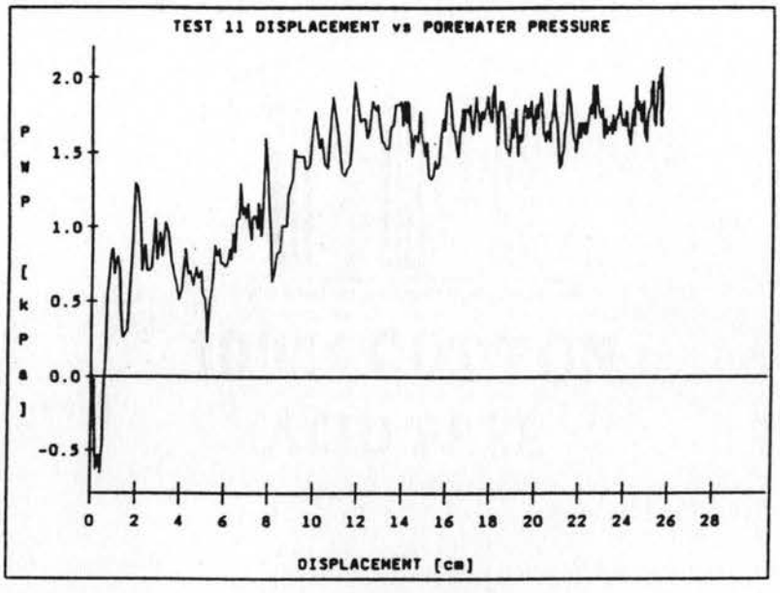

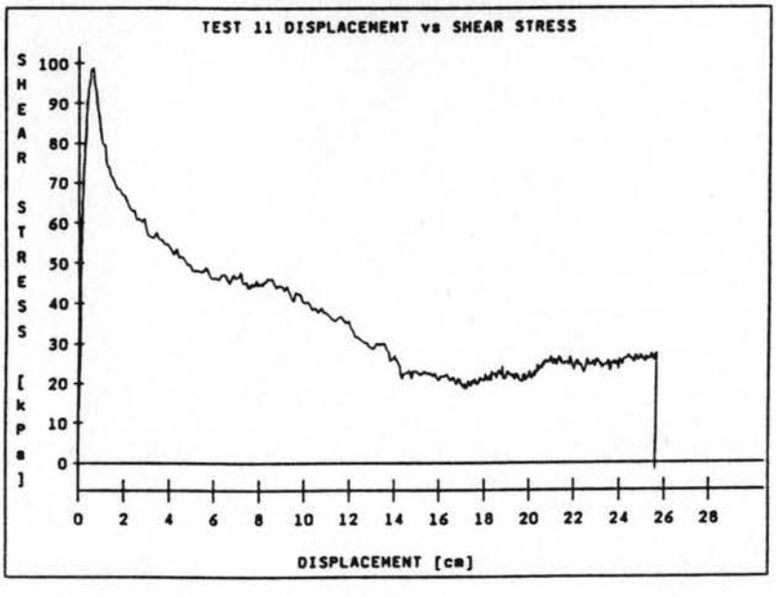

Figure A.11 Piezovane Test No. 11

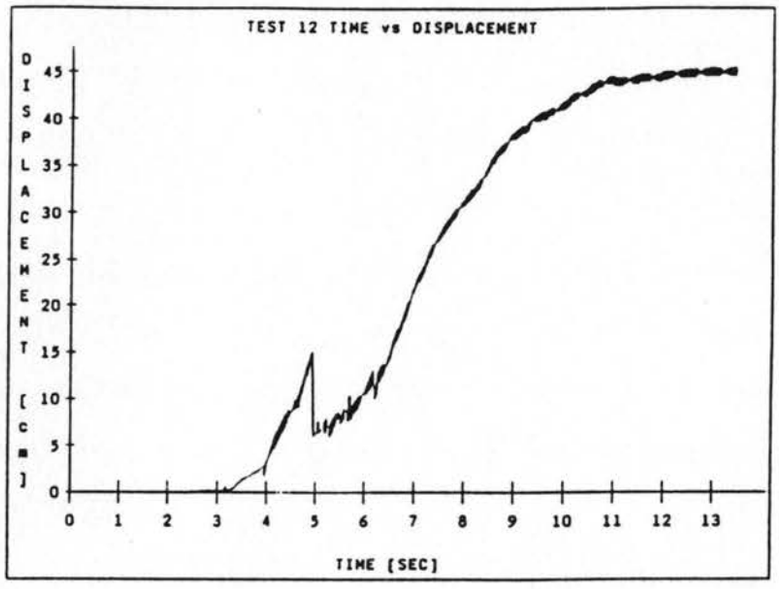

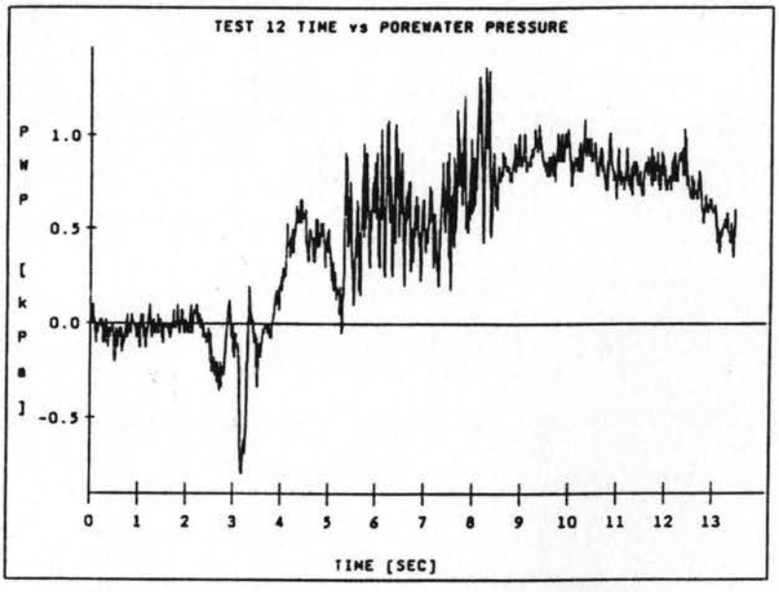

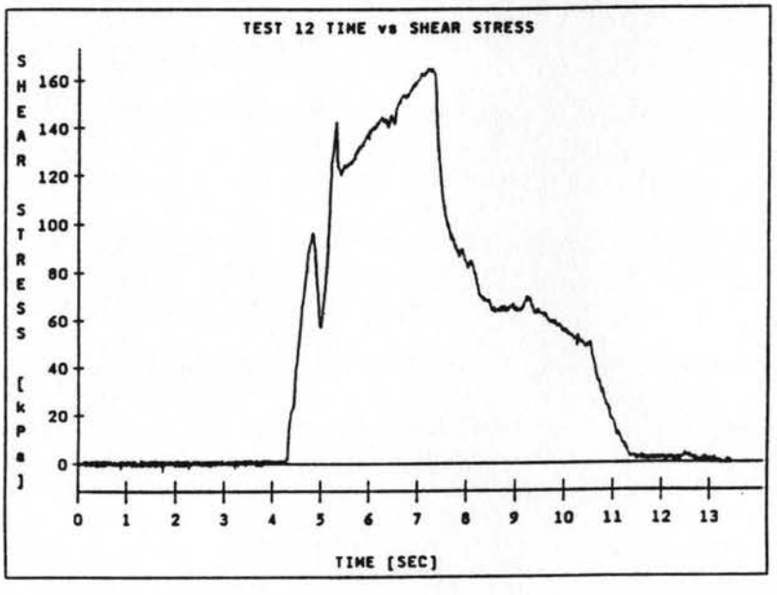

Figure A.12 Piezovane Test No. 12

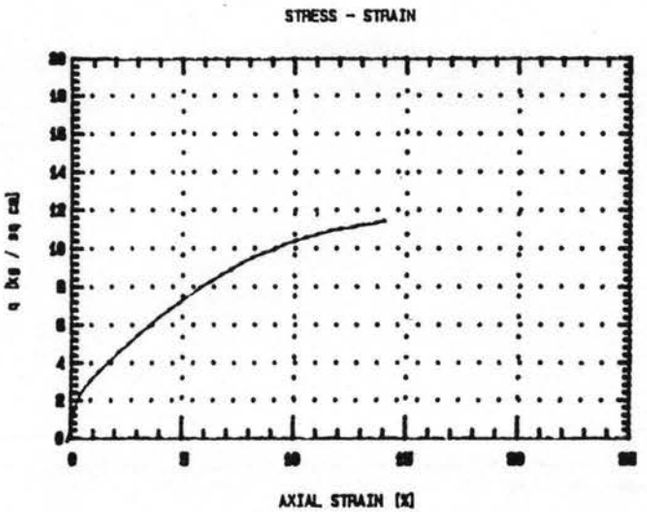

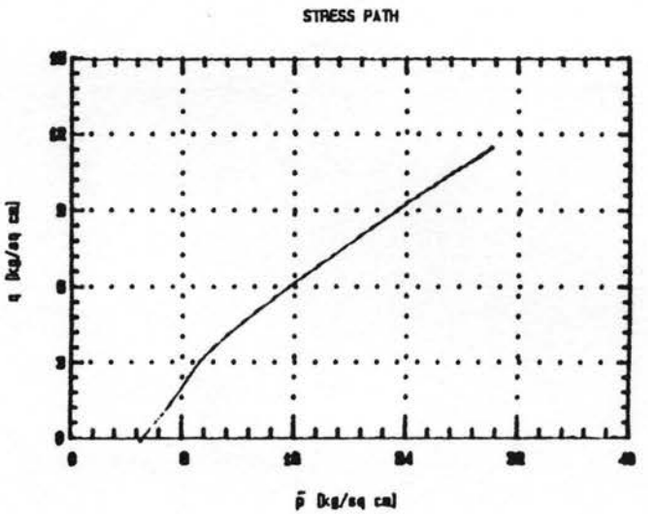

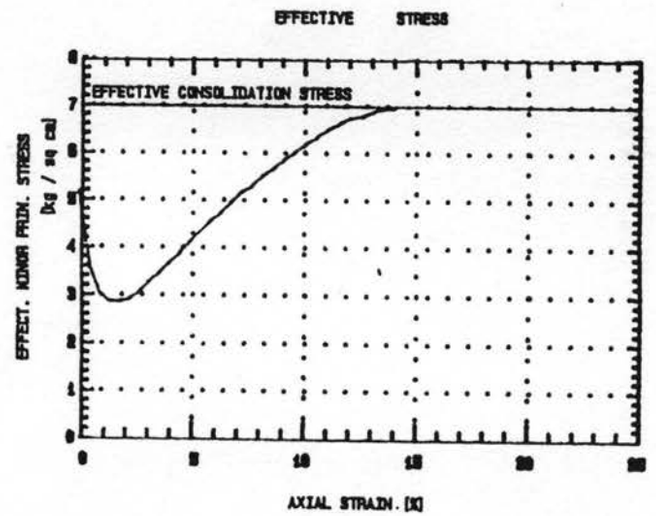

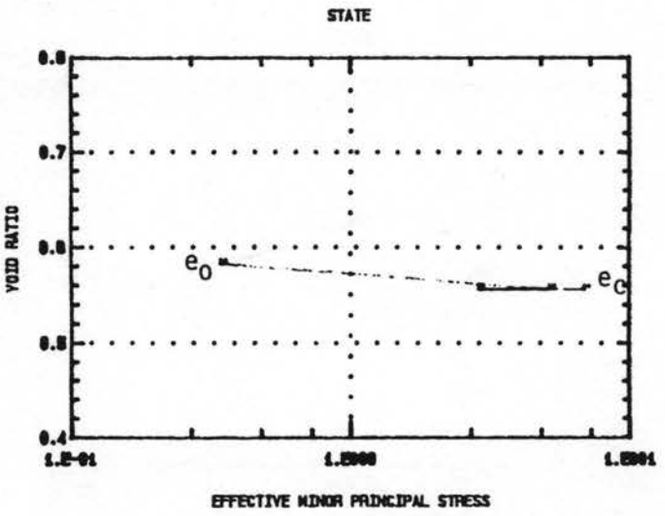

Figure A.13 PVS Triaxial Test 1

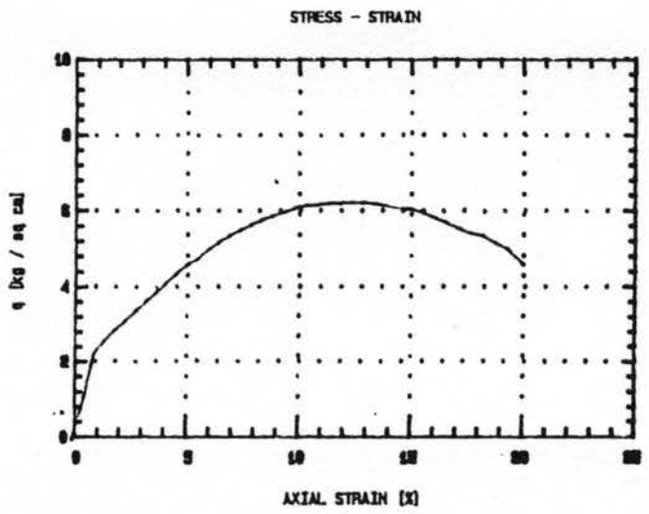

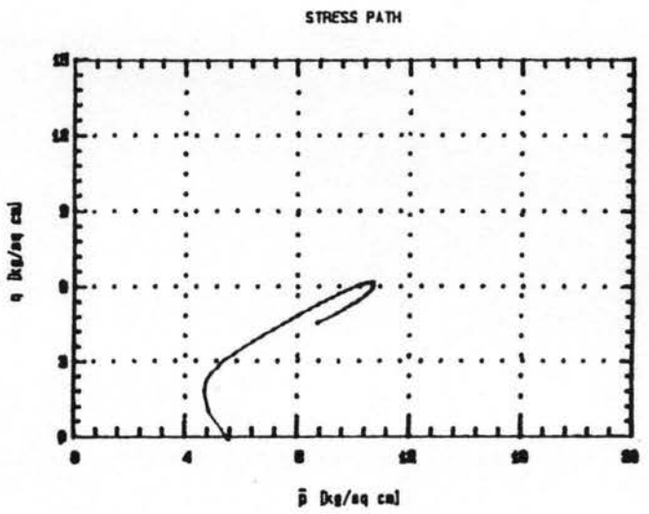

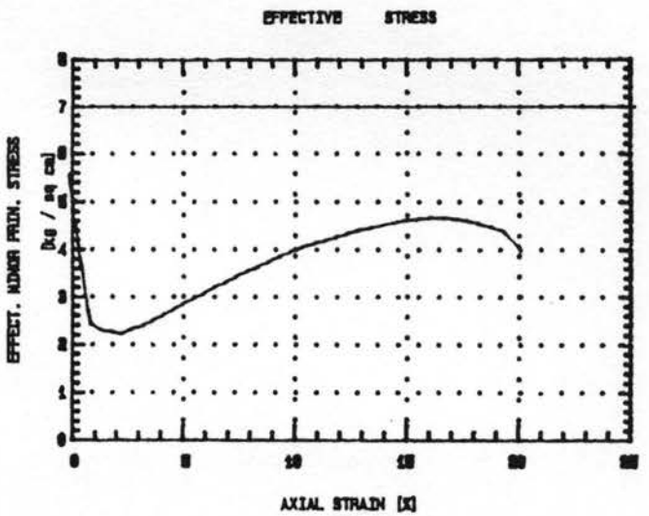

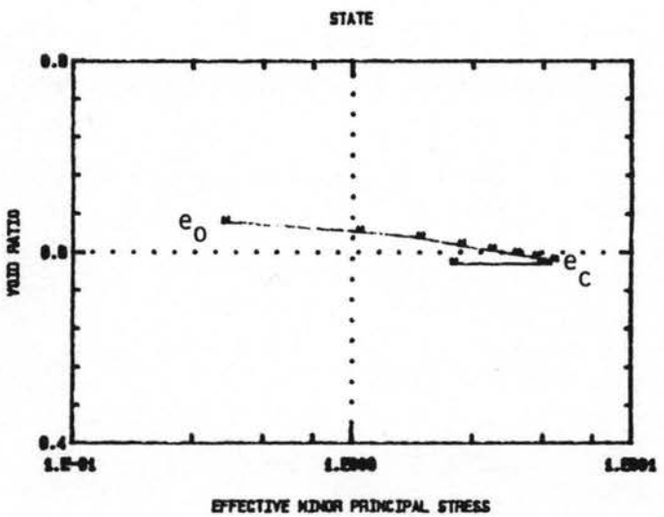

Figure A.14 PVS Triaxial Test 3

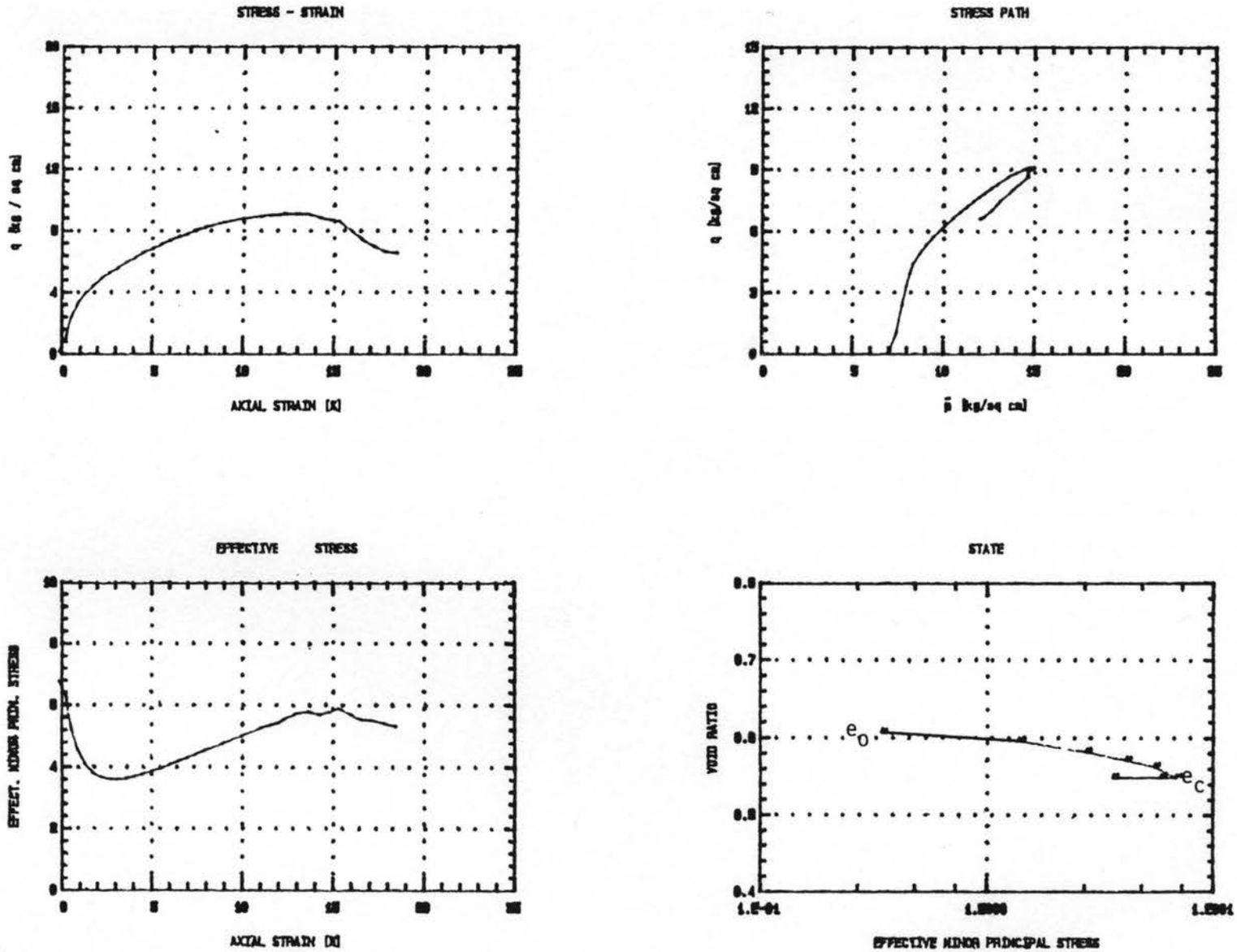

Figure A.15 PVS Triaxial Test 5

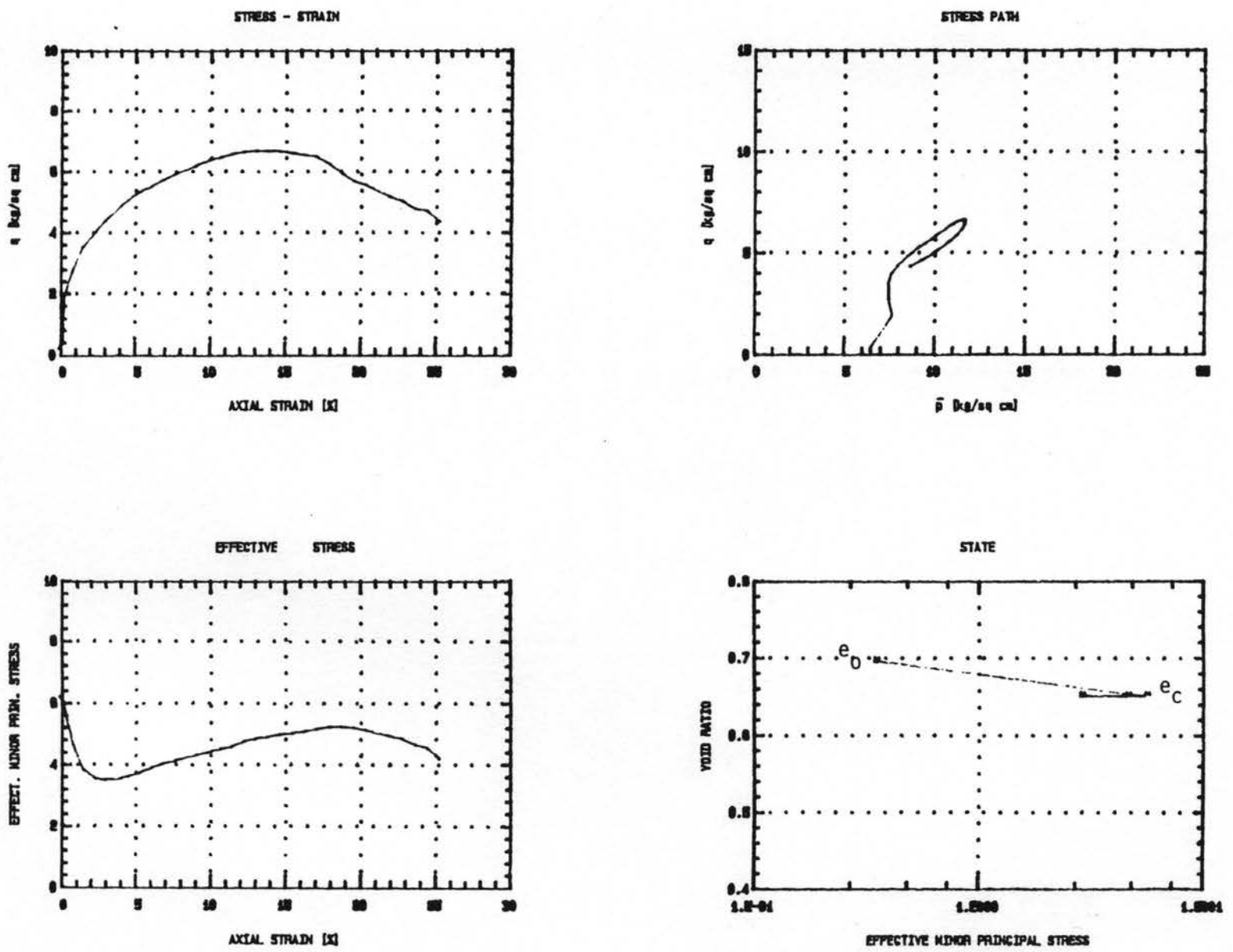

Figure A.16 PVS Triaxial Test 6

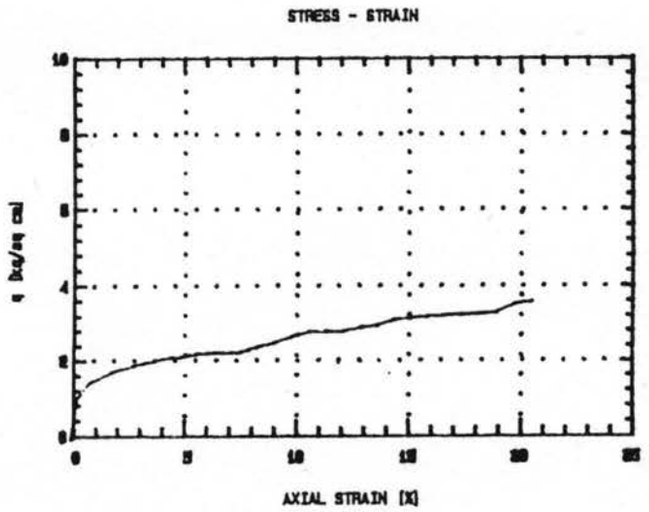

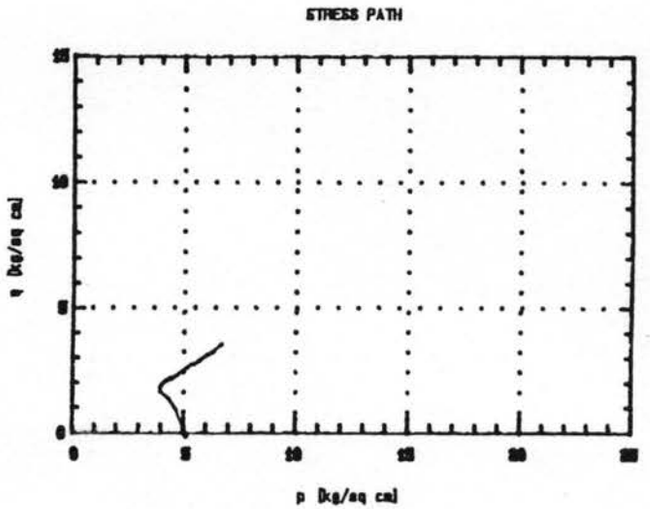

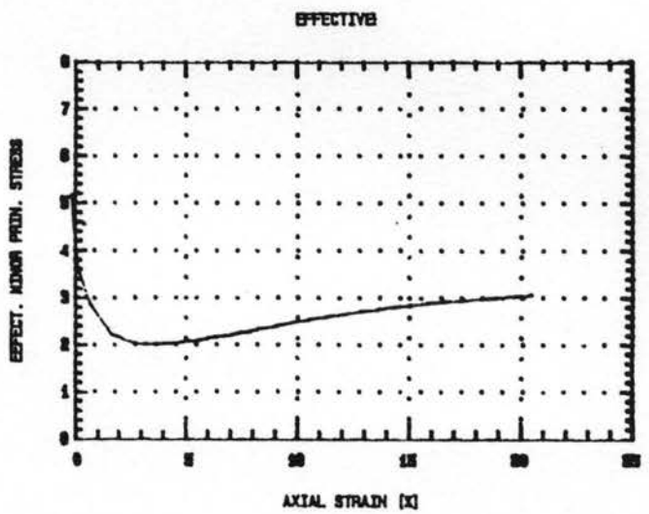

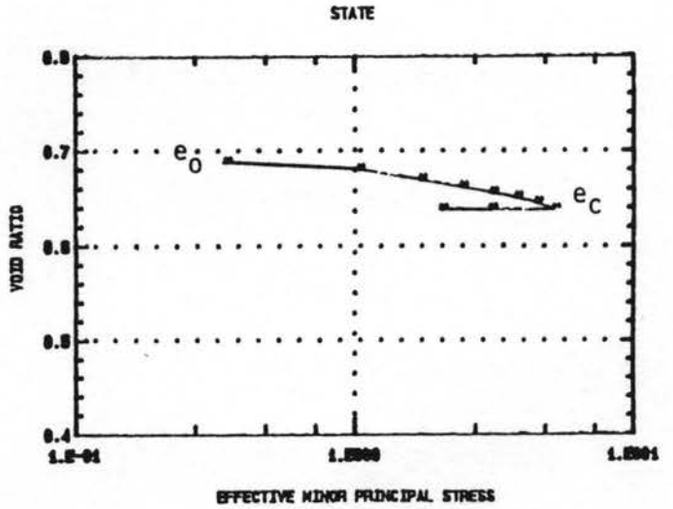

Figure A.17 PVS Triaxial Test 7

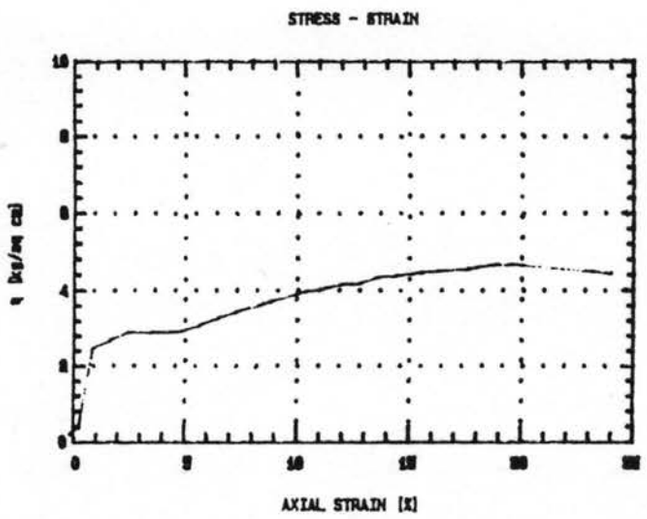

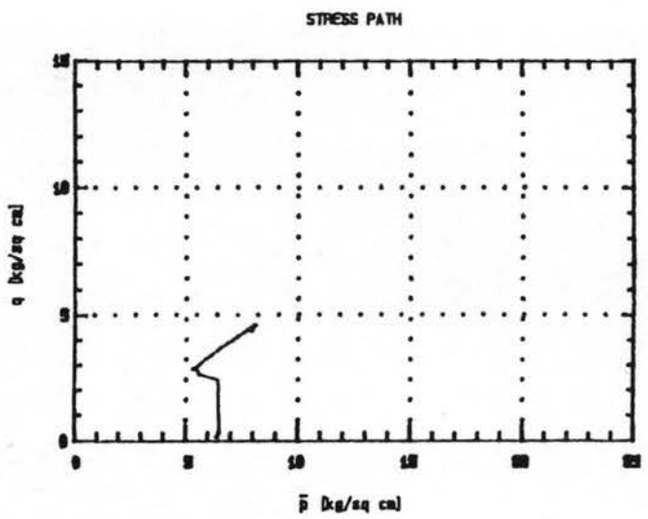

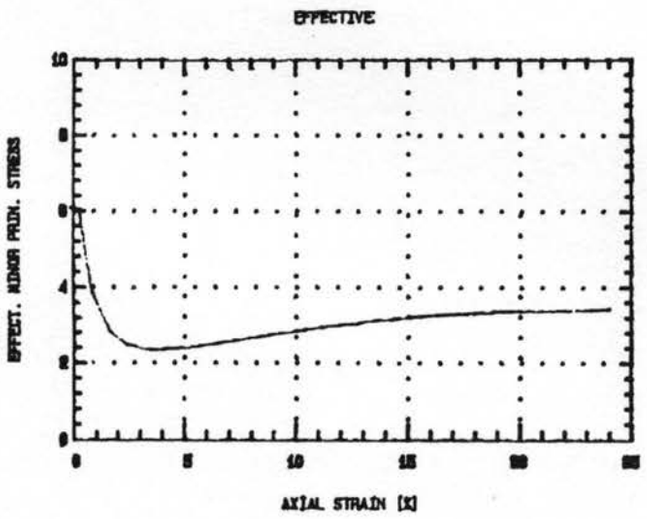

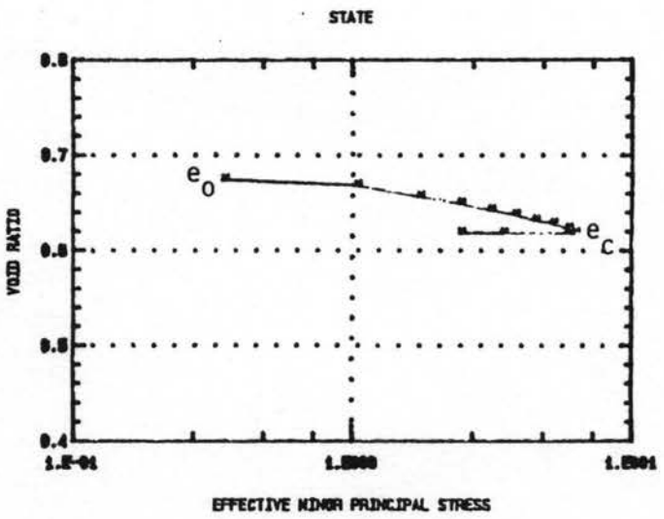

Figure A.18 PVS Triaxial Test 8

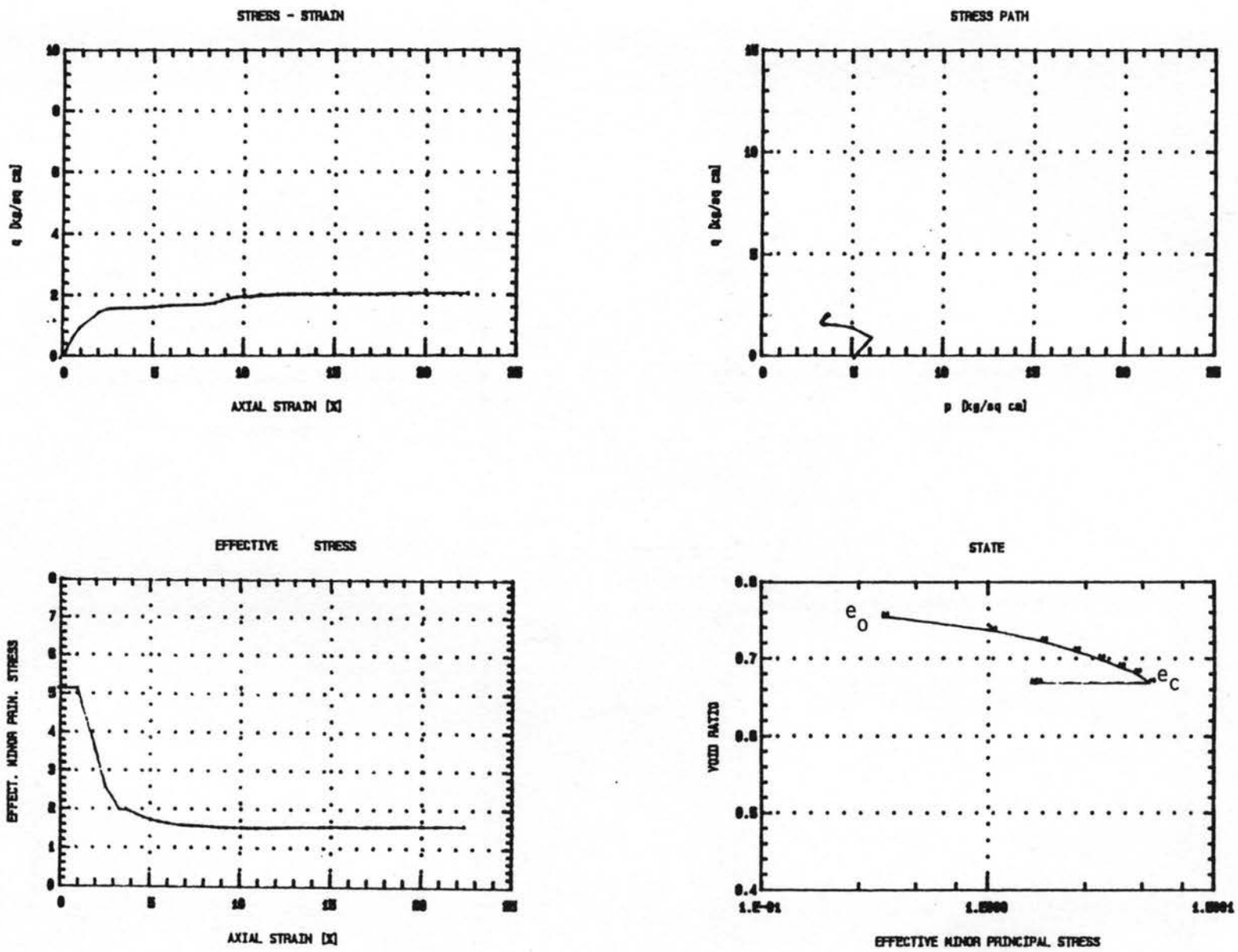

Figure A.19 PVS Triaxial Test 9

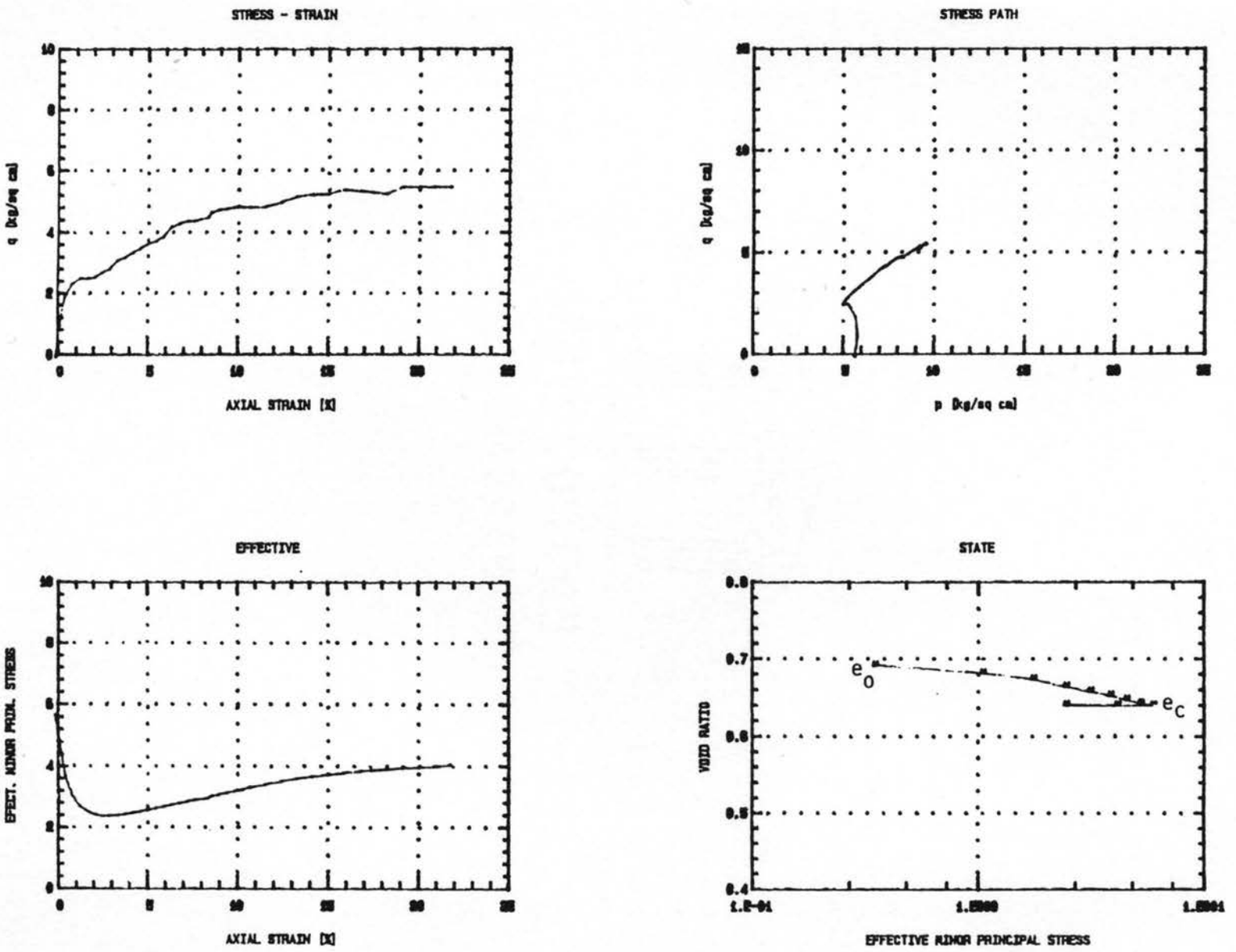

Figure A.20 PVS Triaxial Test 10